The interaction of mTOR and autophagy in salivary glands

Kawashima, Naomasa

Awarding institution:
King's College London

The interaction of mTOR and autophagy in salivary glands

Thesis submitted for degree of Doctor of Philosophy

by Naomasa Kawashima

Division of Mucosal and Salivary Biology

King's College London Dental Institute

March 2018

Supervisors: Dr Guy Carpenter & Prof Gordon Proctor

ABSTRACT

Radiation therapy to treat head and neck cancer damages salivary glands, leading to decreased salivary flow which can cause xerostomia (perception of dry mouth), mucositis and dysphagia. These symptoms of salivary gland hypofunction are a major cause of patients stopping their treatment and greatly decrease their quality of life after treatment. Protecting from damage is essential to avoid these problems so this thesis examined some of the damage mechanisms present in salivary glands. Two intracellular processes seem to be particularly relevant. Mammalian Target of Rapamycin (mTOR) is a growth pathway often activated in cancers, repair and regeneration whereas autophagy is a self-digestion of cellular contents often associated with damage that helps to protect cells from apoptosis. Normally the two processes are linked by an enzyme UNC-like kinase (ULK) in a mutually exclusive way so that growth and degradation do not occur at the same time. However, both mTOR and autophagy have been shown to have beneficial effects after irradiation. Therefore, we decided to study the interactions between mTOR and autophagy in order to find an efficient way to uncouple mTOR and autophagy to protect irradiated salivary glands. Since ULK was an important link between mTOR and autophagy, an interesting new ULK inhibitor MRT67307 was used on salivary glands.

In the first part of this study, we evaluated the effects of MRT67307 on cell cultures in order to collect enough data before trying the drug in vivo. Initially NIH 3T3 cells, a well-studied cell model, were cultured to verify the effects of MRT67307. As previously reported, the drug blocked starvation- and Torin 1 (an mTOR inhibitor)-induced autophagy. The next step was to test the effects of the drug on salivary acinar cells which were known to be very sensitive to irradiation. SMG-C6 cells were chosen since they were previously derived from rat submandibular acinar cells. In these cells, in contrast to NIH 3T3 cells, Torin 1 failed to upregulate autophagy, suggesting that mTOR and autophagy were not linked by ULK. This finding was interesting and novel and was further tested in primary-cultured cells (ie in vitro) from mouse submandibular glands. Again, administration of Torin 1 inhibited mTOR but did not activate autophagy and MRT67307 had no effect on marker of autophagy (LC3-I/LC3-II ratios). It could be inferred from these experiments that MRT67307 is a useful tool in examining mTOR/autophagy interactions through ULK1 and that in salivary glands autophagy and mTOR could be activated simultaneously.

In the second part of this study, we carried out whole body irradiation of mice to study damage, mTOR-autophagy interactions and saliva flow variation in irradiated salivary glands. A dose escalation study appeared to cause minimal damage to salivary glands when the maximum dose of 11 Gy was given. To determine if salivary hypofunction had occurred whole mouth saliva was collected under temporary gaseous anaesthesia by the administration of pilocarpine ($_{I.P.}$). Surprisingly, despite minimal histological indications of damage an increase in salivary function occurred. Biochemical analyses of the salivary glands indicated autophagy was transiently and weakly activated a few hours after irradiation whereas mTOR activity occurred a few days later. The use of a whole body irradiator limited the dose of irradiation to the salivary glands. Thus as a model system, transient mTOR activation probably had a beneficial effect, since pilocarpine stimulated saliva flow experiment showed a transient increase of saliva flow. However, this model system did not yield the expected salivary gland damage seen in other studies so instead another model of salivary gland damage, ductal ligation was studied.

The third part of this study attempted to use autophagy-inhibitors in vivo, using the ligated salivary gland since autophagy activation was weak and did not last in irradiated salivary gland. Whole body injection of autophagy inhibitors chloroquine and MRT67307 (at two different doses and injection intervals) did not appear to have any beneficial effect on submandibular glands, except a slight delay of atrophy in both chloroquine and MRT67307 treated glands. Autophagy appeared to be mainly mTOR independent since MRT67307 failed to inhibit autophagy.

This thesis contains novel data to indicate that autophagy and mTOR are independent of each in mouse submandibular glands. To the best of our knowledge, this is the first time that MRT67307 was used in vivo and no paper demonstrates an mTOR independent activation of autophagy in salivary glands. It provides the basis for further studies to protect salivary glands from irradiation damage by upregulating both mTOR and autophagy simultaneously, something that has not, so far, been tested.

CONTENTS

AKNOWLEDGEMENTS

I would like to express my sincere appreciation to my first supervisor Dr. Guy Carpenter for guiding me throughout my doctorate. I am most grateful for all the support and encouragement you have given me. My sincere thanks also go to my second supervisor Prof. Gordon Proctor and to my postgraduate coordinator Prof. Agamemnon Grigoriadis for their valuable advices and helps.

I would also extend my thanks to all the staff of the Division of Mucosal & Salivary Biology for their help, moral support and kindness.

TABLE OF FIGURES AND TABLES

TABLE OF ABBREVIATIONS

Akt: protein kinase B

AMPK: 5'-AMP-activated protein kinase

AQP5: aquaporin 5

ATG, Atg: autophagy related

BCA: bicinchoninic acid

Bcl-2: B-cell lymphoma 2

BFU-E: burst forming unit erythroid

BMI1: B lymphoma Mo-MLV insertion region 1 homolog

CFU: colony forming unit

C3H10T1/2 cells: C3H mouse embryo cells

DAB: 3,3' diaminobenzidine

DEPTOR: DEP domain-containing mTOR-interacting protein

DMEM: Dubelcco's Modified Eagle's Medium

DME/F-12: Dubelcco's Modified Eagle's Medium/ Ham's Nutrient Mixture F-12

EDTA: ethylenediaminetetraacetic acid

EGF: epidermial growth factor

eIF4E: eukaryote translation initiator factor 4E

ER: endoplasmic reticulum

Erk: extracellular signal-regulated kinase

GβL: G protein beta subunit-like

GADPH: glyceraldehydes-3-phosphate dehydrogenase

GAP: GTPase activating protein

GEMM: granulocyte erythrocyte monocyte megakaryocyte

GRP: glutamine acid-rich proteins

GTP: guanosine-5'- triphosphate

Gy: gray (unit of ionizing radiation dose)

FAT C domain: FRAP ataxia telangiectasia mutated

FIP200: focal adhesion kinase family interacting protein of 200 kDa

FRB: FKBP12-rapamycin binding

HEAT: Huntington elongation factor 3, subunit of protein phosphatase 2A and yeast TOR1

HBSS: Hank's Balanced Salt Solution

HRP: horseradish peroxidase

hVPS: human vacuolar protein sorting

H & E: hematoxylin and eosin

H2AX: H2A histone family, member X

IGF: insulin-like growth factor

IKKε: inhibitor of nuclear factor kappa-B kinase subunit epsilon

IKK2: inhibitor of nuclear factor kappa-B kinase subunit beta

IL-1β: interleukin-1 β

IMS: industrial methylated spirit

IP: intraperitoneal, intraperitoneally

IR: ionizing radiation

KO: knock-out

LC3: microtubule-associated protein light chain 3

LG5: leucine-rich repeat-containing G-protein coupled receptor 5

LKB1: liver kinase B1

LKS^{+}: $lin^{-}c\text{-}kit^{+}Sca1^{+}$

MAPK: mitogen-activated protein kinase

MAP4K3: mitogen-activated protein kinase kinase kinase kinase 3

mAtg13: mammalian autophagy related protein 13

mLst8: mammalian lethal with SEC13 protein 8

mTERT: mouse telomerase reverse transcriptase

mTOR: mammalian target of rapamycin

mTORC: mTOR complex

NSPC: neural stem and progenitor cell

PAS: periodic acid Schiff

Pax: paired-box

PBS: phosphate-buffered saline

PDK1: phosphoinositide-dependent kinase-1

PE: phosphatidylethanolamine

PI3K: phosphoinositide 3-kinase class I

PRAS40: protein-rich Akt substrate of 40 kDa

protor: protein observed with rictor-1

PRP: proline-rich proteins

PRR5: proline rich protein 5

PTEN: phosphatase and tensin homolog

$p16^{Ink4a}$: cyclin-dependent kinase inhibitor 2A

$p21^{WAF1}$: cyclin-dependent kinase inhibitor 1A

p53: tumour protein p53

p62: nucleoporin 62 kDa

raptor: regulatory associated protein of mTOR

REDD: regulated in development and DNA damage

Rheb: Ras homolog enriched in brain

rictor: rapamycin insensible companion of mTOR

RIPA: radioimmunoprecipitation assay

ROS: reactive oxygen species

sin 1: stress-activated protein kinase-interacting protein 1

SDS-PAGE: sodium dodecyl sulfate polyacrylamide gel electrophoresis

SLC: solute-linked carrier

SMA: smooth muscle actin

SMG: submandibular gland

SOD1: superoxide dismutase 1

S6K1: ribosomal protein S6 kinase 1

TSC: tuberous sclerosis complex

TBS: tris-buffered saline

TTBS: tris-buffered saline with 1% tween 20

T3: triiodo-L-thyronine

ULK: Unc-51 like autophagy activating kinase

4E-BP1: eukaryotic translation initiator factor 4E-binding protein 1

A. INTRODUCTION

I. SALIVARY GLANDS

Salivary glands are exocrine glands producing saliva and secreting some enzymes to begin digestion. The main salivary glands are the parotid, the submandibular and the sublingual glands [1]. **Figure 1** shows the location of the main salivary glands in humans [67].

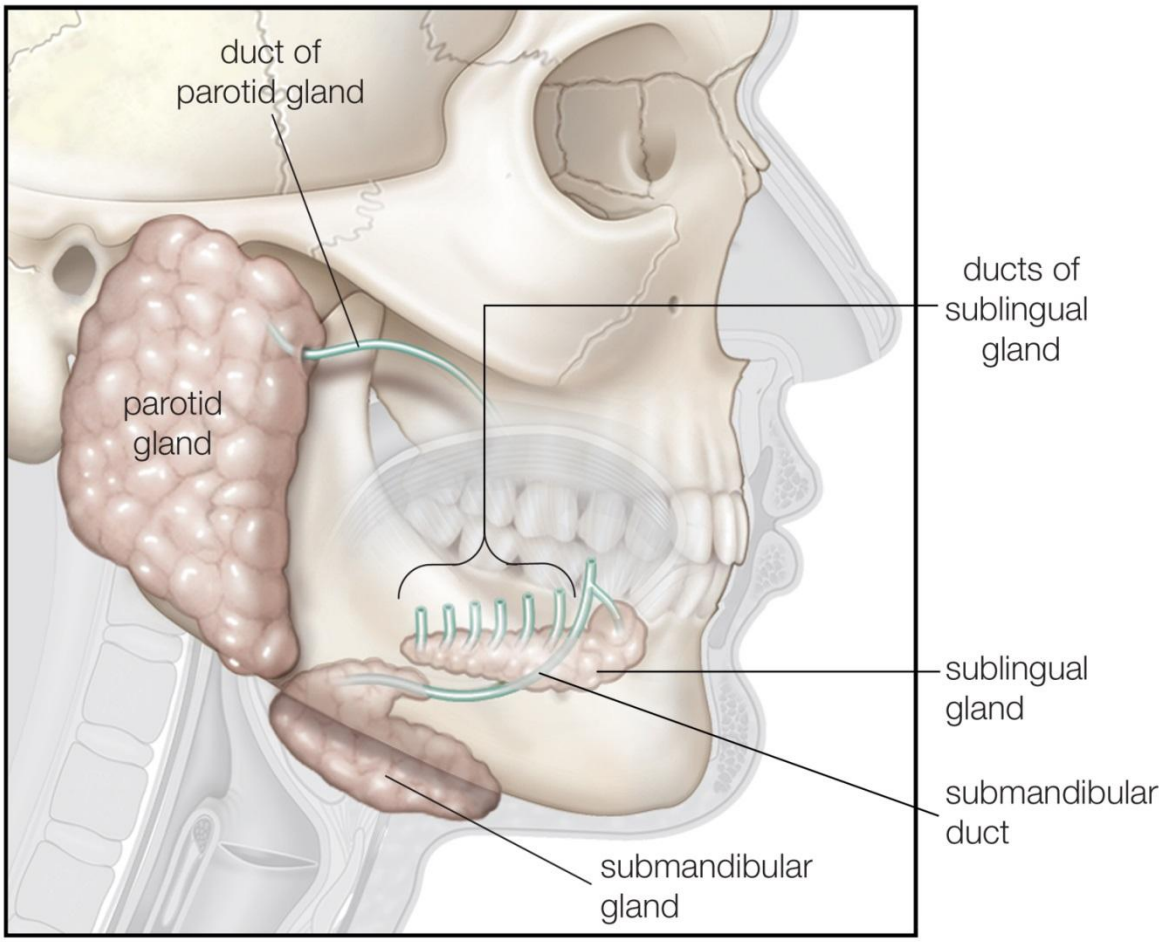

Fig. 1. Location of human parotid, submandibular and sublingual glands [67].

1. Different types of salivary glands

1.1. Parotid glands

The human parotid glands are the largest salivary glands. They contain serous acini. Their secretion is watery. Mature mouse and rat parotid glands myoepithelial cells surround only the intercalated duct, which is not the case in human parotid glands and most of other glands as well. The adipocytes are prominent in human parotid glands, which is not the case in rodent parotid glands [1, 110].

1.2. Submandibular glands

The human submandibular glands have essentially serous acini. There are also mucous acini with serous demilunes, so they are mixed glands. On the other hand, the rodent submandibular glands contain seromucous acini appearing serous with H & E staining and they are connected to a complex duct system. Mucin, glutamine/GRP, peroxidase and PRP are the contents of the acinar secretory granules. Serous demilunes can be easily found in human submandibular glands, whereas none can be observed in rodent submandibular glands [1, 110].

1.3. Sublingual glands

The sublingual glands of humans and rodents are mixed glands and contain mucous acini with serous demilune. Their secretion is mucous [1].

1.4. Minor salivary glands

There are also minor salivary glands:
-von Ebner’s glands of tongue (posterior dorsal and lateral)
-palate, base and lateral border of tongue
-lip, cheek, apex of tongue

No glands can be found in the labial mucosa, hard palate and ventral tongue of mice and rats [1].

2. Salivary gland cells and microstructures

In salivary glands, the acini produce the primary secretion which firstly pass through the intercalated duct, secondary through the striated duct and thirdly through the collecting (or excretory) duct. Myoepithelial cells surround the acini and intercalated ducts [1]. The ductal system resorbs sodium and chloride and when flow rate reduces their concentration diminish [8]. **Figure 2** shows the general structure of a salivary gland [76].

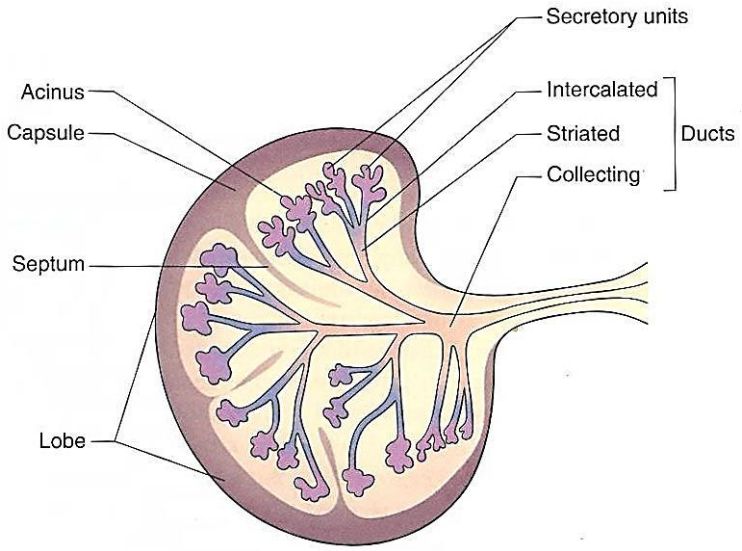

Fig. 2. General structure of a human salivary gland [76].

Acinus can be serous, mucous, or mixed. Serous cells secretion contains higher amount of proteins and lesser carbohydrates than mucous cells. These latter produce a viscous secretion rich in mucin. In mixed acini, the serous cells form a demilune surrounding the mucous cells (**fig. 3**) [76].

The cytoplasm of serous cells is rich in secretory products contained in zymogen granules. They include protein and glycoprotein, as well as ptyalin (amylase) or its intracellular precursor. The granules stain strongly with basic dyes and mask details of the cells in the light microscope. The cell nucleus is large and has round shape. Despite the fact that it can be found near the base, it is not flattened (**fig. 3**). The cytoplasm of serous cells is also rich in granular endoplasmic reticulum and Golgi apparatus [77].

Large pale-staining droplets can be found within mucous cells cytoplasm. They are so closely packed that there is almost no intervening cytoplasm. As it is difficult to maintain these droplets structure in a stained preparation, they often look like soap bubbles (**fig. 3**). The droplets contain a higher amount of highly glycosylated proteins compared to those of serous cells. The nucleus is commonly found near the basal border of the cell, so it is frequently flattened and curved. The cytoplasm, which contains granular endoplasmic reticulum and a big Golgi apparatus, is just a rim at the base and the sides of the cell as droplets occupy a big portion of the cell [77].

Myoepithelial cells clasp acini with their cytoplasmic extensions. Their cytoplasm is full of fibrils similar to those of smooth muscle cells. These cells probably help acini secreting primary secretion by contracting [77].

In intercalated duct cells, nuclei are prominent because the cytoplasm is rather scanty. Their luminal and basal surfaces are smooth. In their cytoplasm, apical secretory granules can occasionally be found, and few organelles involved in protein production can also be observed (**fig. 3**) [76].

In striated duct cells, the volume of cytoplasm is important, and their nuclei are big and located at the centre (**fig. 3**). These cells are strongly polarized, as short microvilli can be observed at their luminal surfaces, whereas the basal surface has many striations. Between the infoldings, numerous mitochondria are located. This structure is not surprising as the striated ducts are known to resorb electrolytes, especially sodium and chloride. That requires a large surface area and a high amount of energy provided by the mitochondria. Therefore the fluid which was initially isotonic becomes hypotonic after passing in striated duct. Besides, tiny secretory granules containing epidermal growth factor, lysozyme, kallikrein and secretory IgA can be found on the luminal side of striated duct cells. These granules are not numerous in humans and they are seldom found in parotid gland than in submandibular gland [76].

Concerning the collecting duct, its role is to transport saliva, whereas intercalated and striated ducts modify saliva composition and transport it too (so they can be called secretory ducts) [76].

Besides, sublingual glands often lack striated ducts and acini are frequently connected to collecting ducts. Minor salivary glands generally lack both intercalated and striated ducts. Therefore, these glands produce a saliva rich in sodium [76].

In rodent submandibular gland, the granular convoluted tubule (or granular duct) can be found between the intercalated duct and the striated duct. It is mainly made up of high-columnar secretory cells. Pillar cells cans also be seen sandwiched between the

main granular convoluted tubule cells. The granular convoluted tubule is known to produce many polypeptides, hormones and cell growth factors such as EGF, NGF, BDNF, HGF, IGF-1, TGF-α and β. The pillar cells produce FGF2. These factors are certainly secreted into the saliva and pass through the upper digestive tract. Besides, granular convoluted tubules are more frequently found in male than in female rodents. It is due to the fact that testosterone favours their apparition [101].

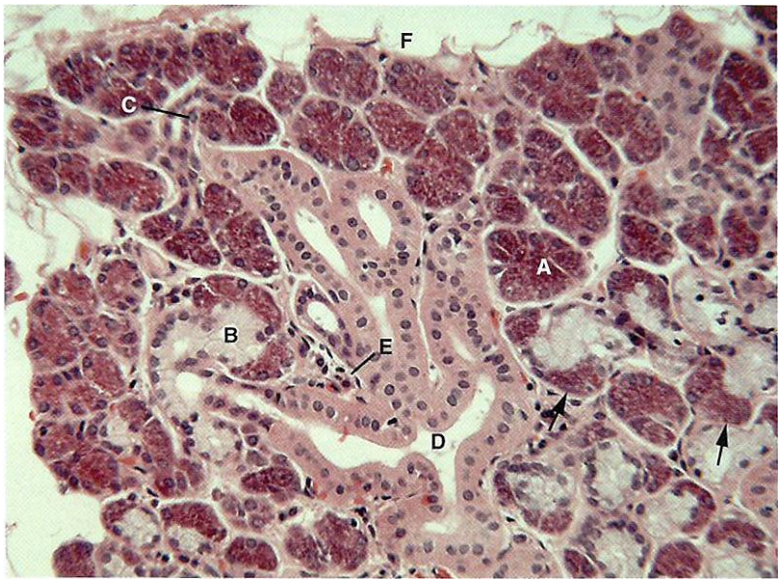

Fig. 3. Human submandibular gland showing serous acini (A), mucous acini (B), serous demilunes (arrows), intercalated duct (C), and striated duct (D). Plasma cells (E), and fat cells (F) can also be observed [76].

Concerning salivary gland stem/progenitor cells, they are not clearly identified at the moment. However, it seems that they are located in ducts. Indeed, after ligation of salivary glands, many acinar cells undergo apoptosis, whereas intercalated and excretory duct cells proliferate. After deligation, glands quickly regenerate as the number of acinar cells promptly increases. Most of the new acinar cells were originally ductal cells, but a small portion of these new cells comes from residual acinar cells mitosis [93, 94]. Nonetheless, Aure et al. ligation experiment showed that the new acinar cells were mainly formed from residual acinar cells mitosis instead of progenitor/stem cells [95]. Therefore it is not clear which type of cell is essential to promote salivary gland regeneration.

3. Innervation

Acinar, duct, and myoepithelial cells are generously supplied with parasympathetic nerves. Nonetheless the sympathetic innervation intensity is not the same between the glands. Human parotid glands are supplied with lesser sympathetic nerves than submandibular glands, and the labial glands have probably no sympathetic secretory innervation. Parasympathetic innervation is involved in strong saliva secretion, while sparse saliva flow is due to sympathetic innervation. Protein secretion is favoured by both parasympathetic and sympathetic innervation. These two autonomic nerves are activated by gustatory reflexes, while parasympathetic innervation is mainly involved in masticatory reflexes. Protein concentration is low in parasympathetic stimulated saliva because of the stronger saliva flow. If the secretory cells are innervated by parasympathetic and sympathetic nerves, they both interact synergistically regarding to the response. Parasympathetic stimulation favours vasodilation, increasing the glandular blood flow up to 20-fold, supplying the water required for saliva secretion [78].

4. Aquaporins

Aquaporins are water channels which can be found in both animals and plants. These are hydrophobic transmembrane proteins of roughly 270 amino acids. They are monomers weighing ~30 kDa. They are made up of six transmembrane helices, three extracellular and two intracellular loops (**fig. 4**). Two repeating Asn–Pro–Ala (NPA) sequences, which are the signature amino acid sequence motifs, are localized in the first intracellular and the third extracellular loop (**fig. 4)**. These two loops combine in the centre of the lipid bilayer creating a hydrophilic pore allowing the water passage through the lipid bilayer. AQP1 forms tetramers (thus, containing four water channels) in the cytoplasmic membrane [79].

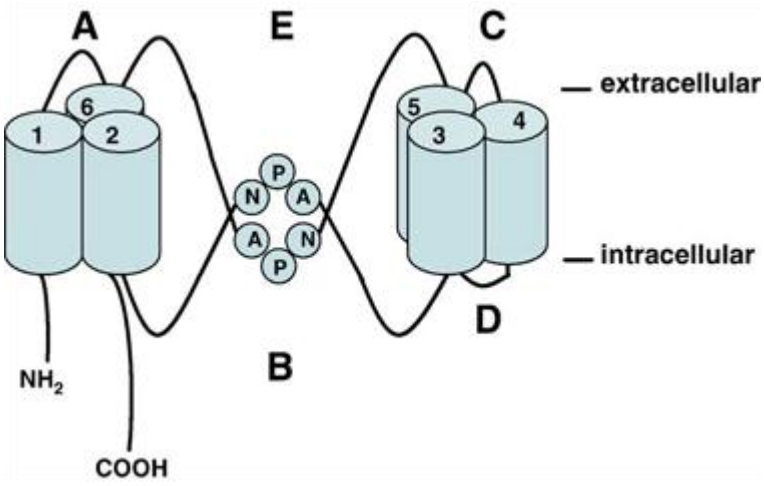

Fig. 4. Hourglass model of AQP1. AQP1 consists of six transmembrane domains, three extracellular and two intracellular loops. The aqueous pore is formed by B and E loops [79].

Concerning AQP5 which interests us the most, **fig. 5** shows the recent proposed structure of human AQP5 [82].

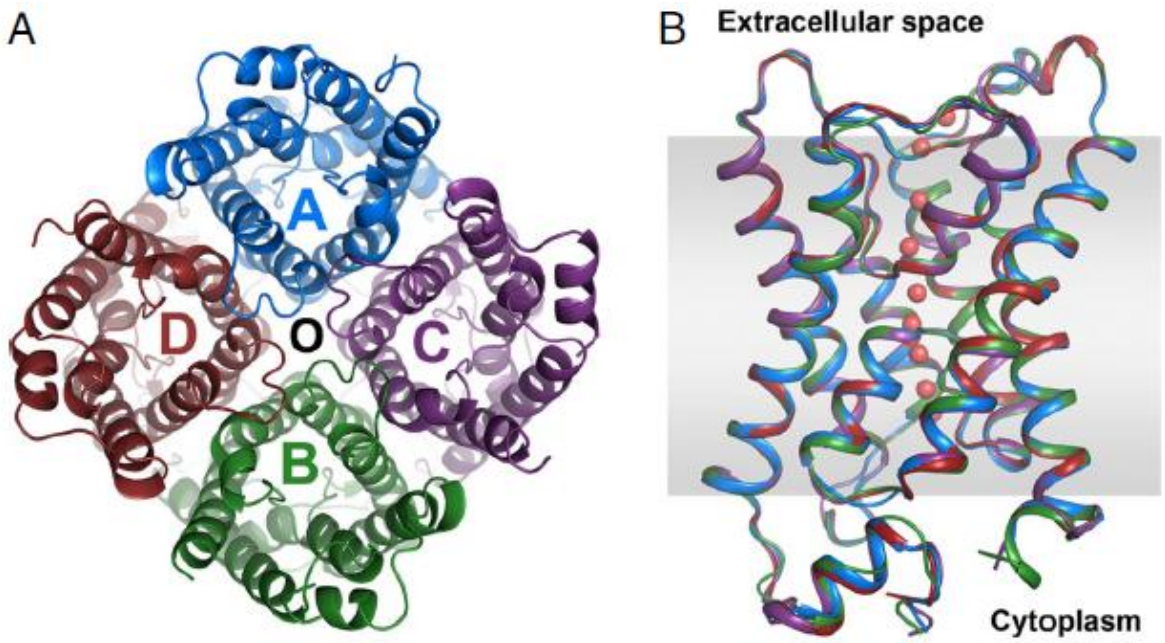

Fig. 5. Human AQP5. **(A)** Top view of the tetramer from the cytoplasm along the membrane normal. The protomers A, B, C, D are presented in blue, green, purple, and red, respectively. The water channel in each protomer is labelled A, B, C, and D. O represents the hypothetical central pore. **(B)** Side view of a structural overlay of all four protomers parallel to the membrane, with the same color scheme as in **A**. Waters for protomer A and the approximate membrane are presented (red spheres and gray shading) [82].

AQP0, AQP1, AQP2, AQP4, AQP5, AQP6, and AQP8 are permeable to water, but AQP3, AQP7, AQP9 and AQP10 can transport glycerol and small solute as well.

$HgCl_2$, which is a mercurial-sulfhydral-reactive compound, is known to inhibit many aquaporins [79].

Many types of aquaporins are expressed in salivary glands. In human glands, capillaries and myoepithelial cells of all salivary glands possess AQP1. AQP3 is localised at the basolateral membrane of serous and mucous acinar cells in all salivary glands. Ductal cells do not express it. Concerning AQP4, although its mRNA can be detected in all salivary glands, its protein has not been detected yet. AQP5 is expressed to the apical membrane of serous acinar cells in all salivary glands. It cannot be found in ductal and mucous acinar cells. Concerning AQP6 and AQP7, their mRNA can be detected in submandibular gland [80].

In mouse glands, AQP1, AQP3, AQP4, AQP5 mRNA and proteins are expressed, whereas only mRNA is expressed for AQP8 [81].

AQP5 is the main water channel allowing saliva secretion (**fig. 6**). Indeed, AQP5 knock-out mice showed a 60 % decrease saliva flow (stimulation with pilocarpine) and the saliva was more viscous and hypertonic, whereas AQP1, AQP4 and AQP8 knock-out mice did not show saliva flow modification [80].

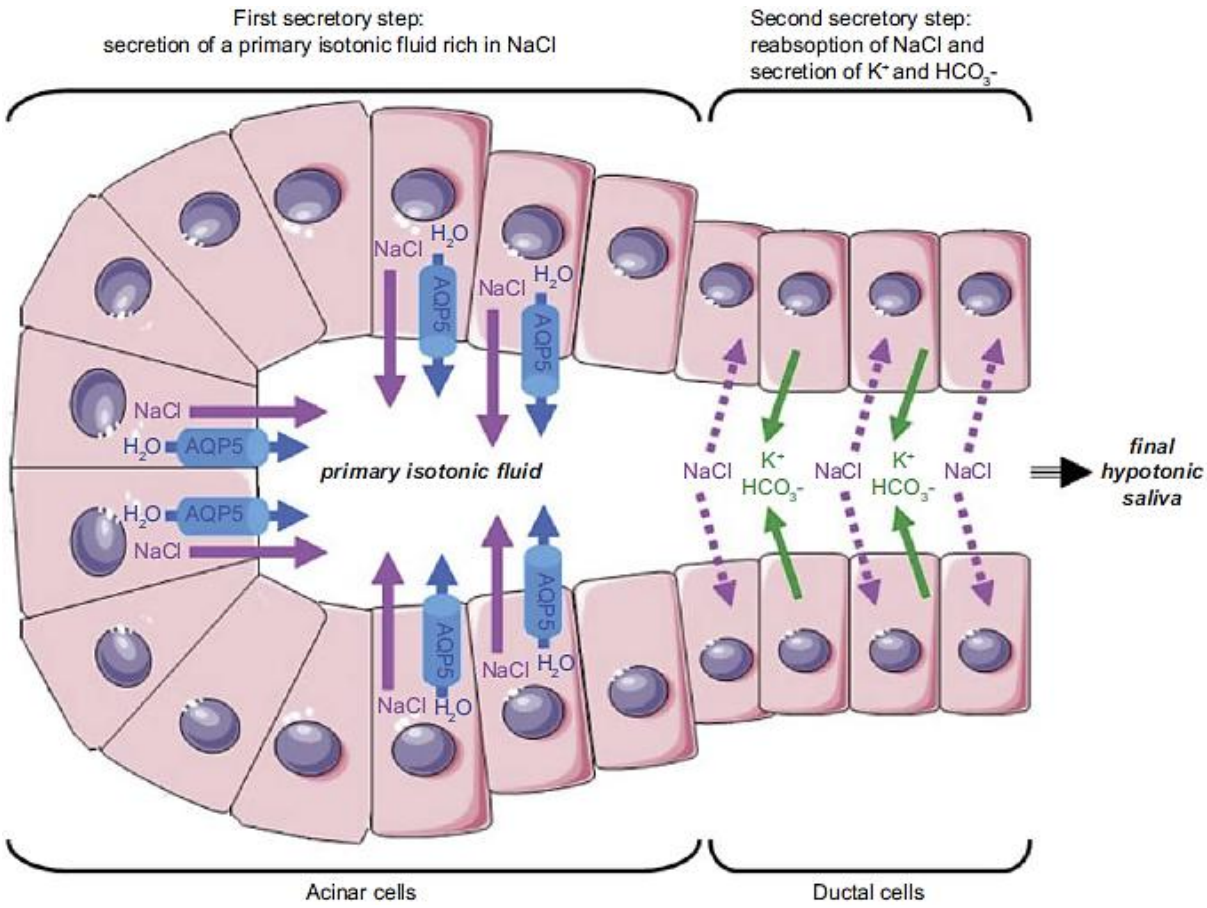

Fig. 6. Molecular mechanisms of saliva secretion. A primary isotonic fluid containing NaCl is secreted by acinar cells. Ions accumulation in the acinar lumen creates a trans-epithelial osmotic gradient generating a water flow via apical AQP5 and maybe paracellular pathways. Then this isotonic fluid passes through the ductal lumen. The ductal cells, which are rather impermeable to water, reabsorb NaCl and secrete K^+ and CO_3^- [80].

Besides, LPS, which is the main constituent of the outer envelope of Gram negative bacteria, was shown to decrease mRNA and protein level of AQP5 in mice, possibly via cross-coupling of NF-κB and p-c-Jun/c-Fos [85].

5. Saliva

Human salivary glands excrete 1 to 1.5L/day saliva. Individual glands contribution to the total volume of saliva differs depending on whether they are stimulated or not (**table 1**) [86].

	submandibular	parotid	sublingual
rest	71%	25%	4%
stimulation	63%	34%	3%

Table 1. Contribution of each gland to the total saliva volume before and after stimulation [86].

Saliva helps mastication and swallowing food. It aids for speaking too. It contains water but also mucins and other glycoproteins. There are also electrolytes like bicarbonate, calcium, chloride, fluoride, magnesium, phosphate, potassium and sodium which furnish the pH and mineral reservoir that maintains homeostasis of tooth structure. They decrease chemical erosion and dental caries. Some salivary proteins, like mucins and statherin, favour this function by transporting minerals in a supersaturated state, although it can create dental calculus [1].

At rest, saliva is hypotonic with a sodium concentration of less than 5 mEq/L (5 mmol/L) and potassium concentration of about 30 mEq/L (30 mmol/L). Following stimulation, the concentration of potassium declines, whereas sodium concentration rises toward the plasma concentration. Their concentrations increase after stimulation. Stimulation modifies the pH too: at rest, the pH is less than the blood pH, whereas it may be slightly greater than blood pH (7.8) after stimulation [86].

5.1. Salivary proteins

Saliva contains enzyme like α-amylase and ribonucleases which not only begin digestion but also help in washing the oral mucosa and teeth of food debris. There are also salivary peroxidase, agglutinins, cystatins, defensins, histatins, lysozyme, proline-rich proteins, and secretory immunoglobulins which protect against ingested poisonous substances and infection by microorganisms. Proline-rich proteins (PRP) are produced and are stocked in the secretory granules of the serous acini of human parotid and submandibular glands, but in the rat glands their concentration are low. However, they can be induced by dietary tannins or strong β-adrenergic stimulation like injection of isoproterenol [1].

5.2. Salivary mucins

Mucins are glycoproteins and are the main organic constituents of mucus. They generally contain more than 50% carbohydrate in the form of neutral and acidic oligosaccharides chains O-glycosidically linked to threonine and/or serine. Within these units, galactose, N-acetylgalactosamine, N-acetylglucosamine, and sialic acids can be found. Sometimes sulfate can be covalently attached to galactose or N-acetylglucosamine. Mucin peptides contain 30 to 40% serine and threonine, and high level of proline, glutamic acid, glycine and alanine [87].

Mucins can be classified by their molecular weights: high molecular mucins with a molecular weight greater than 1000 kDa, and low molecular mucins weighing 200 to 300 kDa. Human salivary mucins contain roughly 30% high molecular weight form and up to 70% low molecular form [88].

Several types of mucins were identified in human: MUC1, MUC2, MUC3, and so on. They can be separated into two groups: secreted soluble mucins (MUC2, MUC5AC, MUC5B, MUC6, MUC7) and membrane-associated mucins (MUC1, MUC3, MUC4, MUC12). Except the small monomeric MUC7, all secreted soluble mucins form disulphide-linked multimer weighing more than 20-40 million Daltons, so they are gel-forming mucins. On the other hand, membrane associated proteins are monomeric [89]. Among the membrane-associated mucins, MUC1 is probably the most important. It favours pellicle and mucus layer formation, and seems to be involved in signal transduction in the immune system function. Concerning secreted salivary mucins, MUC5B and MUC7 are the most important. MUC5B binds to enamel, which is vital to maintain the oral mucosa. It can also form a gel which acts as a barrier against pathogens. MUC7 improves pellicle immune functions by creating a complex with sIgA and lactoferrin [90].

In saliva, mucins are mostly provided by minor salivary glands (up to 70% of the total mucin). Submandibular and sublingual glands are also involved in mucins production [87].

A decrease of mucin production can drive to xerostomia (dry mouth), ulceration, deglutition problem, dental caries, and non-oral infections such as candidosis. Mucins are essential for the nonimmune protection of the oral cavity. By covering epithelial surfaces, they ensure lubrication, maintain moisture and protect against external insult. They can also favour adherence and proliferation of some microorganisms while they eliminate others by aggregation [87, 88].

II. IRRADIATION EFFECTS ON SALIVARY GLANDS

Each year, more than 500,000 patients develop head and neck cancer worldwide [2]. Radiation therapy damages the salivary glands and leads to a decrease of saliva production and its quality [1].

Many serous acini undergo degeneration and cell death after moderate IR such as 34 Gy [4]. Mild doses of IR (6 to 16 Gy) inflict minor damage, resulting in an efficient regeneration of acini. After heavy doses of IR (more than 60 Gy), most of the serous acini of the parotid gland perish and regeneration is almost impossible. The mucous acini of the sublingual and submandibular glands are less damaged. Ductal cells near acini seem to regenerate acini by differentiating into acinar cells. **Figures 7 and 8** show the effects of moderate IR to a rat submandibular gland and strong IR to a human submandibular gland respectively [1].

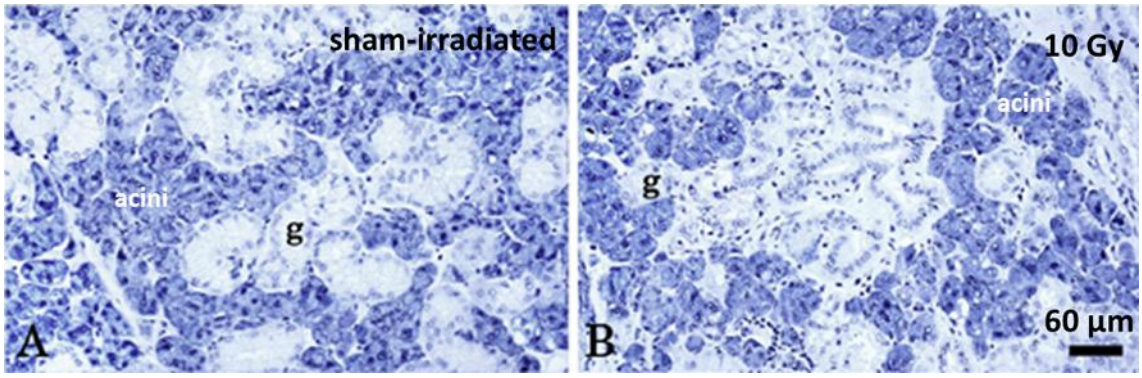

Fig. 7. Male rat submandibular glands at age 10 months. A) Sham-irradiated gland. Acini (blue secretory granules) are tightly spaced in large clusters, several and big granular convoluted tubules (g) can be seen, and the stroma is dense only around the bigger ducts. B) Gland eight months following 10 Gy irradiation. Acini and glandular convoluted tubules are less numerous. Stroma is more predominant, and the granular convoluted tubules became smaller, compared to A). Alcian blue and hematoxylin [1].

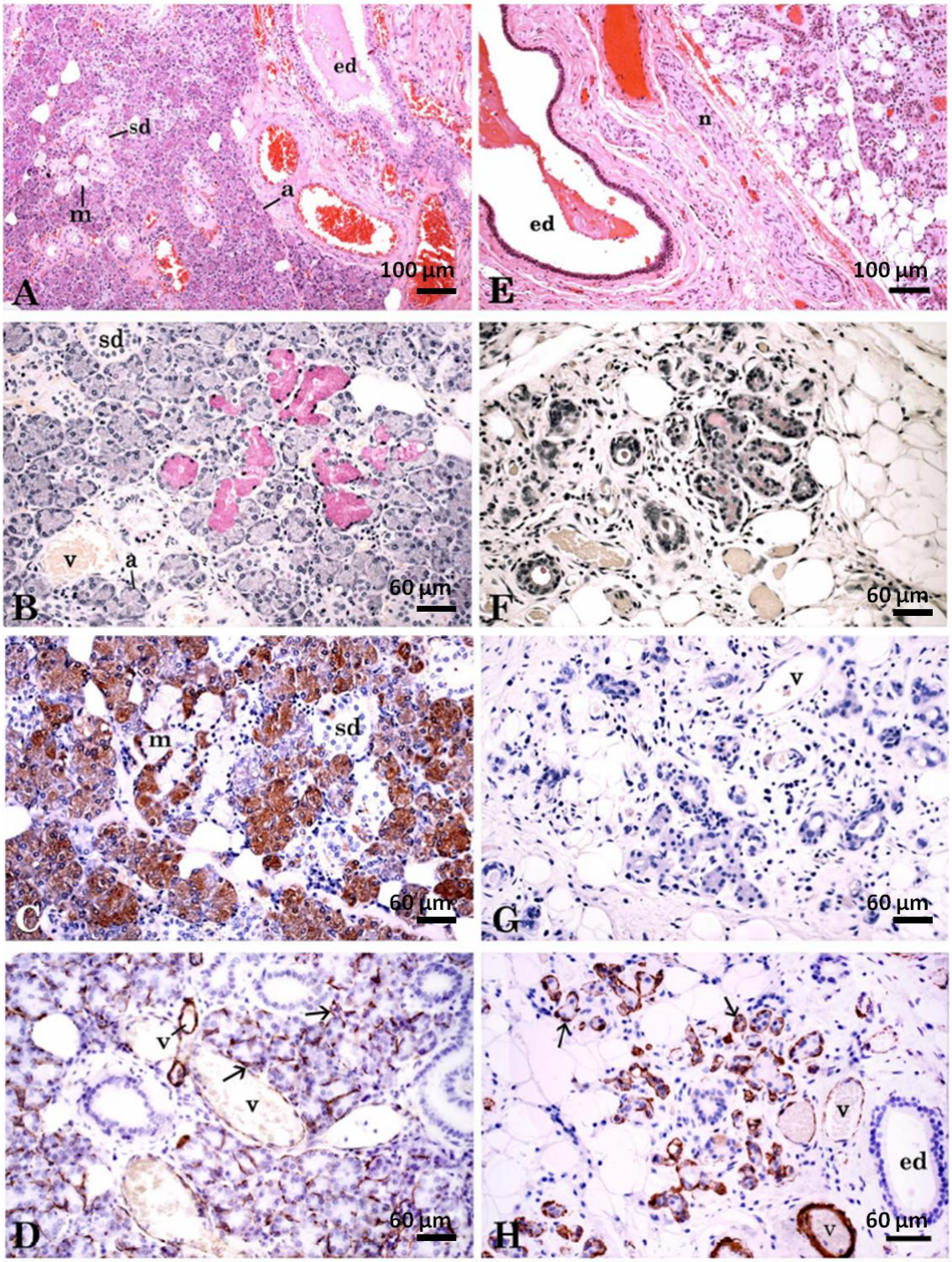

Fig. 8. Human submandibular glands. A-D) Non-irradiated gland. E-H) Gland extracted from a man 4 weeks after receiving 70.34 Gy irradiation in fractionated doses. In the non-irradiated gland, serous acini have abundant secretory granules staining darkly with H & E (A), grey with mucicarmine (B), blank with anti-SMA (D), and brown with anti-amylase (C). Secretion product in mucous acini appears magenta with mucicarmine (B), whereas myoepithelial cells (arrows) and smooth muscle in blood vessels appear brown with anti-SMA (D). In the irradiated gland, serous acini are not identifiable as such. The number, the size, and the coloring intensity with mucicarmine of mucous acini are decreased (F). Columnar cell size of ducts is decreased too, and the adipocytes (big, unfilled cells) and stroma occupy are more abundant. Large nerves seem to be unharmed (E). Labels: a, serous acini; ed, excretory ducts; m, mucous acini; n, large nerves; sd, striated ducts; v, blood vessels; H & E (A, E), mucicarmine (B, F) and immunohistochemical localization (peroxidase-DAB-H_2O_2 reaction) of α-amylase (C, G) and SMA (D, H), counterstained with hematoxylin [1].

In the secretory proteins of serous cells, transition metal ions can be found such as copper, iron, manganese and zinc. These metals are known to generate free radicals under irradiation, so it could explain serous cells vulnerability [3, 5]. More precisely, ROS production leads to lipid peroxidation driving release of proteolytic enzymes packed into granules, thus lysing cells [195]. It was demonstrated that administration of secretagogues before irradiation decreased acinar cells damages in rat parotid glands (no beneficial effect on submandibular glands) [6, 7].

Irradiation also damages nerves, blood vessels and stroma. Chomette et al. [9] noticed permanent damage in secretory nerve endings of rat submandibular gland through 70 days after IR (20 to 30 Gy). This damage led to stimulation arrest, thus contributing to the cycle of regeneration, congestion with secretory granules, and acinar cells death noticed during the 70 days after IR.

Ducts are harmed by IR as well [3, 10]. Their lowered function is obvious in elevated sodium and chloride concentration in stimulated saliva [11].

In rat salivary gland, stromal fibrosis was noticed after strong dose IR [4]. The blood vessel endothelium is radiosensitive and disturbed blood supply has been noticed after ^{131}I treatment for thyroid cancer [10]. These stromal modifications may decrease nutrients, minerals and oxygen transport to parenchymal cells, and thus may disturb regeneration and function by remaining acinar cells [1].

Irradiation is known to decrease the expression of AQP5, and thus, saliva flow. In mouse submandibular glands, after 15 Gy irradiation, both APQ5 fluorescence intensity and AQP5 mRNA expression decreased [83]. In rat submandibular glands, similar results were found after 15 Gy irradiation. The protein level of AQP5 was around 60% of those of control glands 3 days after irradiation, and 44% 30 days irradiation. Concerning the mRNA level, there was a 19% decrease on day 3 and 34% on day 30 [84]. Araujo et al. noticed that in rat submandibular gland, even a moderate dose such as 7.5 Gy could downregulate AQP5 expression and AQP1 as well. They hypothesised that the slight increase of ductal lumen was due to a decrease of water resorption caused by downregulation of AQP5 in intercalated duct cells and AQP1 in the blood vessel endothelium [196].

Aurophagy and mTOR are activated [47, 48], and cellular senescence is upregulated [126] following irradiation. mTOR activation seems to be detrimental, as well as senescence. Details can be seen in **2. Radiation activates first autophagy then mTOR** page 49 and **6. Molecular therapy** page 55 respectively.

The irradiation induced bystander effect could also be a factor which favours salivary gland cell damages, as it was demonstrated in many cell lines that the co-culture of non-irradiated and irradiated cells led to an increase of DNA damage in non-irradiated cells [121].

Previous studies on rats have shown that there are not one but two phases in salivary gland damage. The first phase is the acute phase (day 0 to 60) in which a 50% decrease of saliva flow rate, a glandular shrinkage and a decline of acinar cells can be observed. Water and protein composition of saliva are also altered. The second phase is the chronic phase (day 60 to 240) in which saliva flow is only 30% of control value while no change occurs in cell number and protein composition from acute phase [197]. During chronic phase an increase of fibrosis and dental caries, a decrease of parenchymal cells, blood vessel damage xerostomia, chronic inflammation and mucositis can be observed as well [8, 48]. On the other hand, Coppes et al. described four phases in rat parotid glands. The first phase (day 0 to 10) where a quick decrease of saliva flow occurs but no changes can be noticed in amylase secretion and acinar cell number, the second phase (day 10 to 60) during which amylase secretion and acinar cell number decrease, the third phase (day 60 to 120) where no variation can be observed in amylase secretion and acinar cell number, and the fourth phase (day 120 to 240) characterized by a further dysfunction of salivary gland and a multiplication of acinar cells with aberrant morphology [6]. According to Li et al., parotid glands of patients receiving moderate doses such as <25 Gy can recover 1 year after irradiation, and surprisingly stimulated saliva flow is stronger than pretreatment value at 18 months and 2 years. Concerning non-stimulated saliva flow, the value for 25 Gy was 86% of pretreatment at 2 years. At dose >30 Gy, stimulated and non-stimulated saliva flow do not return to the pretreatment value even after 2 years [198].

The parotid gland is particularly sensitive since many studies noticed an over 50% decrease in its function few days following irradiation at low doses [197]. This sensitivity is due to the fact that this gland contains mainly the most radiosensitive serous cells. The sublingual gland, containing mostly mucous cells, is the most radioresistant. Concerning the submandibular gland, which is a mixed gland, its radiosensitivity is intermediate [3].

III. RODENT STEM CELL IRRADIATION

1. Irradiation effects on bone marrow stem cells

The radiosensitivity of multipotent progenitor cells varies depending on cell type. Bone marrow multipotent progenitor cells such as CFU-Mix, CFU-GEMM and progenitors for granulocytes and monocytes resist well whereas pluripotent and self-renewal hematopoietic stem cells CFU-S-10 (spleen), BFU-E, and CFU-E (erythroid) are sensitive. The most resistant seems to be CFU-F (fibroblast). Besides, after IR, CFU-Mix, BFU-E and CFU-S-10 cells do not recover totally and the recovery speed is low. On the other hand, CFU-E recovering speed is high. Concerning CFU-C and CFU-F, their decrease is slower and they recover totally 10 to 14 days after IR. Besides, the more the stem cell is primitive, the more it is resistant. However, in mouse fetal spleen, CFU-S-8 which is relatively mature is more resistant than the more primitive CFU-S-12. Therefore, sensitivity of adult mice cells is not the same as fetal ones [12].

According to Wang et al. [13], IR promotes senescence in murine hematopoietic stem cells. They noticed an increase in cellular senescence markers such as $p16^{Ink4a}$ and senescence-associated β-galactosidase in LKS^{+} hematopoietic stem cells. They hypothesized that senescence could be a way to repair damages.

The long-term effect of IR depends on mouse age. After single dose irradiation of 7 Gy, a strong decrease of CFU-S, CFU-GM, and BFU-E at around 30% of normal level occurs during the first year in adult mice (12-week-old). CFU-GM and BFU-E lightly recover, around 60% of normal level, 20 months after IR. On the other hand, 8-day-old mice recover more efficiently, as one year after IR, CFU-S and BFU-E reach normal level. Therefore, young mice have a much efficient capacity to repair damages [14].

Concerning the DNA, the level of γ-H2AX foci (marker of DNA double strand break) stays high one year after 7 Gy IR in bone marrow stem cells, whereas no such a thing is noticed in control mice. The repair capacity of young mice (4-month-old) are stronger than old mice (16-month-old), as 24 hours after 1 Gy irradiation, there are more γ-H2AX foci in old mice stem cells than in young mice one. Besides, it seems that there is no difference in the DNA repair capacity between mice pre-irradiated at 7 Gy and non-pre-irradiated one [15].

DNA damage accumulation also occurs in LKS^+, which could be due to a lack of DDR [16]. IR also induces a permanent rising in ROS in hematopoietic stem cells, which could partly explain the continuing damage of DNA [17]. After 3 Gy IR, surviving stem cells division can increase more than 10 times than control cells. This increase allows maintaining hematopoiesis, but accelerates ageing as well [18].

2. Irradiation effects on intestinal stem cells

Small intestine contains many types of stem cells: LG5, BMI1, and mTERT. At the moment, only LG5 cells reaction seems to have been tested. In vitro experiments showed that irradiating single crypt cell decreased the formation of organoids if the dose is ≥ 1 Gy, and organoids were less numerous when the dose was stronger: 45, 20 and 4% of that of the control at 1, 2, and 3 Gy respectively. Surprisingly, irradiation increased organoid size, which means that proliferation capacity was upregulated by IR [19].

3. Irradiation effects on NSPCs (neural stem and progenitor cells)

The NSPCs are very sensitive to IR. According to Li et al. [20] who irradiated mice at 8 Gy, 2 days after irradiation, caspase-1 and IL-1β expressions were significantly elevated, which led to a cellular senescence. The p16-pRB pathway was also involved in cell senescence, as in senescent cells, p16 expression was strong, whereas pRB expression was weak. Inhibition of caspase-1 reduced p16 expression, whereas pRB expression increased. Therefore, IR promotes senescence of NSPCs by activating caspase-1.

Besides, Schneider et al. [21] noticed that in mice, IR (10 Gy) leads to astrocytic differentiation, not only of NSPCs, but of glioblastoma stem cells as well.

It is worth mentioning Semont et al. experiments on murine embryonic telencephalic cells [22]. Cells were irradiated at 2 Gy. 24 hours after, there was an increase in apoptosis and G1 cell cycle arrest too. Irradiation upregulated p53 and its downstream target $p21^{WAF1}$ as well. Cells lacking p53 had less apoptosis, which means that p53 is required for cell response to IR.

4. Irradiation effects on mesenchymal stem cells

According to Su et al. [25], murine mesenchymal stem cells are quite sensitive. They irradiated C3H10T1/2 cell at 4 Gy. The level of apoptosis increased 3 hours after IR, and then it peaked 12 hours after and returned to normal level 24 hours after. Cellular senescence was observed 72 hours after IR as several cells expressed senescence-associated β-galactosidase and their cycle stopped at G1 phase. There was also an up-regulation of Wnt3a (canonical) and especially Wnt5a (non-canonical). Therefore, senescence could require the non-canonical pathway.

5. Irradiation effects on epithelial stem cells

Mouse epithelial cells are rather sensitive as intestinal epithelial cells are strongly damaged with 9 Gy [49], and in lens epithelial cells (C57BL/6J strain) dose lower than 1 Gy is enough to induce DNA double strand breaks [50].

Concerning salivary epithelial stem cells, mainly localized in ductal structures [52], they are more radioresistant [51, 52], although irradiated stem cells produce less salispheres (cell clumps obtained by culturing salivary stem cells) [43]. However, irradiation can damage parasympathetic nerve which is required for regeneration [51].

IV. MTOR COMPLEXES

1. mTOR

mTOR is a serine/threonine protein kinase regulating growth, proliferation, motility, survival, protein synthesis and transcription [26]. Its carboxy-terminal region contains the kinase domain, the amino-terminal region includes 20 HEAT repeats domains, and the FAT C domain (**fig. 9**) [27].

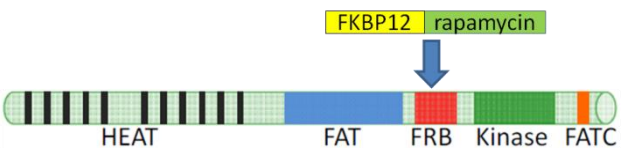

Fig. 9. Domain structure of mTOR [27 modified].

mTOR activity is regulated by insulin, growth factors (like IGF-1 and IGF-2) and amino acids. It also functions as nutrient, oxygen and energy levels sensor [29]. Rapamycin is a well-known inhibitor. It binds to FKBP12 and this complex inhibits mTOR by binding to its FRB domain (**fig. 9**) [30].

2. Complexes

mTOR is the catalytic subunit of mTORC1 and mTORC2 [31]. mTORC1 is a complex formed with mTOR, raptor, GβL/mLst8, PRAS40 and DEPTOR. mTORC2 is made of mTOR, rictor, GβL/mLst8, sin 1, PRR5/protor and DEPTOR (**fig. 10**) [26].

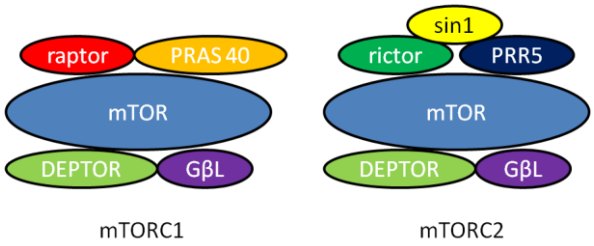

Fig. 10. mTORC1 & mTORC2 composition.

2.1. mTORC1

It senses nutrient, energy and redox levels, and controls protein synthesis. Its role is to activate translation of proteins [31, 32, 33, 34].

2.1.1. Role in autophagy and cell growth

Amino acids, particularly leucine controls mTOR activity. Amino acid signalling is transmitted mostly by Rag GTPases and MAP4K3 [26].

SLC family proteins localised at the plasma membrane are involved in amino acids influx and efflux. L-glutamine influx is ensured by SLC1A5. Concerning leucine influx, it is carried out by SLC7A5/SLC3A2 which simultaneously expels L-glutamine. mTORC1 cannot be activated if SLC1A5 is inhibited (**fig. 11**) [35].

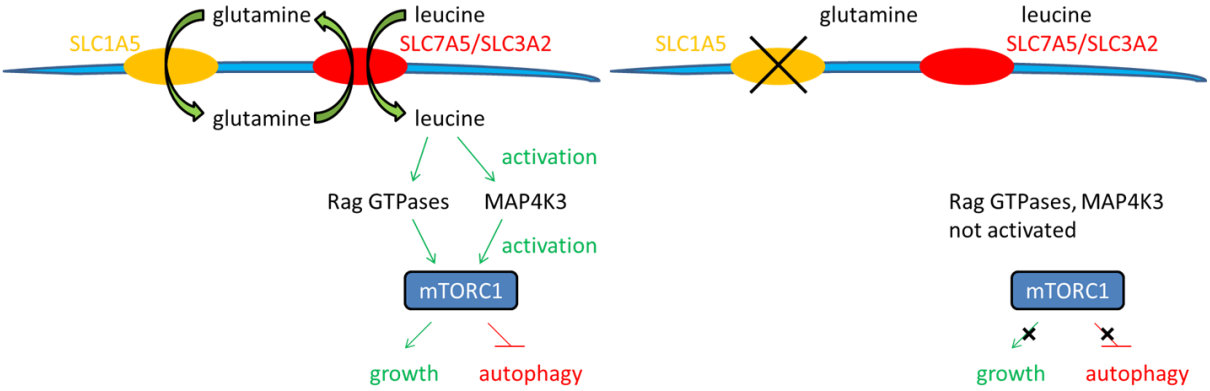

Fig. 11. Leucine signalling upstream of Rag GTPases and MAP4K3. On the left, thanks to SLC1A5 activity, leucine is transported into the cell, activating mTORC1 and promoting cell growth. On the right, inhibition of SLC1A5 stops leucine transport, promoting autophagy.

Glucose level controls cell growth as well. Lack of glucose decreases the ratio of ATP/AMP and activates AMPK which activity is increased by LKB1. AMPK activation inhibits mTORC1 directly (by phosphorylating raptor) or through phosphorylation of TSC2 (forms a complex with TSC1**)** [26, 189]. The lack of ATP and amino acid inhibits mTOR, even if growth factors such as insulin are available [36]. GAPDH is also sensitive to glucose level. If the latter is low, GAPDH inhibits Rheb activation of mTORC1. Therefore AMPK might monitor energy status and stress, while GAPDH might supervise the glucose metabolic status (**fig. 12**) [26].

Autophagy can be triggered by reduced growth factor signalling, the insulin/IGF-1-PI3K (class I)-Akt pathway which regulates mTORC1. The following regulators are implicated in this pathway: the positive regulators PDK1 and Rheb, the negative regulators PTEN and TSC2. TSC2 binds to TSC1 and the complex functions as a GAP for Rheb. This GAP activity is under the influence of the phosphorylation of TSC2 by Akt (**fig. 12**) [26].

Stresses can promote autophagy too. Hypoxia induces REDD1 and its related protein REDD2. REDD1 inhibits mTORC1 by activating the TSC1-TSC2 complex. REDD1 is also induced by ER stress (**fig. 12**). The inhibitory effects of ROS on the mitochondrial function might lead to the mitophagy (degradation of mitochondria by autophagy) and mTORC1 could be involved in this process. Autophagy induced by defective mitochondria could involve mTORC1 as it is localised near mitochondria, and oxidative stress and mitochondrial dysfunction inhibit it. Mitochondrial signal could directly control mTORC1 but the LKB1-AMPK-TSC1/2 branch could inhibit mTORC1 under oxidative stress [26].

Besides, it was recently demonstrated that trehalose favoured autophagy by inhibiting SLC2A leading to decreased glucose transport [39]. mTORC2 promotes growth by activating Akt (**fig. 12**) [26].

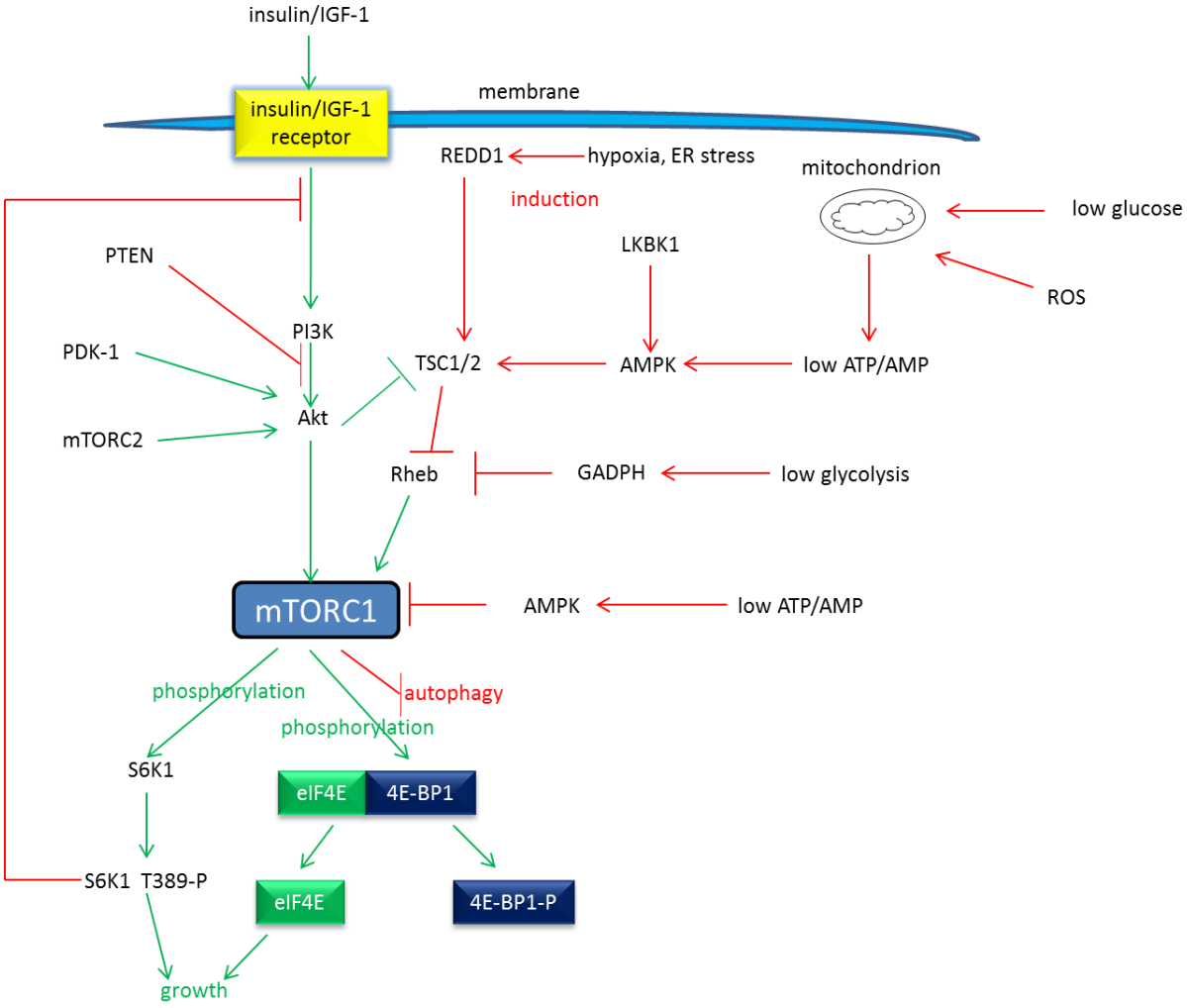

Fig. 12. Regulation of the mTOR pathway by glucose, stress and insulin/IGF-1.

It is worth mentioning that mTORC1 activity in senescent cells cannot be inhibited by serum and amino acid starvation. This is probably due to the fact that the basal autophagy in senescent cells is higher than in young cells, thus elevating the concentration of intracellular amino acids which allows mTORC1 to remain active under starvation. The depolarization of plasma membrane could also contribute to the persistent mTORC1 activity as restoration of plasma membrane potential favours starvation induced Akt inhibition and then mTORC1. It means that when growth factor sensing is restored, senescent cells become sensitive to amino-acid and serum starvation [118].

2.1.2. Feedback

The translation repressor 4E-BP1 inhibits 5'-cap-dependant mRNA translation by binding and neutralising eIF4E. The release of eIF4E by 4E-BP1 phosphorylation promotes initiation of translation. mTORC1 phosphorylates S6K1 at Thr389 as well. Active S6K1 increases ribosome biogenesis and translation elongation. Feedback from the mTORC1/S6K1 pathway inhibits growth factor signalling PI3K (**fig. 12**) [28].

2.2. mTORC2

It phosphorylates Akt/protein kinase B at a serine residue S473 [37, 38], facilitating Akt phosphorylation at a threonine T308 residue by PDK1. Then Akt is totally activated [38].

mTORC2 is regulated by insulin and nutrient levels. Chronic exposure to rapamycin inhibits free mTOR, preventing new mTORC2 synthesise [40]. Recently, it was demonstrated that ammonium, which is a metabolic waste, could activate mTORC2 at least in human breast cancer cells MCF-7 [119].

3. mTOR inhibitors

3.1. Rapamycin and rapalogs

Rapamycin is a well-known inhibitor of mTORC1 and also inhibits new mTORC2 synthesis. Rapalogs, such as temsirolimus, everolimus and deforolimus (or ridaforolimus), are rapamycin derivatives [41]. They bind to the same sites for mTOR and FKB12 [42]. However, since active mTORC1 inhibits the PI3K (class I)-Akt pathway, the use of rapamycin may enhance cancer cells survival by promoting this pathway [72]. Besides, it was shown that p53 and rapamycin had additive effects on mTORC1 inhibition [73].

3.2. mTOR catalytic inhibitors

These are ATP competitive inhibitors of mTOR and are effective on mTORC1 and mTORC2. Among them there are Torin 1, PP242, PP30, Ku-0063794, WAY-600,

WYE-687 and WYE-354. They have stronger effects on 4E-BP1 phosphorylation and autophagy than rapamycin. However, S6K1 feedback loop inhibition increases Akt phosphorylation at Thr308 through PDK1 signalling, leading to mTORC1 activation [27]. It is worth mentioning that recently Park et al. noticed that resveratrol could inhibit mTOR through ATP competition as well [114].

3.3. Dual specificity inhibitors

There are several dual specificity inhibitors: GNE477, NVP-BEZ235, PI-103, XL765, WJDOOS, LY294002, and BGT226. They deactivate PI3K (class I), mTORC1, mTORC2, Akt and PDK1, so they do not selectively inhibit mTOR [27]. Torin 1 and PP242, which are ATP-competitive kinase inhibitors, are also known to inhibit both mTORC1 and mTORC2 [71].

3.4. miRNAs (micro RNAs)

These RNAs represent a family of noncoding small, single-stranded RNA molecules (roughly 22 nucleotides in length). They post-transcriptionally controle gene expression by disrupting translation, suppressing the target mRNA expression and hindering translation to control multiple biological processes. They can interact with mTOR itself or with key genes within the mTOR pathway, such as IGF-receptor, PI3K, Akt and PTEN. In cancer, up-regulated miRNAs could function as oncogenes, whereas down-regulated miRNAs function as tumour-suppressors [27].

V. AUTOPHAGY

Autophagy (derives from the Greek and means self-eating) is a mechanism degrading bulk cytoplasmic contents, aberrant protein aggregates, and surplus or impaired organelles. Starvation activates it, but development, differentiation, neurodegenerative diseases, stress, infection, and cancer do it as well. mTOR activation abolishes autophagy, whereas its inhibition promotes it [46, 53, 54, 55].

There are many types of autophagy: macroautophagy which encompasses canonical and non-canonical autophagy, microautophagy and chaperone-mediated autophagy.

1. Macroautophagy

It is the main form of autophagy, and for that reason when the term “autophagy” is used, it refers to macroautophagy in general. It uses autophagosome to sequester and degrade materials, so it can be activated by either canonical or non-canonical autophagy [65].

1.1. Canonical autophagy

When mTORC1 is activated, it blocks ULK1 by phosphorylating it at Ser757, thus inhibiting autophagy [91]. During starvation, mTORC1 is inhibited by AMPK activation [23]. The latter activates ULK1 (serine/threonine kinase) by phosphorylating it at Ser467, Ser555, Thr574 and Ser637 [91]. Activated ULK1 phosphorylates and forms a complex with Atg13 and FIP200 at the beginning of autophagy [23]. The hVps34 PI3K complex, containing Beclin 1, Atg14 and hVps15 is also involved in the nucleation of phagophore. The autophagosome formation is controlled by Atg12 and LC3. LC3 is cleaved at its C-terminal arginine residue by Atg4 and becomes the cytosolic LC3-I. Then, the latter is conjugated to PE to become the lipidated LC3-II. This lipidation requires Atg3, Atg7 and the Atg12-Atg5-Atg16 complex (formed by Atg12, Atg5 and Atg16 binding) [23]. Then the autophagosome fuses with the lysosome becoming autolysosome and the content is degraded [65]. Since LC3-II is localized in the autophagosome, it is used as an evidence of autophagy activation [23]. However, an increase of LC3-II levels is not necessarily an evidence of autophagy activation as in human neuroblastoma SH-SY5Y cells, the administration of 3-methyladenine, which totally inhibits autophagy, does not prevent LC3-II accumulation in rapamycin and dopamine treated cells [64]. **Figure 13** summarizes canonical autophagy pathway.

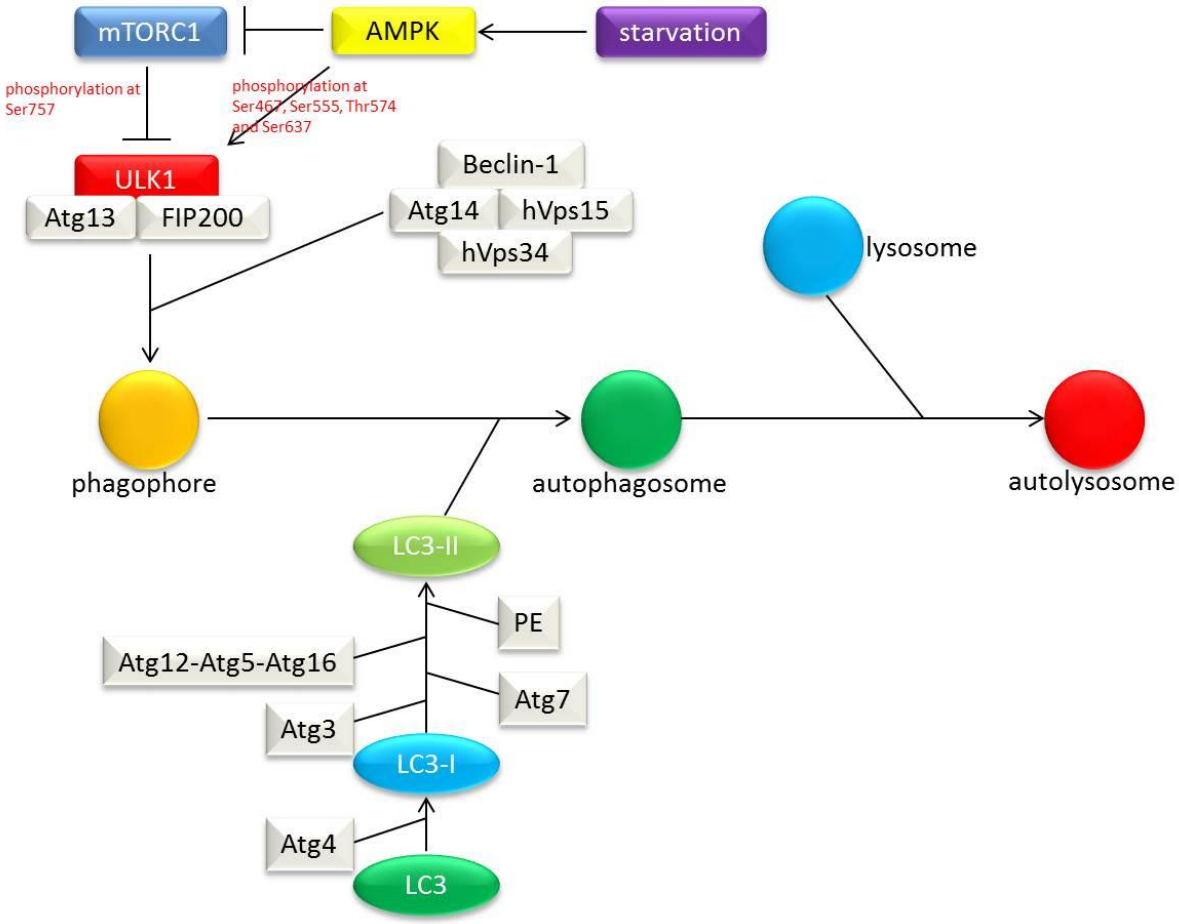

Fig. 13. Canonical autophagy pathway. mTORC1 activation blocks ULK1 by phosphorylating it at Ser757, thus inhibiting autophagy. Starvation activates AMPK which triggers autophagy by inhibiting mTORC1 and activating ULK1 by phosphorylating it at Ser467, Ser555, Thr574 and Ser637. This leads to the formation of autophagosome. The latter requires many Atg (4, 5, 7, 12 and 16). LC3 is also involved. Firstly, LC3 is cleaved at its C-terminal arginine residue to become the cytosolic LC3-I. Secondary, LC3-I is conjugated to PE and becomes LC3-II (lipidated) which is attached to the autophagosome membrane. Next the autophagosome fuses with the lysosome forming the autolysosome and its content is degraded.

ULK1 plays an important role as its inhibition by compounds such as MRT67307 blocks autophagy [56]. On the other hand, it was shown that autophagy could occur in ULK1 knock-out MEF and mice. The most likely reason is that ULK2, which shows more than 50% homology to ULK1, has redundant functions [57]. However, they have also different roles. In adipocytes, it was demonstrated that ULK1 knock-down blocked fatty-acid oxidation and favoured fatty acid absorption, while ULK2 knock-down effects were opposite [145].

It is worth mentioning that it was recently found that in Atg5 and Atg7 knockout mouse cells, phagosome maturation occurred, which means that Atg proteins are not always involved in this process [24]. It was also demonstrated that in 4E-BP1 knock-out

cells, no increase of LC3-II was observed when cells were starved or treated with rapamycin. Therefore non phosphorylated 4E-BP1 is involved in autophagy activation [69].

1.2. Non-canonical autophagy

This autophagic pathway has the following features [58]:
- it does not necessitate the hierarchical intervention of all of the Atg proteins to form the double-membraned autophagosome.
- the double membrane does not always elongate from a single source.
- a pre-existing membrane, different from the phagophore, can recruit a set of Atg proteins.

The exact mechanism leading to non-canonical autophagy is not fully understood. At the moment, it is known that administering pro-apoptotic compounds leads to Beclin 1 independent autophagy [58]. Trehalose, a well-known disaccharide which promotes non-canonical autophagy, inhibits SLC2A (solute carrier 2A), thus blocking glucose transport and activating ULK1 and AMPK [39]. Lithium, carbamazepine and valproic acid trigger autophagy by lowering inositol via the inositol signaling pathway. Verapamil, loperamide, amiodarone, nimodipine and nitrendipine, which are L-type calcium channel antagonists, activate the Ca^{2+}/calpain pathway, thus promoting autophagy [61]. It was shown that chemical inhibition of LRRK2 (leucine rich repeat kinase 2) favoured autophagy without modifying mTOR and ULK1 activity but required the activation of Beclin 1 containing class III PI3-kinase [63].

1.3. Roles

1.3.1. Adaptative metabolic response

Macroautophagy is the main pathway to produce amino acids in non-starved cells. When cells are starved, this production is increased. Lack of any nutrient favours autophagy. However nitrogen starvation in yeast and amino acid starvation in mammalian cells are the most efficient inducers. It is not surprising as autophagy

produces mainly amino acids from cellular proteins. If cells are provided enough amino acids, it reactivates mTOR, thus decreasing autophagy [65].

If yeast cells are incubated without nitrogen, autophagy-deficient cells show a quick decrease of intracellular amino acid levels and immediately die. Concerning mice, if they are Atg3, Atg5 or Atg7 KO, starvation leads to a rapid decrease of plasma and tissue amino acid levels and they promptly die. Therefore autophagy is an essential survival system during starvation [65].

Amino acids provided by autophagy can be used as an energy source, as amino acids are converted into intermediates of the Krebs cycle and ensure ATP synthesis. It was shown that in Ras expressing cancer cells, autophagy was essential to maintain Krebs cycle metabolites. It is noteworthy that citrate, isocitrate and aconitate, which are exclusively produced by mitochondria, are specifically decreased, which could mean that autophagy is vital to produce metabolites for Krebs cycle as well as for quality control for mitochondria [65].

In the liver, amino acids seem to be the main source for gluconeogenesis. Indeed, if Atg7 is knock-out in the liver of mice, one day starvation leads to a significant decrease of glucose and amino acids levels. Therefore amino acids produced by liver ensure gluconeogenesis and preservation of the plasma pool of amino acids [65].

Amino acids provided by autophagy are not solely used to produce energy. Indeed, in one day starved mice, if autophagy is strongly activated in most of its organs, their contents of lipids are not significantly reduced, even though glycogen could provide enough energy at least one day. Actually, autophagy produced amino acids can be used to synthesize proteins required for starvation adaptation. It is well known that starvation decreases protein synthesis. However some types of proteins are still anabolized and can even be strongly stimulated. Among these proteins, there are vacuolar/lysosomal enzymes, proteins of respiratory chain, antioxidant enzymes and proteins required for amino acids synthesis. In yeast, autophagy deficient cells cannot synthesise these proteins if they are starved. This leads to a loss of respiratory function and accumulation of stronger amount of reactive oxygen species, driving to a reduction of their mitochondrial DNA content. This phenomenon is certainly the main cause of rapid cell death observed when yeast cells are nitrogen starved [65].

1.3.2. The interdependence of apoptosis and autophagy

1.3.2.1. Autophagy inhibits apoptosis

In order to inhibit apoptosis, mitophagy can occur. This is not surprising as damaged mitochondria tend to strongly activate apoptosis, so their elimination is essential for cell survival. Inhibition of apoptosis can also be achieved by specifically eliminating pro-apoptotic proteins, such as active caspase 8, and SQSTM1 which can favour the synthesis of reactive oxygen species and cell death if it is overexpressed [68].

1.3.2.2. Apoptosis inhibits autophagy

Despite the fact that autophagy has protective effects, it can be overwhelmed if the stress is too strong or lasts too long. In that case, cells activate apoptosis in order to kill themselves. In general, when apoptosis occurs, caspases (apoptotic proteins) are strongly activated. The consequence is the digestion of many proteins, including autophagy proteins. This leads to the inhibition of autophagy, thus stopping cellular survival mechanism and accelerating cell death. Among the targeted proteins, there are Atg3 and Beclin 1. Their digestion neutralises their autophagy stimulating activity. Besides, AMBRA1, a protein regulating autophagy, is degraded by caspases and calpains (proteases). Mutant cells having AMBRA1 without the caspase 3 cleavage site are rather insensitive to apoptosis induction. Yet, the inhibition of caspase activity could be due to cleavage of site-mutated proteins into pseudo-substrates. Therefore it is difficult to interpret experiments in which the expression of a mutated protein is stronger than its endogenous equivalent. The resistance to apoptosis could be to the inhibition of caspase instead of lack of cleavage of target protein [68].

After having been cleaved by caspase, many autophagy protein fragments seem to favour apoptosis. When Beclin 1 is cleaved by caspase 3, caspase 6 or caspase 9, a carboxy-terminal fragment is produced (downstream of the BH3 domain). This fragment is found in mitochondria in cells, and favours cytochrome *c* release by permeabilizing isolated mitochondria *in vitro*. After having been cleaved by caspase 3, Atg4D becomes pro-apoptotic as well. It is also known that the calpain-mediated cleavage of Atg5 leads to the release of an amino-terminal fragment that translocates to

mitochondria and cells become more sensitive to apoptosis. This amino-terminal fragment also binds to BCL-X_L, blocking its anti-apoptotic function. From these data, it can be inferred that the increase of Atg4D, Atg5 and Beclin 1 expression, if it favours autophagy, can also produce protein precursors that, upon caspase activation, can stimulate apoptosis [68].

There is only one example of caspases regulation of autophagy. It is the degradation of BCLAF1 (BCL-2- associated transcription factor 1) by caspase 10. The latter helps the induction of apoptosis in response to TNF binding to death receptors. Yet, in multiple myeloma cells, caspase 10 degrades BCLAF1, thus preventing the formation of BCL-2-Beclin 1 complex. If caspase 10 is inactivated, it leads to an uncontrollable increase of autophagy that ends to apoptosis independent cell death [68].

1.3.2.3. Autophagy activates apoptosis

Autophagic cell death involves specific inhibition, depletion or deletion of different autophagy proteins and/or genes to cause cellular death. Apoptosis and necroptosis are not involved in this process. On the other hand, in many cases, autophagy induction favours apoptosis activation. Proteins having an important role in autophagy seem to take part in pro-apoptotic signalling. It is also necessary to mention that some Atg genes can be involved in cellular processes other than autophagy, such as endocytosis and protein secretion. Consequently, it is vital to differentiate the function of proteins and/or genes from the process [68].

It was demonstrated that the creation of the autophagosome was involved in caspase 8 activation after administration of SKI-I (pan-sphingosine kinase inhibitor) and bortezomib (protease inhibitor) to cells. More precisely, caspase 8 forms a complex with the death receptor adaptor FADD (FAS –associated death domain) and Atg5, colocalizes with LC3 and p62/SQSTM1. Its activation is Atg5, FADD and p62/SQSTM1 dependent. In Atg3 or Atg5 knock-out cells autophagy is inhibited by administration of SKI-I or bortezomib which drives a decreased activation of caspase 8 and that of the effector caspase 3. Concerning the inhibition of the late steps of autophagy, administration of bafilomycin A1 increases caspase dependent cell death. It can be inferred from these data that only the formation of autophagosome, and not the whole autophagic process, is required to create a platform for the activation of caspase 8.

Nonetheless, during autophagy caspase 8 is often not activated. It is not clear which mechanisms determine if autophagosomes favour caspase 8 activation [68].

Autophagy can decrease the endogenous inhibitor of cell death pathway, favouring apoptosis. It is known that in *Drosophilia melanogaster*, apoptosis is essentially controlled by the interaction between caspases and IAPs (inhibitors of apoptosis proteins). Bruce (BIR-containing ubiquitin-conjugating enzyme), which is an IAP, can be degraded by autophagy. Therefore it is not surprising that the inhibition of Atg1, Atg13 or Vps34 genes stops the development apoptosis of nurse cells in late oogenesis [68].

Necrosis, which is a cell death lacking many characteristics of apoptosis such as karyorrhexis and pyknosis, can be triggered by autophagy as well. It was demonstrated that in mouse L929 fibrosarcoma cells, autophagy favoured necrosis by degrading catalase which is known to neutralize hydrogen peroxide. Autophagy is beneficial in myocardial ischaemia, but the accumulation of autophagosome becomes noxious if oxygen supply is restored after blood circulation recovery. Immediately after reperfusion, autophagosomes are built but they are not eliminated. This could be due to the expression of LAMP2 (lysosome-associated membrane protein 2), which is necessary to merge autophagosome and lysosome, is decreased because of tissue damage. Interestingly, if LAMP2 expression level is restored and if Beclin-1 gene expression is partially knocked down, autophagosome processing is restored, thus decreasing cell death. In fact, autophagosomes accumulation drives a mitochondrial pathway of necrosis, which can be prevented by administration of cyclosporine A, known to inhibit mitochondrial PTP^{86} (permeability transition pore 86). At the moment, it is not clear how autophagosomes accumulation favours opening of the mitochondrial PTP^{86} [68].

Atg proteins are probably involved in cell death signalling separately of the autophagic activity. Atg12 certainly plays a role in activation of caspases through the mitochondrial pathway, since its deficiency decreases caspase activation induced by apoptotic stresses. Under pro-apoptotic stimuli, it can inhibit Bcl-2 and MCL1 (myeloid cell leukaemia sequence 1), favouring apoptosis. Atg7 can also induce apoptosis following lysosomal photodamage, probably by inducing lysosomal membrane permeabilization leading to apoptosis (similar to mitochondrial outer membrane permeabilization) [68].

1.3.2.4. Intercellular crosstalk

Crosstalk occurs not only within the same cell, but also between different cells in organs. When cells undergo apoptosis, they release soluble substances which can activate autophagy in nearby cells. It is well known that many DAMPs (danger-associated molecular patterns), such as HMGB1 (high mobility group box 1), S100 proteins and DNA complexes take action on a series of PRRs (pattern recognition receptors), therefore favouring autophagy. DAMPs are certainly highly expressed during a strong necrosis in which cellular debris cannot be efficiently eliminated. Besides it was demonstrated that autophagy protected cardiomyocytes and neurons during ischaemia. This could be explained by the fact that components released by dead cells induce autophagy in neighboring cells, helping them to survive [68].

2. Microautophagy

Here the lysosome directly envelops elements of the cytoplasm by invaginating the lysosomal membrane [65, 66]. Microautophagy is coordinated with other autophagic pathways. It can be activated by starvation and rapamycin, probably due to macroautophagy induction [66].

3. Chaperone-mediated autophagy

This kind of autophagy selectively targets soluble cytosolic proteins. The chaperone protein Hsc70 (heat shock cognate 70) and cochaperones specifically recognize proteins containing a KFERQ-like pentapeptide. Then the substrate proteins binds to the transmembrane protein LAMP2A (isoform of LAMP2) and translocation occurs (proteins are unfolded) [68].

4. Autophagy inhibitors

4.1. ULK1 and ULK2 inhibitors

MRT67307 and MRT68921 are both competitive ATP-binding site inhibitor. They potently and specifically inhibit ULK1 and ULK2 [70]. SBI-0206965 is known to inhibit more specifically ULK1 [74].

4.2. PI3K inhibitors

Mammalian cells have three classes of PI3Ks. Class I PI3K inhibits autophagy, whereas class II PI3K seems not to play important role in autophagy. On the other hand, class III PI3K is known to activate autophagy. Its inhibition by 3-methyladenine, wortmannin and LY294002 which are class III PI3K blocks autophagy. However, these compounds can also favour autophagy. 3-methyladenine stimulates autophagy if cells are cultured in nutrient-rich medium and incubated for a long time. Wortmannin has constant effects on class III PI3K whereas it has temporary effects on class I PI3K (opposite effects of those of 3-methyladenine), but it can also induce the formation of vacuoles which look similar to autophagosomes. It was demonstrated that LY294002 could inhibit the class I PI3K signalling pathway, thus activating autophagy [75].

4.3. Cycloheximide

This compound inhibits protein biosynthesis in eukaryotic organisms. It was demonstrated that cycloheximide blocked autophagy induced by hyperosmotic sucrose or cadmium chloride in mouse pancreatic acinar cells. In seminal cells, a regression of autophagic vacuole was observed. This compound could block autophagy by inhibiting the segregational steps occurring prior to the formation of autolysosomes [75].

4.4. Vacuolar-type H (+)-ATPase inhibitors

Vacuolar-type H (+)-ATPases are included in numerous organelles membranes such as lysosomes, endosomes, and secretory vesicles. Bafilomycin A1 and concanamycin A

inhibit specifically these enzymes. They suppress the acidification of lysosomes and endosomes [75].

4.5. Lysosomal lumen alkalizers

The mostly used compounds are chloroquine, hydroxychloroquine, NH_4Cl, and neutral red. They impair lysosomes, thus inhibiting autophagy. Recently, new forms of chloroquine were created: Lys01 which is a dimeric form of chloroquine, and a water-soluble salt of Lys01 known as Lys05. They are both more efficient than hydroxychloroquine to block autophagy [75].

4.6. Acid protease inhibitor

Leupeptin is a well-known to inhibit cysteine, serine and threonine peptidases. It inhibits autophagy by blocking digestion of the cytoplasm enclosed in lysosomes, driving to autolysosomes accumulation and/ or cytoplasmic inclusions in the central vacuoles. It was demonstrated that if cycloheximide was administrated at the same time, autophagic vacuoles formation, as well as the sequestrations of cytoplasmic and lysosomal enzymes were immediately blocked. E64d and pepstatin A can also inhibit autophagy by blocking lysosomal proteases, especially cathepsins [75].

4.7. Genetic intervention

Since many chemical inhibitors are not totally specific, genetic manipulation can be undertaken. Atg genes are crucial in autophagy process, so they can be deleted, inactivated or knocked down by using RNAi in order to obtain more accurate results [75].

VI. LIGATION AND RADIATION EFFECTS ON MTOR AND AUTOPHAGY EXPRESSION IN SALIVARY GLANDS

1. Ligation simultaneously activates mTOR and autophagy

In normal condition, mTOR and autophagy are switched off in salivary glands. Nonetheless, it was demonstrated that in rats, after ligation-induced atrophy of submandibular glands, autophagy and mTOR were activated at the same time [44]. Both mTOR and autophagy activity were detectable at day 3 and they remained active beyond [44]. This can appear paradoxical as mTOR activation should inhibit autophagy according to most literature. However, in this particular case, mTOR activation could trigger autophagy. This hypothesis is supported by a follow-up study in which rapamycin inhibited mTOR and autophagy [45]. In other cells, if mTOR is activated in the later recovery stage of acute pancreatitis [59], and that S6K1 is required in autophagy induced by serum deprivation or sulforaphane [60].

2. Radiation activates first autophagy then mTOR

Concerning irradiation effects, Morgan-Bathke et al. [47] saw a little conversion of LC3-I to LC3-II and no change in Atg5 and Atg7 proteins levels in mice parotid glands 8 hours after 5 Gy irradiation of the head and the neck. So, autophagy was increased. They also noticed that autophagy deficient mice were more radiosensitive. In another experiment in which mice were irradiated in the same manner [48], they uncovered that irradiation promoted hyperplasia and strong cellular proliferation in autophagy deficient mice. They also noticed that mTOR was hyperactivated as phosphorylated S6K1 level strongly increased in the parotid glands 4 to 5 days after irradiation and salivary gland function was disturbed at the same time.

VII. VALUES AND LIMITATIONS OF ANIMAL MODELS AND CELL CULTURES

Concerning animal models, although all animals are sensitive to irradiation, it is important to know that the dose required to inflict damage can vary depending on the species. A single dose of 5 to 40 Gy is required for rat, 1 to 15 Gy for mouse, 2.5 to 15

Gy for rhesus monkey and 15 to 20 Gy for miniature pig. The effects can be different as well. Infiltration of inflammatory cells is regularly noticed in miniature pig and rhesus monkey, whereas in rodents this infiltration does not always occur. Fractionated radiation, if it better simulates clinical radiation, can have different effects too. Indeed, in rats 30 x 2 Gy (over 6 weeks) irradiation led to a gradual decrease of function, serous acini, and increase of fibrosis and inflammation 6 months after irradiation. In comparison, in miniature pigs 35 x 2 Gy irradiation led to a strong downregulation in saliva flow rates, a significant acinar degeneration, fibrosis and parenchymal shrink 1 month only following radiation [199]. The immediate cell death following irradiation seems to occur more in primates than in rodents [5]. It is worth mentioning that in mice, the radiosensitivity is strain dependent. Kamiya et al. noticed in C57BL/6 mouse a strong inflammation which severely damaged the submandibular gland structure, whereas in ICR-nu/nu mouse, if no acute inflammation was observed, many cells underwent apoptosis before salivary gland malfunction 4 to 8 weeks following irradiation (25 Gy, single dose) [137]. Besides it has been reported in rats that recovery of submandibular glands were weaker than parotid glands [200]. Concerning ligation experiments they are often carried out on mice and rats. Results are highly reproducible since in both species ligation leads to gland atrophy, dilation of ducts, shrink of acini, inflammatory cell infiltration, activation of mTOR and autophagy [44, 45, 169]. After deligation salivary glands can regenerate in both species [201**,** 202]

Regarding cell cultures, the mouse embryonic fibroblasts NIH 3T3 cells is probably the most used cell line. These cells were extracted from *Mus musculus f. domenstica* [203]. They have been cultured for mTOR and autophagy studies [132] and irradiation as well [204]. However, results obtained on these cells are not always transposable in vivo. Fonseca et al. demonstrated that extract of Kalanchoe brasiliensis was toxic to NIH 3T3 cells (mouse embryonic fibroblasts) when administrated at 10^4 µL/mL (DMEM + 10% fetal bovine serum) since impairment in cell viability was around 80% at 72 hours, whereas the biochemical and haematological analysis of mice receiving the extract at 1000 mg/kg per os showed no acute toxicity. They only noticed a slight damage of liver since tissue sections revealed that some cells underwent apoptosis to mice receiving the extract at 500 and 1000 mg/kg [205]. Concerning primary cells, it was shown in hepatocytes that many genes can be upregulated or downregulated following extraction, so primary cells genes expressions are altered [206]. This means that the effects of irradiation and/or drugs of primary salivary gland cells could be different to those obtained in vivo. Besides concerning salivary primary

cells, they are known to grow slowly, to have a limited lifespan and tend to de-differentiate. For that reason tumour-derived and immortalised cell lines are often used in salivary gland research. HSY cells are neoplastic epithelial cell line derived from human parotid gland adenocarcinoma intercalated ducts. Their morphology and their behaviour are similar to those of intercalated ducts, since when they are administrated muscarinic and β-adrenergic autonomic agonists an upregulation of intracellular free calcium concentration and intracellular cyclic AMP occurs respectively. HSG cells are also neoplastic intercalated ducts but they derived from irradiated human submandibular gland. Like HSY cells, their calcium concentration can be upregulated by administration of muscarinic and purinergic agonists. SMG-C6 and SMG-C10 cells are immortalised rat submandibular acinar cells. They both upregulate intracellular cyclic AMP when exposed to β-adrenergic agonists. These cells are reliable to study Na^+ channels and Epithelial Na^+ Channel Protein [207]. Even though these cells behaviours are very similar to those of cells in salivary glands, there is at least one problem: they continuously undergo mitosis, so mTOR is activated, which is not the case in normal salivary glands [44]. It is also important to know that even though cells in a culture are all the same, the behaviour of each cell can vary following irradiation, so results obtained on single cells are not always reliable [208].

VIII. PROMOTING SALIVARY GLAND PROTECTION AND REGENERATION

1. Bioengineering

Replacing patients damaged salivary glands by bioengineered glands is not possible at the moment. However, encouraging results were recently obtained in mice. Ogawa et al. extracted E13 and E14 mice salivary gland cells (parotid, submandibular and sublingual) and put the cell pellets into collagen drops, forming cell aggregates. Two days after incubating at 37℃, H & E staining revealed salivary gland germs (parotid, submandibular and sublingual) had salivary gland structures. Then they removed all salivary glands from 7 weeks mice, and sutured the salivary gland germ ducts to parotid gland ducts. After 30 days, the connection was well established and bioengineered salivary glands secreted saliva [127].

2. Shield and 3-DTP

It is possible to protect major salivary glands from irradiation by placing shields. However, shields can almost not be used in case of larynx and oral mucosa tumour [1]. Targeting more precisely the areas to irradiate by using the 3-DTP (three-dimensional planning technique) is an alternative to limit salivary glands damages. Nonetheless, this technique is not efficient on patients with large midline cancers and bilateral metastases [1].

3. Antioxidants

As mentioned in paragraph II (p. 34), irradiation favours free radicals production. So administration of antioxidants should have protective effects. Indeed, amifostine is often used as it is a free radicals scavenger. However, it has many side effects such as nausea and vomiting [1].

Many other antioxidants were tested in patients, mice, and rats. Some of them seemed to be efficient. Fallahi et al. administrated vitamin E orally 800 IU/day to patients with thyroid cancer for 5 weeks, from 1 week before to 4 weeks after ^{131}I therapy. Salivary gland function was better preserved in vitamin E treated patients than those who received placebo [96].

Babicová et al. noticed an improved survival of whole body irradiated rats (8 Gy) receiving acetyl-L-carnitine. Moreover the plasma concentration of malondialdehyde (oxidative stress marker) was similar to control rats [97].

Üçüncü et al. administrated vitamin E 60 IU/mg/kg/day and L-carnitine 200 mg/kg/day simultaneously to cranium irradiated rats (15 Gy), but this combination was not more efficient than vitamin E only or L-carnitine only treated rats [98].

Yamada et al. tested the effect of astaxanthin to Sjögren syndrome patients, HSY cells (human salivary gland epithelial cell line) cultured with H_2O_2, and irradiated mice. A modest increase of saliva flow was observed in Sjögren syndrome patients, but the level of HEL (hexanoyl-lysine, oxidative stress marker) strongly dropped. Pretreatment of HSY cells with astaxanthin partially eliminated H_2O_2 induced ROS. Concerning mice, astaxanthin was efficient only if it was administrated before irradiation, which means that it has only preventive effect [99].

Şimşek et al. tried resveratrol on whole body irradiated rats (720 cGy). A significant protective effect was obtained in rats receiving high dose of resveratrol (100 mg/kg) as glutathione (antioxidant) level was increased, whereas nitric oxide and malondialdehyde levels were lowered. Moreover, few damages were observed in submandibular and parotid gland tissue sections [100].

Funegård et al. supplemented β-carotene and α-tocopherol to head and neck irradiated rats (7 Gy per day during 5 days). Although irradiation decreased saliva flow, supplemented rats had higher flow rate compared to rats fed with basic diet. Submandibular and parotid gland tissue sections did not show any morphological changes in supplemented rats [101].

Takahashi et al. tested the effect of quercetin on mice. Mice were fed with food containing quercetin 2 weeks before irradiation (15 Gy). The level of malondialdehyde in submandibular gland tissues was significantly lower in irradiated + quercetin treated mice than in irradiated-only mice. The gene expression of TNF-α and IL-10 (inflammatory cytokines) was elevated in irradiated-only mice gland tissues, while in irradiated + quercetin mice it was lower. Saliva flow of irradiated mice decreased, whereas the flow of irradiated mice receiving quercetin increased. Besides non-irradiated mice receiving quercetin had higher saliva flow than control mice. It is not surprising as the gene expression of AQP5 was strong in irradiated + quercetin mice and non-irradiated + quercetin mice. So quercetin not only protects against oxidative stress but also increases AQP5 expression even if the salivary gland was not irradiated [116].

4. Secretagogues

We saw in paragraph II (p. 34) that irradiated transition metals generated free radicals, and administration of secretagogues before irradiation decreased damage in rat parotid glands [6, 7]. Concerning the effect of secretagogues in human, it was demonstrated that administration of pilocarpine or bethanechol before irradiation limited the loss of saliva flow rates of parotid glands [1]. However, in patients receiving more than 50 Gy, gland damage was strong enough to decrease saliva flow rates and its quality as well [1].

5. Cell therapy

Repairing damaged salivary glands by injecting new cells is another option to restore their function. Since bone marrow stem cells are known to differentiate into many cells, some research teams tested the effects of their injection into irradiated mice. Sumita et al. injected (tail vein injection) male mice bone-marrow-derived cells to 18 Gy irradiated female mice. The saliva flow rate was strongly improved, acinar cells regeneration and vascularisation were apparent, and chromosome Y was detected in salivary glands [102]. Schwarz et al. carried out similar experiment on mice with ligated submandibular glands. As expected, injected cells migrated into ligated glands but they were also found in the contralateral glands too [103].

Adipose-derived stem cells have also the capacity to differentiate into many cells. Wang et al. irradiated miniature pigs at 20 Gy (local irradiation), and injected adipose derived-stem cells into parotid glands. Stem cells helped maintaining gland weight, flow rate, and amylase production. Tissue sections showed that stem cells transplanted into irradiated parotid glands had relatively well-preserved structures, contained more acinar cells and had higher microvessel density than in irradiated only glands [104].

Culturing and injecting salivary gland stem cells is another possibility to regenerate irradiated salivary glands. Nanduri et al. cultured mouse salispheres from submandibular glands. From 3 day old salispheres, they selected cells expressing different stem cell markers (c-kit, CD133, CD49f, and CD24) and injected into submandibular glands of locally irradiated mice (15 Gy). One hundred and twenty days after irradiation, stimulated saliva flow rate was stronger in mice transplanted with stem cell marker expressing cells than in irradiated only mice. The most efficient cells were c-kit expressing ones [105]. Concerning human salivary gland stem cells, Feng et al. succeeded in culturing salispheres from parotid and submandibular gland. After dispersion, they grew the cells in Matrigel. They formed new salispheres which transformed into duct-like and acinar-like structures [106]. Pringle et al. cultured salispheres from human submandibular gland and injected dispersed salisphere cells into the submandibular gland of locally irradiated mice (5 Gy). Human cells proliferated and formed acinar- and duct-like cells. Moreover, this injection significantly restored saliva flow [115]. For their part, Andreadis et al. cultured human minor salivary gland cells (lower lips) which are easily accessible. They obtained two different types of cells: fibroblast-like (majority) and flat-shaped epithelial-like cells. These cells had osteogenic,

adipogenic, and neurogenic differentiation capacity. They also expressed many mesenchymal stem cell markers such as CD90, CD105, nestin, CD49f, and CD81. Approximately 40% of cells expressed CK7 and CK8, which suggests an epithelial phenotype [107].

The use of iPS cells which can differentiate into many cells could be another way to favour salivary glands regeneration. Ono et al. [108] injected mouse iPS cells into mice submandibular glands. As expected, teratomas containing many types of tissues formed but some tissues were similar to submandibular gland and sublingual gland ones. They also co-cultured mouse embryonic submandibular gland cells with mouse iPS cells. Epithelial structures were more developed in this mixture than in monoculture of mouse embryonic submandibular gland cells. Undifferentiated markers of salivary gland cells were significantly lower than in monoculture as well. Therefore iPS cells can speed up cellular differentiation and regeneration too.

6. Molecular therapy

Since it was known that injection of bone marrow cell lysate had beneficial effects in mice with acute myocardial infarction, Fang et al. tested the effect of bone marrow cell lysate in head and neck irradiated mice (15 Gy). They noticed that when the proteins of lysates were deactivated, it could not restore saliva flow rate. Acinar cell area, the number of blood vessels and cells expressing PCNA were lower compared to sham irradiated mice and intact proteins lysates injected mice. Therefore, they hypothesized that bone marrow cells released many protein factors which contribute to restore salivary glands. Indeed, they identified MMP-8 and 9, FGF-1, HGF, OPN and SDF-1 which are tissue repair/regeneration factors [109].

For their part Choi et al. tested the effect of KGF-1 (keratinocyte growth factor-1) on human parotid epithelial cells and rats (head and neck irradiation, 15 Gy). Human parotid epithelial cells were irradiated at 15 and 20 Gy irradiation. This led to morphological changes, low mitosis, and elevated cytotoxicity by LDH release. Those which received KGF-1 just after irradiation were less damaged. Concerning KGF-1 effects on rats (injection into submandibular gland, 1 hour before and immediately after irradiation), submandibular gland tissue sections showed that in irradiated-only rats the staining of AQP5 (acinar cell marker), CK18 (ductal cell marker) α-SMA (myoepithelial cell marker) decreased, while in rats receiving KGF-1 it was stronger. Moreover, in irradiation + KGF-1 rats, saliva flow rate was higher, the expression of

pro-apoptotic proteins (p53, PUMA, Bax, cytochrome c, and cleaved caspase-3 and -9) was considerably inhibited and the level of anti-apoptotic protein Bcl-2 was stronger than in irradiated-only rats. The protective effect of KGF-1 is probably due to the inhibition of p53 mediated apoptosis [117].

The bFGF (basic fibroblast growth factor) which is known to favour wound healing may also favour regeneration of irradiated salivary gland. Kobayashi et al. surgically wounded the submandibular glands of rats, and filled the hole with collagen gel with or without bFGF. Wound healing was faster in collagen + bFGF group as there were numerous myoepithelial cells, stem cells ductal cells, and acinar cells compared to collagen only group [122]. Concerning irradiation experiments, Li et al. tested the effect of bFGF on irradiated mice thymocytes and splenocytes. They extracted these cells from whole body irradiated mice (0.5 and 1 Gy) and cultured them with or without bFGF. They did not observe significant decrease of apoptosis and cell proliferation was not improved in bFGF treated cells [123]. On the other hand Kinoshita et al. who irradiated the skin of CLAWN miniature pigs at 10 Gy, uncovered that the administration of bFGF alone had few beneficial effects, whereas the combination of bFGF with expander (bFGF inserted through the edge of the tissue expanded flap immediately after irradiation) greatly improved dermo-epidermal proliferation and angiogenesis as well [124]. For their part Matsuu-Matsuyama et al. noticed that in rats, injection of bFGF prior to irradiation (whole body, 8 Gy) decreased the number of apoptotic cells, and increased mitosis and the number of Ki-67 (proliferation marker) positive cells in the jejunal crypts. Expression of p53, CDKN1A, PUMA and cleaved caspase 3 was decreased [125].

Recently, Marmary et al. uncovered a surprising effect of IL-6. This cytokine, which is a senescence associated marker, is upregulated after irradiation. In irradiated IL-6 knockout mice and in anti-IL-6 antibody injected wild type mice, senescence was reduced. Therefore senescence is one of the causes of salivary gland hypofunction, and IL-6 favours it. However, injection of IL-6 prior to irradiation decreased senescence and salivary gland hypofunction, and improved DNA repair. The mechanism is not clear but IL-6 pretreatment has protective effects [126].

7. Parasympathetic nerve stimulation

Parasympathectomy is known to block salivary gland regeneration. For that reason Knox et al. hypothesized that irradiated salivary gland did not regenerate because of parasympathetic nerve damage. They noticed that in E13 mice submandibular gland, irradiation (5 and 7 Gy) decreased the number of end buds, parasympathetic submandibular ganglion, and the expression of TUBB3 (tubulin beta 3 class III, axonal marker in the parasympathetic nerves), whereas K5+ progenitor cells were not harmed. Moreover, the expression of NRTN (neurturin), a factor ensuring parasympathetic nervous system function and survival, in submandibular gland epithelium was diminished as well. By providing NRTN to irradiated E14 mice submandibular gland, they observed a rise in the number of end buds and a decrease of neuronal apoptosis. On the other hand, NRTN administration to non- irradiated samples did not show any increase of epithelial morphogenesis. These findings tend to prove that parasympathetic nerve stimulation is required to ensure salivary gland regeneration [120].

8. Activating or inhibiting mTOR

Experiments with mice showed that rapamycin delayed salivary gland atrophy following ligation [45]. Up to 3 days, gland weights were maintained and mTORC1 remained totally inhibited. Acinar cells were preserved but not ductal cells. Beyond 3 days, rapamycin efficacy decreased as gland weights decrease and mTORC1 was only partially inhibited because phosphorylated S6K1 and 4E-BP1 were detected. This partial inhibition was probably due to the PI3K (class I)-negative feedback mechanism and the fact that rapamycin could only inhibit mTORC1 (**fig. 14**). However, S6K1 and 4E-BP1 phosphorylation could occur without mTORC1 activation as treatment with Torin 1, which is believed to inhibit all kinase-dependent functions of mTOR, showed similar results to rapamycin [45].

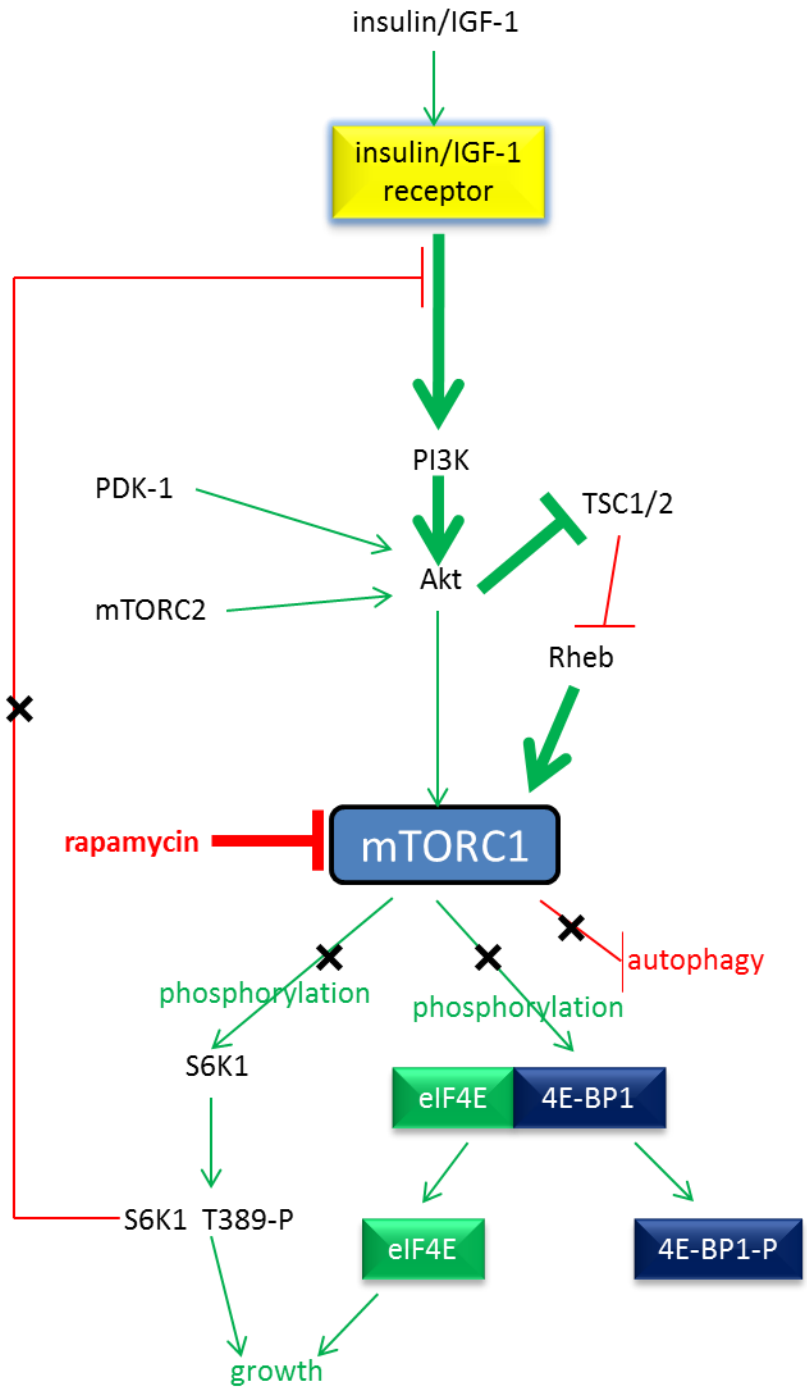

Fig. 14. Rapamycin effect on mTORC1. In the first 3 days of ligation of mouse submandibular glands, firstly, mTORC1 is inhibited by rapamycin, leading to inhibition of S6K1 and 4E-BP1 phosphorylation. Secondly, as PI3K (class I)-negative feedback mechanism does not occur, mTORC1 is re-activated, thus phosphorylating 4E-BP1 and S6K1. This phenomenon is observed beyond 3 days.

Morgan Bathke et al. uncovered that administration of IGF-1, which was supposed to favour mTOR activation and thus inhibit autophagy by blocking ULK1, before 5 Gy irradiation (head and neck) improved autophagy as Atg5, Atg7 and LC3-II proteins levels strongly increased 8 hours after irradiation. This effect was not observed

in autophagy deficient mice. Moreover, transmission electron microscopy showed that autolysosomes and autophagosomes were more numerous in IGF-1 treated mice than in control mice. It is not clear if IGF-1 induced mTOR activation triggers autophagy but it is known that if tissues are pretreated with IGF-1, cell cycle is interrupted after damage, so it favours cellular repair [47]. In another experiment, they noticed that inhibition of mTOR by administration of the rapalogue CCI-779 (tensirolimus) after irradiation (5 Gy, head and neck) had protective effect as salivary flow rate of irradiated mice which received the drug was almost similar to control mice, and was stronger than irradiated-only mice. The reason is not clear, but they observed that after irradiation, mice with conditional knock-out of autophagy genes had excessive acinar cell proliferation. Therefore, inhibition of mTOR could help improve salivary gland homeostasis by stopping excessive acinar cell growth [48].

Zhu et al. [113] tested the effects of rapamycin on irradiated swines and human submandibular gland cells. Swines which received rapamycin injection before irradiation (parotid gland, 7.5 Gy/day for 5 days, injection before each irradiation) had better saliva flow than irradiated only ones. AQP5 expression was stronger in the rapamycin treated irradiated group than in irradiated only group as well. H & E staining showed that the parotid glands of irradiated only group had few acini and were atrophied. There were also duct luminal dilatation, lack of glandular lobule, and an increase of adipose and fibrosis tissue. On the other hand, the irradiated + rapamycin group parotid glands looked almost normal. There were only a slight decrease of acini numbers and their size as well. Concerning human submandibular gland cells, administration of rapamycin on non-irradiated cells decreased its proliferation. mTOR was activated in non-irradiated cells and irradiation increased its activation. However, when rapamycin was administrated 72 hours before 8 Gy irradiation, this overactivation of mTOR was blocked, and the level of γ-H2AX was decreased while the expression of MnSOD increased. After replacing rapamycin containing media with normal media, cells proliferated better than non-irradiated cells. The authors hypothesised that the blocking of mTOR with rapamycin allowed cells to repair damage as cell cycle is stopped. Moreover rapamycin increased the level of MnSOD which protects against ROS, which might explain why there was less γ-H2AX. Therefore the beneficial effect of rapamycin can be attributed to the fact that it protects DNA from irradiation damage, allowing a strong cellular proliferation after irradiation.

B. AIMS

A central paradigm of cell biology is that growth and autophagic pathways are regulated to operate in a reciprocal manner so that during conditions of growth autophagy is down regulated and during atrophy growth pathways are down-regulated. Between mTOR and autophagy is ULK1/2 which regulates autophagy when mTOR is activated. It was surprising then that our group found activation of mTOR and autophagy during ligation-induced atrophy and that inhibition of mTOR delayed atrophy. Others have also found that during ligation of salivary glands that knocking out autophagy had no effect on atrophy. In separate studies the same group found mTOR inhibition during irradiation improved recovery [45, 48, 113], they did not verify if autophagy was upregulated. Therefore, it was uncertain that mTOR dependent autophagy occurred. For that reason we estimated that ULK1 study was essential to determine if beneficial effects of mTOR inhibitors were due to autophagy activation triggered by ULK1 activation or mTOR inhibition only.

A new approach to test for a functional ULK was the availability of the inhibitor MRT67307. NIH 3T3 cells were chosen since mouse embryonic fibroblasts were used in the first publication of MRT67307 and are often used to study mTOR and autophagy [24, 56, 57, 60, 132]. The use of these cells in the present study was to ensure that ULK1 inhibition by MRT67307 could be detected using both mTOR and autophagy biochemical indicators (4E-BPI, S6K and LC3-I/LC3-II). Once confirmed these methods were used on SMG-C6 cells which were immortalised from rat acinar cells. However, there was a risk that results obtained on these cells were not totally representative of salivary glands since mTOR is continuously activated, whereas in normal condition both mTOR and autophagy are supposed to be inactive in salivary glands [44]. Therefore, it was necessary to confirm results obtained on immortalised cells to those of primary submandibular gland cells acutely isolated from mice.

Concerning mouse irradiation, no paper mentions the minimal dose which activates mTOR and autophagy, so it was necessary to do a dose escalation study to find it. Since the radio-sensitivity varies depending on strain [137], it was also necessary to irradiate 2 strains to see if damages could be stronger in one of them and if that could modify mTOR and autophagy activation. To assess damage, H & E staining and immunohistochemistry on tissue sections were used since acinar cells are damaged following irradiation [1, 4, 6, 131] and AQP5 expression is decreased [84, 133].

Pilocarpine stimulated saliva flow was also measured since many papers mention a decrease of the flow following irradiation [47, 48, 83, 84, 160].

Finally the effects of drugs were tested on mice. Because it was demonstrated that autophagy was weakly activated and lasted few hours following irradiation [47], we decided to use ligated submandibular gland in which autophagy is activated during several days [44]. As well as MRT67307 to inhibit ULK1/2, chloroquine, also known to inhibit autophagy by impairing lysosome [75] was tested in vivo.

Thus the overall aim of the thesis was to determine if mTOR and autophagy are linked in salivary glands by a functional ULK1/2. To do this the following objectives were attempted.

1) Determine optimal concentration of MRT67307 to block ULK1/2. NIH 3T3 cell will be used and mTOR activation assessed by 4ebp1 and S6K phosphorylation. Autophagy activity will be assessed by LC3-I/LC3-II ratios. Autophagy will be induced by serum starvation and by mTOR inhibition by Torin. Results to be repeated in SMG C6 cell lines and acutely prepared salivary cells from mouse submandibular glands.
2) Determine if autophagy and mTOR are simultaneously activated in mouse salivary glands following irradiation-induced atrophy. If successful, Torin and/ or MRT67307 will be introduced prior to irradiation to determine if they alter the process of atrophy.
3) Utilise MRT67307 and chloroquine in ligation-induced atrophy to determine if ULK is functional and whether autophagy is activated by mTOR.

C. MATERIALS AND METHODS

1. Animals

All experimental procedures were conducted on adult female ICR or C57BL/6 mice provided by Charles Rivers Laboratories (Margate, UK)

After reception, mice were housed in groups of five or eight, with food and water ad libitum. They were maintained at 20-22 °C with 12 hours light-dark cycle and were provided nesting materials and tunnels. They were allowed to rest at least 1 week before experimental procedures.

All animal studies and procedures were conducted in accordance with UK Home Office Animal (Scientific Procedures) Act 1986.

2. Ligation and irradiation

Submandibular gland duct ligation was carried out as described previously [45]. To anesthetize mice, ip injection of xylazine (5 mg/kg)/ketamine (25 mg/kg) was performed. Then mice were put on a controlled heating pad to avoid body temperature decrease. Pedal reflex was used to assess the depth of anesthezia. While mice were maintained lying on their back, the midline of the neck skin was incised (~0.5 cm long), the fat tissue surrounding the left submandibular gland was removed, then the gland duct was ligated by using a 6-0 Ethicon suture (Johnson and Johnson Intl, Brussels, Belgium). Next the neck was sutured and the mice were put in a cage placed in a warm room and received 10 mg/kg buprenorphine (analgesic) in order to recover from anaesthesia. To decrease the risk of infection, aseptic conditions were carried out during the surgical procedure. 1 week later, both ligated and contralateral glands were extracted.

For irradiation, we used a gamma irradiator Gp 1200. Mice were placed in a metal tube and were free to move inside. They received a single dose of 1, 3, 5, 7, 9, 11 Gy for the preliminary work, whereas they received a single dose of 11 Gy for subsequent experiments.

3. Saliva collection

Firstly mice were anaesthetized in chamber with isoflurane. After few minutes, when mice were well anesthetized, 200 µL pilocarpine (0.1 mg/mL in saline) was intraperitoneally injected. After 5 to 10 minutes, once breathing rate was seen to increase, a piece of filter paper was put in their mouth during 5 minutes or 10 minutes. Then papers were retrieved and put into ice cooled tubes. As paper + tubes were pre-weighed, it was possible to weigh the amount of saliva retrieved. To eluate saliva, the base of tubes was cut and these tubes were put into new Eppendorf tubes. Next 100 µL PBS was added to the papers and tubes were centrifuged. At the end we obtained a mixture of PBS + saliva.

4. Tissue collection

After sacrificing mice by overdose of euthatal, submandibular glands were extracted, weighed and chopped into small pieces. Some pieces were put into liquid nitrogen or dry ice, and then stored at -20 °C for biochemical analysis, whereas others were fixed in 4% formalin for histological analysis.

5. Haematoxylin and eosin staining

After 24 hours of incubation at room temperature in 4% formalin, submandibular gland tissues were processed in ascending alcohol (industrial methylated spirit) and embedded in paraffin wax. Tissues were sectioned at 5 µm and mounted on super-frost plus-coated slides.

Following 45 minutes incubation at 60 °C or overnight incubation at 37 °C, dewaxing procedure was carried out: 2 x 5 minutes incubation in xylene, 3 x 5 minutes incubation in 100% industrial methylated spirit.

Then, dewaxed tissue sections were incubated in Mayer's Haematoxylin (Thermos Fischer Scientific, Leicestershire, UK) for 5 minutes, washed with tap water, differentiated with 1% acid alcohol, and incubated for 5 minutes in 1% Eosin solution (VWR International, Leicestershire, UK). Next, the slides were dehydrated by incubating in 100% industrial methylated spirit (3 x 5 minutes) and xylene (2 x 5 minutes). Adobe Photoshop 7.0 was used to crop pictures and modify tone.

6. Immunohistochemistry

After dewaxing (same procedure as described in the previous paragraph), tissue sections were soaked in 3% hydrogen peroxide for 10 minutes to quench the endogenous peroxidase. Then they were put in preheated citric acid buffer (pH 6.0) and heated for 10 minutes in microwave oven. This step was required to retrieve antigens which were masked by formalin meshwork. Next, sections were washed with cold tap water, and incubated with 2% bovine serum albumin to decrease non-specific binding of antibodies. Then, sections were washed with 1% TBS and incubated overnight with primary antibodies at 4 °C. Sections were washed again with 1% TBS and incubated 1 hour with secondary antibodies. They were washed again with 1% TBS and incubated with DAB (Thermo Fischer Scientific, Illinois, USA) solution for 5 minutes. Next, they were washed with Milli-Q water and counter stained in Mayer's Haematoxylin for 1 minute. Adobe Photoshop 7.0 was used to modify tone.

7. Gland homogenates

Submandibular gland pieces stored at -20 °C were put in 5% w/v of an ice-cold homogenization buffer containing 1% Triton X-100, 1 mM EDTA and a 1% v/v dilution of protease inhibitor cocktail set 1 (Merck Chemicals Ltd, Nottingham, UK) or RIPA buffer (Sigma-Aldrich, Poole, Dorset, UK) with the same protease inhibitor cocktail and homogenated with Ultra-Turrax TP18/10 (Ika-Werke GmbH & Co. KG, Staufen, Germany) or MP FastPrep-24 (MP Biomedicals, Ohio, USA). Next, samples were placed in Sigma 1-13 Centrifuge and centrifuged at 10000 rpm (~7043 g) and supernatants were collected.

8. Protein assay

Protein concentrations in homogenates were assessed by using BCA Protein Assay Kit (Thermo Scientific, Rockford, USA). Samples were diluted in water (90 µL water + 10 µL sample), poured into microplate wells (2 wells/sample), mixed with reagents and incubated 30 minutes at 37 °C. Absorbance was quantified with BIO-RAD iMark Microplate Reader.

9. Coomassie blue and PAS staining

Samples were mixed with DTT (reducing agent) and lithium dodecyl sulfate (anionic detergent for denaturing native proteins which can replace sodium dodecyl sulfate), boiled at 100 °C for 3 minutes. After having performed SDS-PAGE (NuPAGE Novex 4-12% Bis-Tris Gels, Life Technologies Ltd, Paisley, UK), gels were coloured with Coomassie blue (Sigma-Aldrich, Poole, Dorset, UK), and destained with 10% acetic acid. For PAS staining, gels were incubated in black trays containing periodic acid solution at 20 g/L for 15 minutes with gentle shaking. After washing with ultra-pure water (2 x 5 minutes), they were incubated in black trays containing Schiff's reagent (VWR International, Leicestershire, UK) for 90 minutes with gentle shaking, and then washed with Milli-Q water.

10. Western blotting

After having carried out SDS-PAGE, resolved proteins were transferred to 0.2 µM nitrocellulose membrane (Life Technologies Ltd, Paisley, UK). In order to assess mTOR and autophagy in the same samples the blots were cut horizontally and probed separately. The membranes were blocked with 2% non-fat milk (w/v) in TTBS 1 hour at room temperature or overnight at 4 °C to minimize non-specific binding of antibodies. After washing with TTBS (5 minutes x 3), membranes were incubated in the primary antibodies solutions 1 hour at room temperature or overnight at 4 °C. Then they were washed again with TTBS (5 minutes x 3) and incubated in the secondary antibodies solutions 1 hour at room temperature. Next, they were washed again with TTBS (5 minutes x 3) and they were ready for analysis. Blots were reprobed with beta-actin to normalise for protein loading between lanes.

11. Antibodies

The primary antibodies used for immunohistochemistry and/or western blots were the followings: phospho-4E-BP1 (Thr 37/46, Cell Signaling Technology, Hertfordshire, UK), phospho-S6 ribosomal protein (Ser 240/244, Cell Signaling Technology Hertfordshire, UK), ATG5 (NovusBio, Abingdon, UK), LC3B (NovusBio Abingdon, UK), ULK1 (Abcam, Cambridge, UK), AQP5 (Abcam Cambridge, UK), and beta actin (4A Biotech, Beijing, China). The dilution used was 1/1000 for western blots for all

antibodies. For immuno histochemistry: 1/100 for phospho-S6 ribosomal protein, 1/400 for ATG5, and 1/500 for AQP5.

Secondary antibodies used were polyclonal goat anti-rabbit immunoglobulins HRP or anti-mouse immunoglobulins HRP from Dako Ltd (Ely Cambridgeshire, UK). The dilution used was 1/2000 for western blots and 1/200 for immunohistochemistry.

For protein bands detection, Western Blotting Luminol Reagent sc-2048 (Santa Cruz Biotechnology, Inc., Heidelberg, Germany) or Clarity^{TM} Western ECL Substrate were poured on membranes. To take protein bands pictures, ChemiDoc Imaging System (BioRad Laboratories Ltd, Hertfordshire, UK) was used, with optimized exposure times and built-in high-sensitivity blot detection highlighting over-saturated pixels, to obtain ideal exposure in images of the protein bands. Each band intensity was quantified using Image Lab Software (version 5.2., Bio-Rad), and normalised for beta-actin density when necessary. For autophagy activation, LC3-I and LC3-II band intensities were measured and LC3-I/LC3-II ratios were calculated. An upregulation of autophagy leads to a decrease of LC3-I/LC3-II since an accumulation of LC3-II occurs [23]. Adobe Photoshop 7.0 was used to crop blots.

12. Cell culture

Mouse embryonic fibroblasts NIH 3T3 were cultured in DMEM (Sigma-Aldrich, Poole, Dorset, UK) supplemented with 10% newborn calf serum (Gibco Life Technologies, Paisley, UK), 500 units/mL penicillin and 0.5 mg/mL streptomycin (Sigma-Aldrich, Poole, Dorset, UK), GlutaMax 1X (Gibco Life Technologies, New York, USA).

Rat submandibular acinar cells SMG-C6 cells (provided by Angela Ohm from University of Colorado Denver) cultured in DMEM/F-12 (GE Healthcare Life Sciences, Utah, USA) supplemented with 2.5% fetal bovine serum (Sigma-Aldrich, Poole, Dorset, UK), 0.4 µg/mL hydrocortisone (Sigma-Aldrich, Poole, Dorset, UK), 5 µg/mL (Sigma-Aldrich, Poole, Dorset, UK), 0.08 µg/mL EGF (Gibco Life Technologies, Paisley, UK), T3 0.13 ng/mL (Sigma-Aldrich, Poole, Dorset, UK), 0.03 µg/mL retinoic acid (Sigma-Aldrich, Poole, Dorset, UK), 2.5 mM L-glutamine (Gibco Life Technologies, Paisley, UK), 5 µg/mL insulin, 50 µg/mL gentamycin (Gibco Life Technologies, Paisley, UK).

Both cell lines were cultured at 37 °C with 5% CO_2. Cells were seeded into 6 wells plates (~22500 cells/well or 11250 cells/mL) and harvested when it was 85-90%

confluent (~540000 cells/well or 270000 cells/mL) with trypsin-EDTA 0.25% (Gibco Life Technologies, Paisley, UK). After centrifugation (Sigma 1-13 Centrifuge, 10000 rpm), trypsin solution was discarded and PBS (Sigma-Aldrich, Poole, Dorset, UK) or HBSS (Gibco Life Technologies, New York, USA) were added and centrifuged again in order to eliminate the remaining trypsin. Next, the supernatant was removed and ice-cooled RIPA buffer with 1% v/v dilution of protease inhibitor cocktail set 1 was added to cell pellets and they were sonicated. For Western blotting, cell lysates were mixed with dithiothreitol and lithium dodecyl sulfate and boiled at 100 °C for 3 minutes.

For NIH 3T3 cells ULK1 knock-out experiment, cells were seeded in a 24 well plates (500 µL/well). ULK1 siRNA (m) of Santa Cruz (sc-44849) and ULK1 si RNA I of Cell Signaling (7000) were suspended in HiPerfect Transfection Reagent of Qiagen (301704) and the mixture was added in each well (for both ULK1 SiRNA the final concentration was 20 nM) and cells were incubated 24 hours at 37 °C with 5% CO_2.

Mouse primary submandibular gland cells were prepared as described previously [190]. In brief, after killing mice submandibular glands were extracted, minced and incubated at 37 °C for 1 hours under agitation and gassing with 100% oxygen in a buffer with the following composition: 10 mM sodium pyruvate, 10 mM glucose, 15 mM Hepes, 1 mM magnesium chloride, 0.02% soya bean trypsin inhibitor, 0.1% bovine serum albumin, 130 mM sodium chloride, 5 mM potassium chloride, 1 mM calcium chloride and 1% phenol red (pH 7.4) containing Collagenase P (from *Clostridium histolyticum*, 3.1 U/mg, Boehringer Mannheim, Lewes, UK) at 5 mg/20 mL. Cells where then centrifuged (Sigma 1-13 Centrifuge, 10000 rpm) and washed with PBS, suspended in the same buffer without collagenase (~2000000 cells/mL) and were incubated again with drugs at 37 °C for 1 or 2 hours under agitation and gassing with 100% oxygen. In the new experiments, drugs were added during the enzymatic treatment and cells were incubated 2 hours in the same conditions.

13. Statistical analysis

Results were expressed as mean ± standard deviation. Statistical comparisons were done by using one way Anova (normal distribution), Kruskal Wallis (non-normal distribution) or Student's t-test. Data analysis was carried out with GraphPad Prism version 7 (GraphPad Software, California, USA) and Microsoft Excel 2010 (Microsoft, Redmond, USA).

D. MTOR AND AUTOPHAGY INTERACTIONS STUDIES ON CELL CULTURES

Introduction

mTOR and autophagy interactions are rather complicated since mTOR inhibition and ULK1 activation are not always required to activate autophagy [63] and ligation of submandibular gland activates both mTOR and autophagy [44]. To study the interactions between mTOR and autophagy, it was necessary to test the effects of mTOR and/or autophagy inhibitors on cells. Firstly NIH 3T3 cells were cultured (mouse embryo fibroblast cell line), and administrated mTOR inhibitor Torin 1 as autophagy activator and/or ULK1 inhibitor MRT67307 as autophagy inhibitor to study the interactions between mTOR and autophagy. Since many researchers cultured this cell line to study mTOR and autophagy, it was a very reliable cell model. Secondly we cultured SMG-C6 cells which were previously derived from rat submandibular gland acinar cells. Even though these were immortalised cells, they could provide data on mTOR and autophagy activity in acinar cells which interested us the most. Thirdly drugs were administrated to primary submandibular gland cells. Since these cells were freshly extracted submandibular gland cells, we hoped they could provide more reliable results than those of immortalised acinar cells.

Methods

NIH 3T3 and SMG-C6 cells were seeded into 6 wells-plates (~22500 cells/well or 11250 cells/mL) and drugs were added when it was 85-90% confluent (~540000 cells/well or 270000 cells/mL). All experiments were performed in triplicates: Torin 1 was administrated into 3 wells, 3 others received MRT67307, and so on. Both cell lines were harvested after 2 hours incubation at 37 °C with 5% CO_2. NIH 3T3 cells were used to confirm the effects of Torin 1 and MRT67307, as well as verifying the effect of ULK1 KO on autophagy. Unless otherwise specified, the concentration of Torin 1 in each well was 0.05 mM, whereas MRT67307 was 0.072 mM. To test the effects of Torin 1 on MRT67307 treated cells, MRT67307 was administrated first, and 1 hour later Torin 1 was added and incubated one more hour. The effects of MRT67307 on Torin 1 treated cells were assessed by using the same protocol. For starvation, cells were culture without serum. To knock-out ULK1, NIH 3T3 cells were incubated 24 hours with siRNA m and siRNA I at 37 °C with 5% CO_2 (24 wells plates). The effects of ULK1 KO on autophagy was evaluated by starving cells during 2 hours at 37 °C with 5% CO_2 (~270000 cells/mL). For SMG-C6 cells, Torin 1 concentration was 0.01 mM

while MRT67307 remained at 0.072 mM. The effects of Torin 1 on MRT67307 treated cells and MRT67307 on Torin 1 treated cells were also assessed by using the same protocol as NIH 3T3 cells. Primary SMG cells were seeded into 12 wells plates (~2000000 cells/mL) with drugs under 100% oxygen and under agitation during 1 hour or 2. In the latest experiment, drugs were added during the enzymatic treatment and cells were incubated 2 hours in the same conditions. For cells receiving both drugs, we simultaneously administrated Torin 1 and MRT67307.

In all experiments Western blot was carried out to visualise the variation of proteins expressions. More precisely, after harvesting (with trypsin-EDTA 0.25% for NIH 3T3 and SMG-C6 cells), cells were centrifugated during 5 minutes (Sigma 1-13 Centrifuge, 10000 rpm), the supernatants discarded, then PBS was added and centrifugated again 5 minute. Next, the supernatant was removed and ice-cooled RIPA buffer with 1% v/v dilution of protease inhibitor cocktail set 1 was added to cell pellets and they were sonicated. Cell lysates were mixed with dithiothreitol and lithium dodecyl sulfate and boiled at 100 °C for 3 minutes. Then SDS-PAGE (NuPAGE Novex 4-12% Bis-Tris Gels) was performed, and resolved proteins were transferred to 0.2 µM nitrocellulose membrane. The membranes were blocked with 2% non-fat milk (w/v) in TTBS 1 hour at room temperature or overnight at 4 °C to minimize non-specific binding of antibodies. After washing with TTBS (5 minutes x 3), membranes were incubated in the primary antibodies solutions 1 hour at room temperature or overnight at 4 °C. Then they were washed again with TTBS (5 minutes x 3) and incubated in the secondary antibodies solutions 1 hour at room temperature. Next, they were washed again with TTBS (5 minutes x 3) and they were ready for analysis. western blot was carried out to visualise the variation of proteins expressions in all experiments.

Results

1. Effects of mTOR and/or autophagy inhibitors on NIH 3T3 cells

1.1. Determination of optimal concentration of Torin 1 and MRT67307

Before studying the interactions between mTOR and autophagy in SMG-C6 cells and mouse submandibular gland cells, it was necessary to ensure that we could confirm the results obtained on NIH 3T3 cells by other research teams. Torin 1 is a potent mTOR inhibitor which inhibits both mTORC1 and mTORC2 and is more efficient than

rapamycin. According to Thoreen et al. [132] who tested a wide concentration range (2 to 5000 nM) on mouse embryonic fibroblasts, 250 nM seems to be enough to totally inhibit mTOR as western blot did not detect phospho-S6K1 band at this concentration. However, they did not assess autophagy activity. So it is uncertain if the concentrations tested were sufficient to fully activate autophagy. Therefore, two stronger concentrations were tested: 0.005 mM and 0.05 mM. Chloroquine (0.25 mM) was also added to stop LC3-II degradation [168]. Cells were incubated 2 hours at 37°C. As a positive control cells were starved to induce autophagy, which should inhibit mTOR as shown by a loss of S6K phosphorylation. In the following experiments, mTOR activation is demonstrated by the appearance of phosphorylated S6K, a substrate of the mTORC1 kinase. Autophagy flux is monitored by changes in ratio of LC3-I/LC3-II.

In 0.005 mM experiment, non-starved Torin 1 treated cells LC3-I/LC3-II ratios were significantly lower than control cells ($p<0.01$) but were stronger than 0.005 mM starved cells ($p<0.01$). It means that at this concentration, despite the fact that S6K1 was not phosphorylated, autophagy was not fully activated. On the other hand, in 0.05 mM experiment, non-starved Torin 1 treated cells LC3-I/LC3-II ratio was similar to Torin 1 treated starved cells one, so autophagy was further activated (**fig. 15**). Therefore, 0.05 mM was chosen as the ideal working concentration.

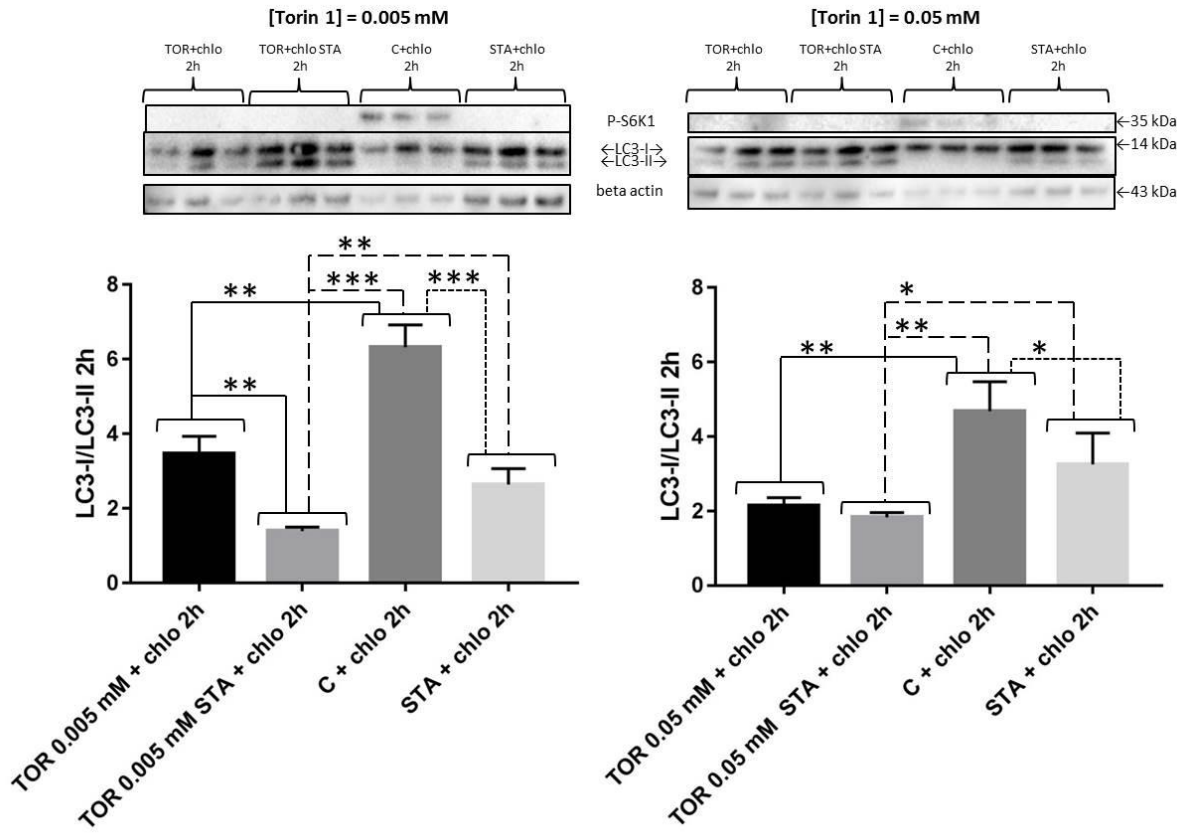

Fig. 15. Determination of optimal concentration of Torin 1 to activate autophagy. NIH 3T3 cells were incubated for 2 hours with either 0.005 mM (TOR 0.005 mM + chlo 2h) or 0.05 mM of Torin 1 (TOR 0.05 mM + chlo 2h). Both concentrations of Torin 1were sufficient to prevent S6K1 phosphorylation, but LC3-I/LC3-II ratios of TOR 0.005 mM were weaker than TOR 0.05 mM. So 0.05 mM was the concentration used in subsequent experiments to activate autophagy by inhibiting mTOR. Cells were all treated with chloroquine (chlo). Cells were starved as an alternative method to activate autophagy. The combination of starvation and Torin 1 was also tried to determine if any additive effects occurred but at the lower concentration was any difference observed. C: control cells: STA: starved cells, P-S6K1: phospho-S6K1. Significant differences (*p<0.05, **p<0.01, ***p<0.001) were determined using a one-way ANOVA followed by a post-hoc Tukey multiple comparisons test for [Torin 1] = 0.005 mM and Newman-Keuls for [Torin 1] = 0.05 mM. Error bar: standard deviation. For each column, n = 3.

MRT67307 is known to block autophagy by inhibiting ULK1 and ULK2 [56]. Before starting the experiment, it was necessary to find the concentration which totally inhibits autophagy. According to Petherick et al. [56], 10 μM of this compound was enough to inhibit ULK1 and ULK2 in mouse embryonic fibroblast cells. However, autophagy was not assessed in this publication.

Therefore, two stronger concentrations: 0.036 mM and 0.072 mM were tested using starvation to activate autophagy. Cells were incubated 2 hours at 37°C. In 0.036 mM experiment, MRT67307 treated starved cells LC3-I/LC3-II ratio was significantly lower than non-starved MRT67307 treated cells ($p<0.01$) and control cells ($p<0.05$),

suggesting that autophagy was still active. In 0.072 mM experiment, MRT67307 treated starved cells LC3-I/LC3-II ratios were similar to non-starved MRT67307 treated cells and control cells (**fig. 16**), suggesting autophagy activation by starvation was inhibited. Therefore, 0.072 mM was chosen for further experiments to block ULK1 activity in further experiments.

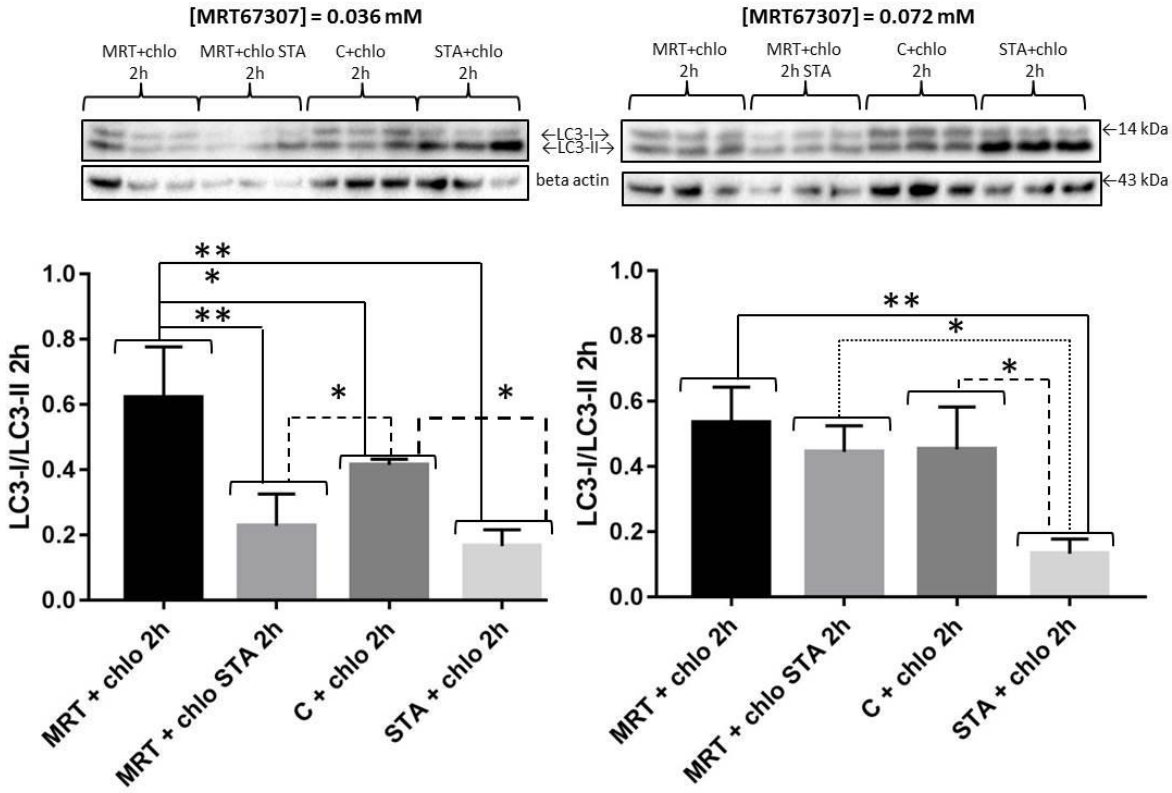

Fig. 16. Effects of ULK1 inhibitor (MRT67307) on the activation of autophagy by starvation. NIH 3T3 cells were incubated 2 hours with either 0.072 mM or 0.036 mM of MRT67307. The lower dose (0.036 mM) was clearly not sufficient as LC3-I/LC3-II ratios of starved MRT67307 treated cells (MRT + chlo STA 2h) were significantly lower than non-starved MRT67307 treated cells (MRT + chlo 2h) and control cells ones (C + chlo 2h). On the other hand, LC3-I/LC3-II ratios of [MRT67307] = 0.072 mM starved cells were similar to those of non-starved MRT67307 cells and control cells. Cells were all treated with chloroquine (chlo). C: control cells. STA: starved cells. Significant differences (*p<0.05, **p<0.01) were determined using a one-way ANOVA followed by a post-hoc Tukey multiple comparisons test for 0.072 mM, and Newman-Keuls multiple comparisons test for 0.036 mM. Error bar: standard deviation. For each column, n = 3.

1.2. The effects of a combination of MRT67307 and Torin 1

As expected in cell lines, starvation activated autophagy by removing the stimuli for growth that activates mTOR. These activities are linked via ULK1 and was confirmed

by MRT67307 inhibition of ULK1. The next step was to see if directly affecting the mTOR kinase could affect autophagy and again if MRT67307 could inhibit this link. Experiments were carried out as following: during the first hour, cells were incubated with either Torin 1 or MRT67307, and then the other compound was added and cells were incubated one more hour. The administration of MRT67307 to Torin 1 treated cells led to an increase of LC3-I/LC3-II ratios (**fig. 17**), which means that autophagy was inhibited, whereas the addition of Torin 1 to MRT67307 treated cells did not activate autophagy. These experiments also showed that the effect of MRT67307 on autophagy was stronger than Torin 1. Surprisingly, a decreased phosphorylation of S6K1 in MRT67307 only treated cells was also noticed. This may suggest broader inhibitory capacity than just ULK1 which was also shown by Ganley et al., in their paper first describing MRT67307 [56].

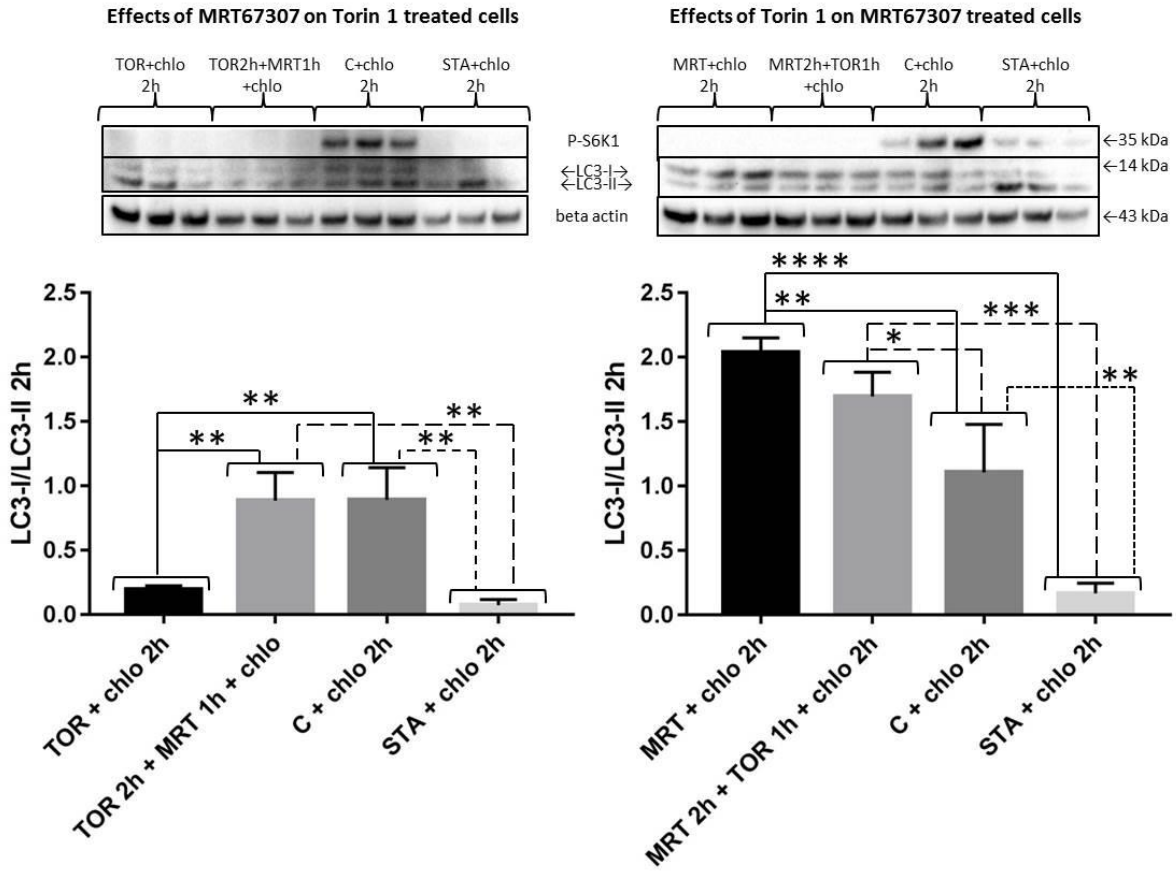

Fig. 17. Administration of both MRT67307 and Torin 1. MRT67307 blocked Torin 1 induced autophagy (TOR 2h + MRT 1h + chlo), whereas Torin 1 could not induce autophagy in MRT67307 treated cells (MRT 2h + TOR 1h + chlo). Cells were all treated with chloroquine (chlo). C: control cells. STA: starved cells, P-S6K1: phospho-S6K1. Significant differences (*p<0.05, **p<0.01, ***p<0.001, ****p<0.0001) were determined using a One-way ANOVA followed by a post-hoc Tukey multiple comparisons test. Error bar: standard deviation. For each column, n = 3.

1.3. Effects of ULK1 knock-out on NIH 3T3 cells autophagy

Since it was known that ULK1 activation led to autophagy activation, the effect of its absence on autophagy was investigated. First siRNA was administrated to NIH 3T3 cells cultured in normal culture medium and medium without serum (necessary for transfection) and incubated 24 hours to see if it was sufficient to knock out ULK1 (cells cultured without chloroquine). This duration was enough to reduce ULK1 protein expression in both media (as shown in **fig 18**). ULK1 expression was stronger in control cells (C) than in starved cells (STA). Surprisingly, the level of phospho-S6K1 was not very strong in control cells (**fig. 18**) but was unchanged in the knock-out cells, starved or not. This suggested that absence of ULK1 was sufficient to prevent and change to mTOR under starvation conditions.

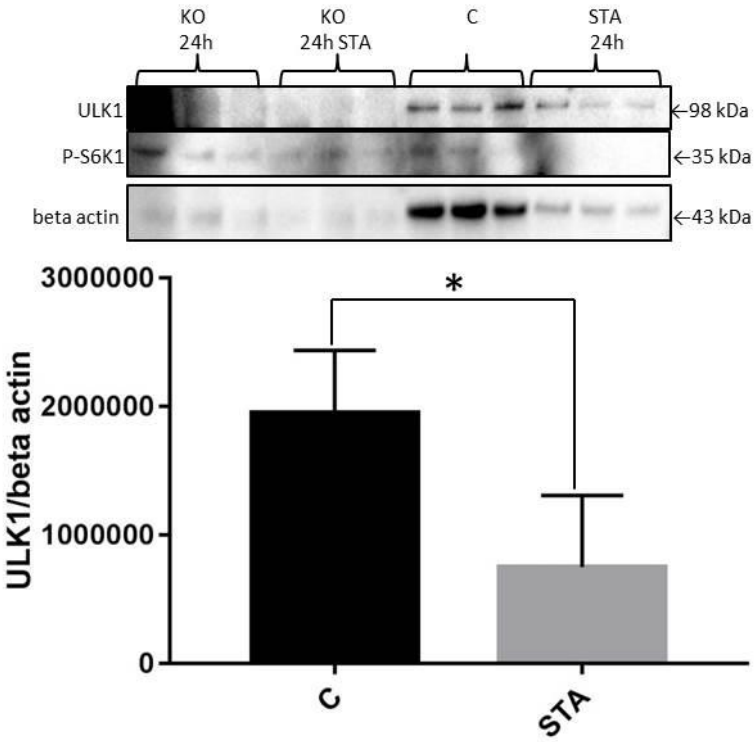

Fig. 18. ULK1 KO test. NIH 3T3 cells were incubated with siRNA during 24 hours. No ULK1 band could be seen in normal media cultured cells (KO 24h) and media without serum cultured cells (KO 24h STA). ULK1 was more strongly expressed in control cells (C) than in starved cells (STA). Cells were cultured without chloroquine. P-S6K1: phospho-S6K1. Error bar: standard deviation. For each column, n = 3. Unpaired Student's t test (*$p<0.05$).

In a repeat of this experiment cultured ULK1 KO cells in normal medium and medium without serum to see if autophagy (by LC3-I/LC3-II ratios) could be activated in the absence of ULK1 (cells cultured with chloroquine at 0.25 mM). It was found that

compared to control cells, autophagy was strongly activated in ULK1 KO starved cells (**fig. 19**). Therefore autophagy could be activated without ULK1 which suggests ULK2 may also be involved and that a pharmacological approach maybe required.

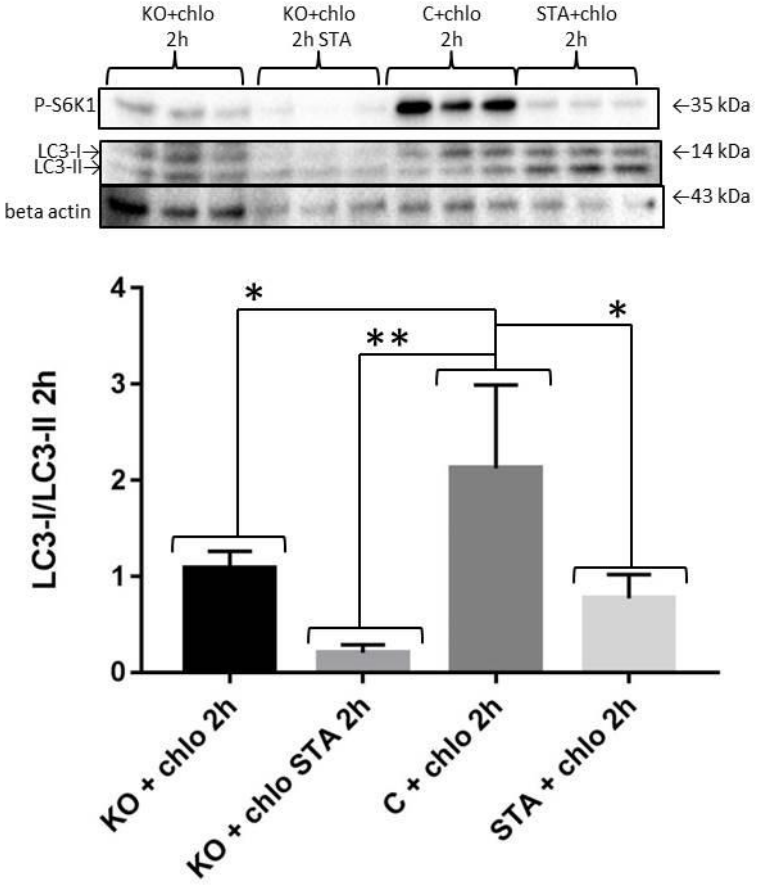

Fig. 19. ULK1 KO autophagy test. ULK1 KO cells were incubated in normal media (KO + chlo 2h) and media without serum (KO + chlo STA 2h). Autophagy was strongly activated in starved ULK1 KO cells. Cells were all treated with chloroquine (chlo). C: control cells. STA: starved cells, P-S6K1: phospho-S6K1. Significant differences (*p<0.05, **p<0.01) were determined using a one-way ANOVA followed by a post-hoc Newman-Keuls multiple comparisons test. Error bar: standard deviation. For each column, n = 3.

2. Effects of mTOR and/or ULK inhibitors on SMG-C6 cells

Although NIH 3T3 cells results confirm MRT67307 can block ULK1/2, they were largely confirmatory of previous studies and not necessarily relevant to salivary gland cells. For that reason SMG-C6 cells were cultured which were previously derived from rat submandibular gland acinar cells. Firstly these cells were incubated with the same concentration of Torin 1 and MRT67307 used for NIH 3T3 cells (as well as chloroquine 0.05 mM). For Torin 1 + MRT67307, Torin 1 was administrated first, and then 1 hour later MRT67307 was added. However, it was discovered that Torin 1 at 0.05 mM was

too toxic as neither LC3-I nor LC3-II bands appeared in both Torin 1 only and Torin 1 + MRT67307 treated cells (**fig. 20**).

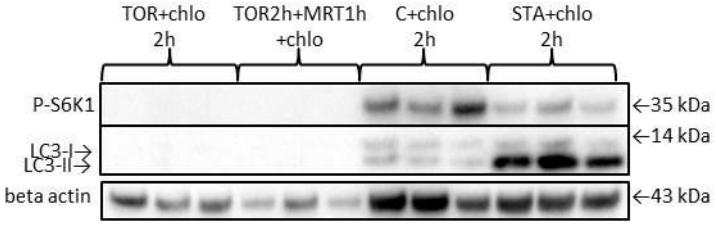

Fig. 20. Administration of both MRT67307 at 0.072 mM and Torin1 at 0.05 mM to SMG-C6 cells. No LC3 bands appeared in Torin 1 (TOR + chlo 2h) and Torin 1 + MRT67307 treated cells (TOR 2h + MRT 1h + chlo). Therefore Torin 1 at 0.05 mM was toxic. Cells were all treated with chloroquine (chlo). C: control cells. STA: starved cells, P-S6K1: phospho-S6K1.

Next Torin 1 was reduced to 0.01 mM while maintaining MRT67307 at 0.072 mM. This time both LC3-I and LC3-II bands clearly appeared, so [Torin 1] = 0.01 mM was the concentration used in subsequent experiments. S6K1 phosphorylation was inhibited as expected. Unlike NIH 3T3 cells, Torin 1- treated SMG-C6 cells failed to induce a change autophagy. Phospho-S6K1 bands were rather strong in starved cells, but remained weaker compared to control cells ($p<0.01$). Since LC3-I/LC3-II ratios of control cells were similar to Torin 1 only treated cells (**fig. 21**) thus further experiments were required to refine the system.

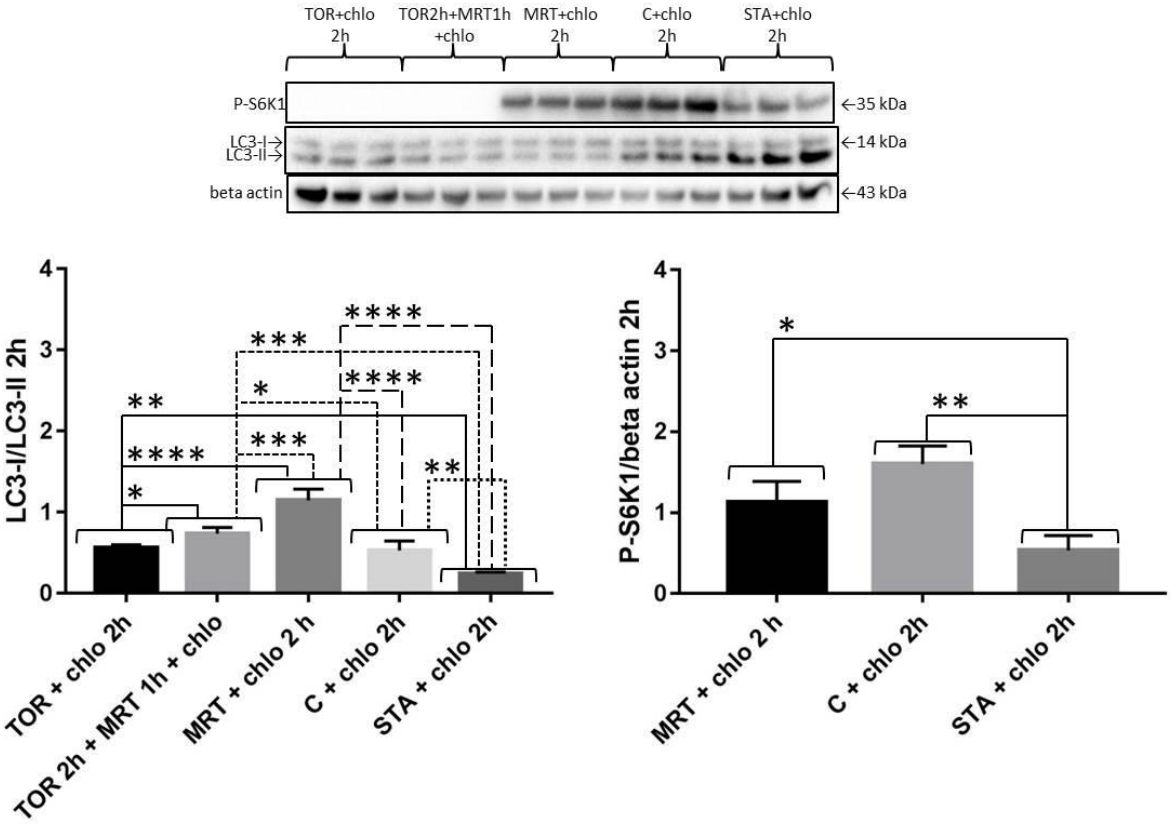

Fig. 21. Administration of both MRT67307 at 0.072 mM (1 h) and Torin1 at 0.01 mM (2 h) to SMG-C6 cells. Both LC3-I and LC3-II bands appeared in Torin 1 (TOR + chlo 2h) and Torin 1 + MRT67307 treated cells (TOR 2h + MRT 1h + chlo 2h), so Torin 1 at 0.01 mM was the right concentration. P-S6K1 bands were rather strong in starved cells but were weaker than control cells. MRT67307 inhibited Torin 1 induced autophagy (TOR 2h + MRT 1h + chlo 2h). Cells were all treated with chloroquine (chlo). C: control cells. STA: starved cells, P-S6K1: phospho-S6K1. Significant differences (*p<0.05, **p<0.01, ***p<0.001, ****p<0.0001) were determined using a one-way ANOVA followed by a post-hoc Newman-Keuls multiple comparisons test for LC3-I/LC3-II and Tukey multiple comparisons test for P-S6K1/beta actin. Error bar: standard deviation. For each column, n = 3.

We also evaluated the effect of Torin 1 on MRT67307 treated cells. Unlike NIH 3T3 cells, SMG-C6 treated Torin 1 cells were not able to induce autophagy. Starvation of these cells did induce autophagy compared to control cells (**fig. 22**).

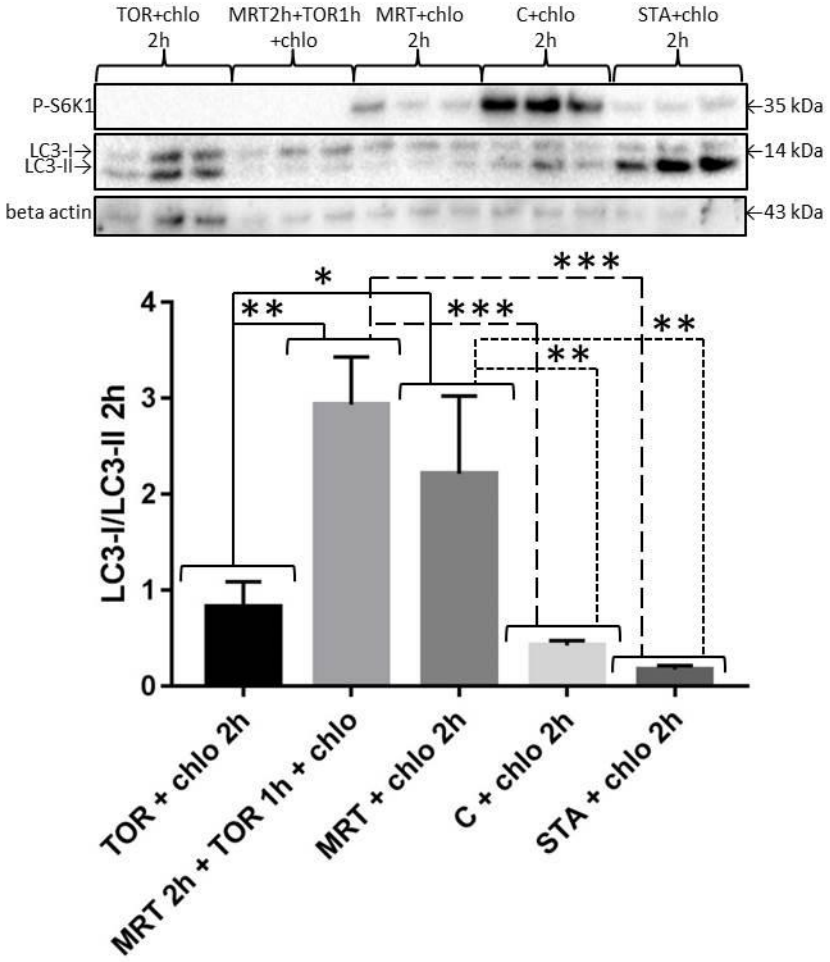

Fig. 22. Administration of both MRT67307 at 0.072 mM (2 h) and Torin1 at 0.01 mM (1 h) to SMG-C6 cells. Torin 1 could not induce autophagy by itself or with MRT67307 (MRT 2h + TOR 1h + chlo). All cells were treated with chloroquine (chlo). C: control cells. STA: starved cells, P-S6K1: phospho-S6K1. Significant differences (*p<0.05, **p<0.01, ***p<0.001, ****p<0.0001) were determined using a One-way ANOVA followed by a post-hoc Tukey multiple comparisons test. Error bar: standard deviation. For each column, n = 3.

3. Effects of mTOR and/or autophagy inhibitors on primary submandibular gland cells

Even though SMG-C6 cells were derived from submandibular gland acinar cells they are immortalized acinar cells and potentially this has altered the mTOR pathway. So it was necessary to culture primary submandibular gland cells to see the effects of Torin 1 and MRT67307 on submandibular gland cells. Various experiments were tried to optimise cell viability since these cells do not last long *in vitro* culture. Initially, we retrieved cells after incubating 1 hour with collagenase, then resuspended in culture medium and cells were seeded in 12 well plates. After administration of drugs (for cells

receiving both Torin 1 and MRT67307, we administrated both drugs simultaneously), cells were incubated 1 hour and then they were retrieved for analysis. Phospho-S6K1 bands were clearly seen in control cells, which meant that mTOR became activated in primary submandibular gland cells. It was noticed that Torin 1 had no effect since S6K1 was phosphorylated in both Torin 1 and Torin1 + MRT67307 treated cells. Concerning autophagy, Torin 1 did not activate it because if it was the case, LC3-I/LC3-II ratio of Torin 1 treated cells would have been lower than control cells ratio. It was not possible to see if MRT67307 could inhibit autophagy as Torin 1 failed to trigger autophagy (**fig. 23**).

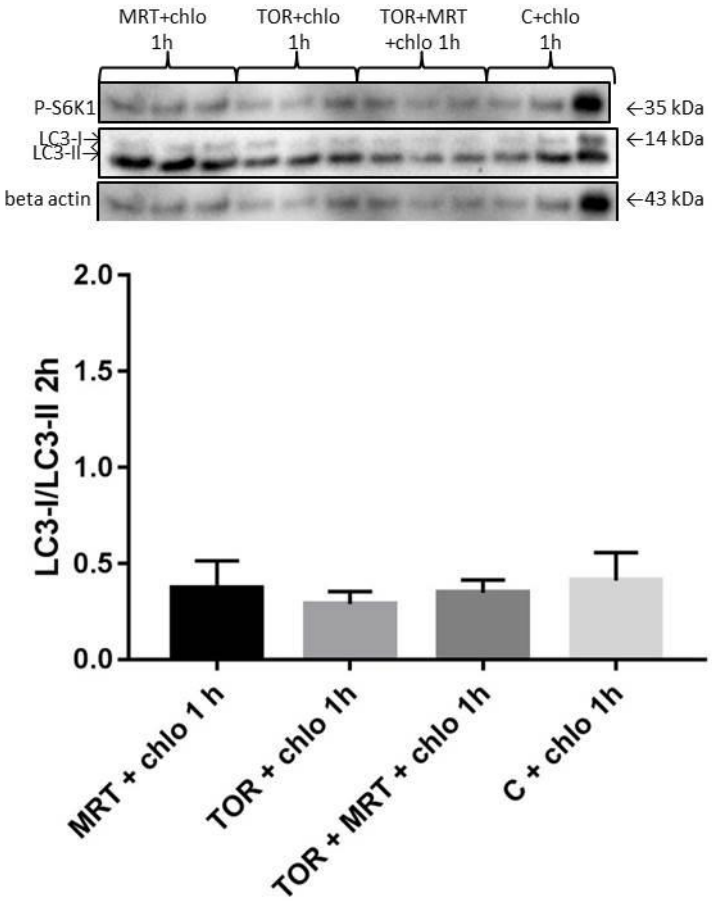

Fig. 23. Administration of both MRT67307 at 0.072 mM and Torin 1 at 0.05 mM to primary SMG cells. S6K1 was phosphorylated in Torin 1 treated cells (TOR+chlo 1h) and Torin 1 + MRT67307 treated cells (TOR+MRT+chlo 1h) so Torin 1 did not block mTORC1. Torin 1 did not favour autophagy since LC3-I/LC3-II ratio of TOR+chlo 1h was not statistically different to control cells ratio (C+chlo 1h). As Torin 1 could not activate autophagy, it was not possible to test the inhibiting effect of MRT67307. P-S6K1: phospho-S6K1. No significant difference was noticed by using a One-way ANOVA followed by a post-hoc Tukey multiple comparisons test. Error bar: standard deviation. For each column, n = 3.

Since Torin 1 did not block mTOR, the concentration of Torin was increased (0.1 mM instead of 0.05 mM) and incubated for 2 hours rather than 1 hour. However, as seen in **figure 24**, despite Torin 1 concentration was stronger and incubation time longer, mTOR was not inhibited (phospho-S6K1 is unchanged) and autophagy was not activated either.

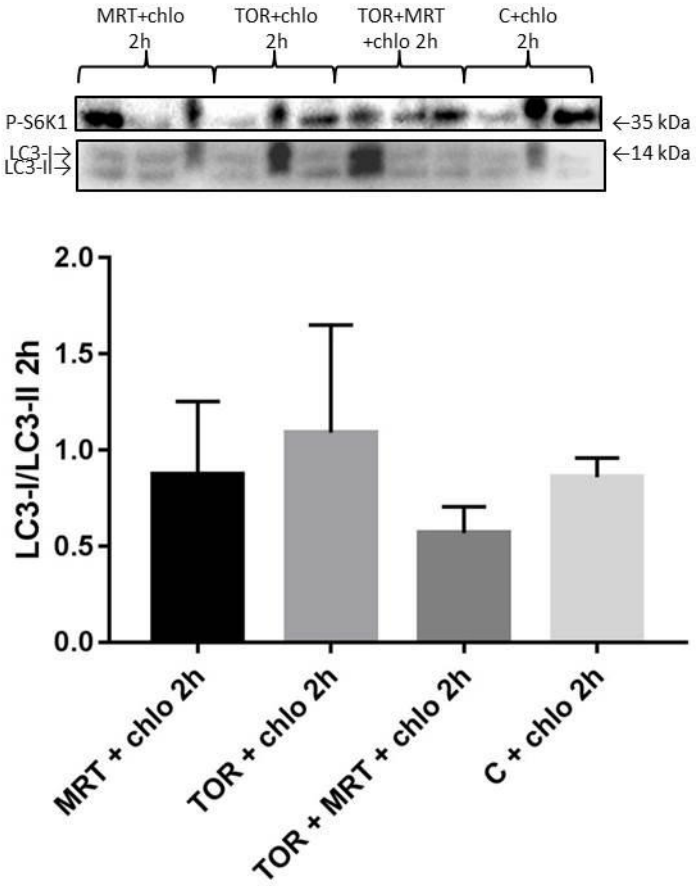

Fig. 24. Administration of both MRT67307 at 0.072 mM and Torin 1 at 0.1 mM to primary SMG cells. S6K1 was phosphorylated in Torin 1 treated cells (TOR+chlo 2h) and Torin 1 + MRT67307 treated cells (TOR+MRT+chlo 2h) so Torin 1 did not block mTOR. Torin 1 did not favour autophagy since LC3-I/LC3-II ratio of TOR+chlo 2h was not statistically different to control cells ratio (C+chlo 2h). Because Torin 1 could not activate autophagy, it was not possible to test the inhibiting effect of MRT67307. P-S6K1: phospho-S6K1. No significant differences were noticed by one-way ANOVA or by a post-hoc Tukey multiple comparisons test. Error bar: standard deviation. For each column, n = 3.

The reason why Torin 1 had no effect was not clear, but it could be hypothesized that administrating this drug immediately after having minced submandibular glands could more efficiently block mTOR. So a new protocol was tried consisting of adding drugs while cells were under collagenase treatment. This time Torin 1 concentration returned to 0.05 mM and incubation time was 2 hours. This protocol was better since no

phospho-S6K1 band appeared in both Torin 1 and Torin 1 + MRT67307 treated cells. Nonetheless, autophagy was not activated again (**fig. 25**).

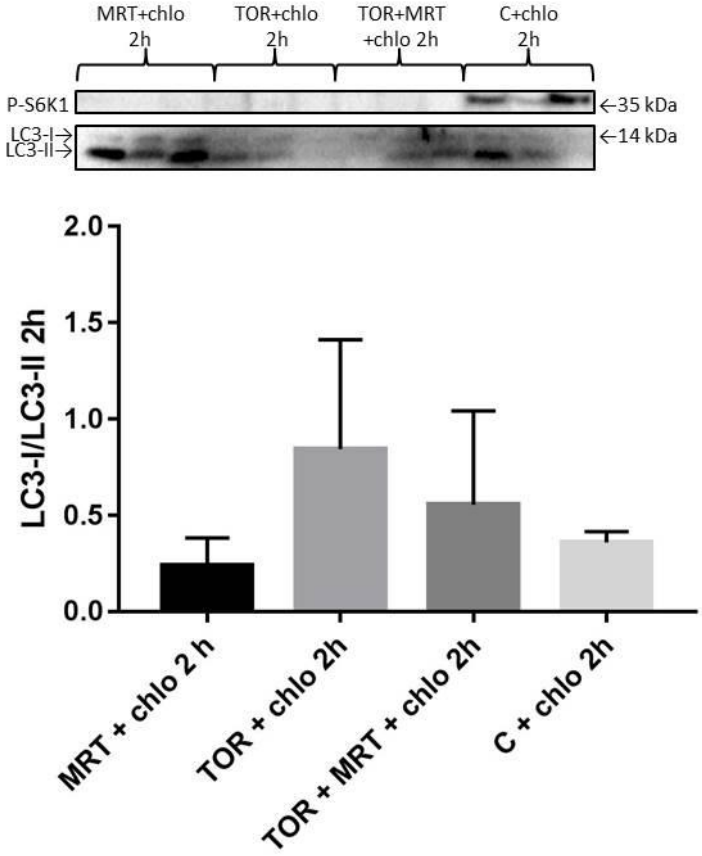

Fig. 25. Administration of both MRT67307 at 0.072 mM and Torin 1 at 0.05 mM during collagenase treatment of primary SMG cells. S6K1 phosphorylation was inhibited in Torin 1 treated cells (TOR+chlo 2h) and Torin 1 + MRT67307 treated cells (TOR+MRT+chlo 2h) so Torin 1 blocked mTORC1. However, Torin 1 did not favour autophagy since LC3-I/LC3-II ratio of TOR+chlo 2h was not statistically different to control cells ratio (C+chlo 2h). Because Torin 1 could not activate autophagy, it was not possible to test the inhibiting effect of MRT67307. P-S6K1: phospho-S6K1. No significant difference was noticed by using a Kruskal-Wallis test followed by a Dunn's multiple comparisons test. Error bar: standard deviation. For each column, n = 3.

Since MRT67307 seemed not to have any effect on autophagy, it was necessary to verify that ULK1 was expressed in submandibular gland cells. **Figure 26** clearly shows that the latter as well as NIH 3T3 cells and SMG-C6 cells contain ULK1.

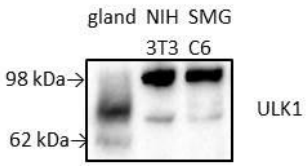

Fig. 26. ULK1 expression in submandibular gland cells, NIH 3T3 cells and SMG-C6 cells.

Discussion

NIH 3T3 experiments showed that when Torin 1 was administrated or during serum starvation, mTOR was efficiently inhibited (loss of phospho-S6K1) and autophagy was activated (LC3-I/LC3-II ratio decreased). Furthermore, the addition of MRT67307 blocked this induction of autophagy. These results confirm previous studies such as Thoreen et al. who tested the effect of Torin 1 on mouse embryonic fibroblasts [132], and Petherick et al. who administrated MRT67307 on the same cells [56]. These studies confirm the usefulness of Torin 1 and MRT67307 as tools to assess the link between mTOR and autophagy. So in NIH 3T3 cells, autophagy is ULK1 dependent.

In SMG-C6 cells the same drug combinations were used to assess the linkage between mTOR and autophagy. These studies showed that Torin 1 was efficient in inhibiting mTOR kinase as levels of phospho-S6K1 were undetectable after treatment. If ULK1 was active this should have been sufficient to activate autophagy and modify the LC3-I/LC3-II ratio. In none of the drug combinations and concentrations tried on SMG-C6 was this found. If MRT67307 was administrated to Torin 1 treated cells, autophagy was blocked despite the fact that mTOR remained inhibited, whereas the administration of Torin 1 to MRT67307 treated cells, it inhibited mTOR but did not activate autophagy. These results suggest that SMG-C6 do not contain a functional ULK1 kinase or at least the kinase does not act in the same way as in NIH 3T3 cells.

Primary submandibular gland cell culture confirmed our previous studies which showed that in normal healthy salivary gland tissue mTOR is inactive. During collagenase treatment it quickly became activated possibly due to impending mitosis [26]. Thus administration of Torin 1 during collagenase treatment should block mTOR and activate autophagy if ULK1 is present and functional. Despite some initial problems mTOR activation was blocked by Torin1 but did not alter autophagy. This suggests that like SMG-C6 cells and primary submandibular gland cells have mTOR independent autophagy.

ULK1 knock-out in NIH 3T3 cells revealed that autophagy could occur in serum starved cells. This result is similar to Kundu et al. experiment [57]. They observed an activation of autophagy in ULK1 knock-out mouse embryonic fibroblast cultured in glucose deficient medium. ULK2, which is structurally similar to ULK1, likely compensated the loss of ULK1. Therefore the inhibition of autophagy by MRT67307 (alone or combined with Torin 1) in NIH 3T3 and probably SMG-C6 cells were caused by inhibition of both ULK1 and ULK2. However, in some cell lines, such as HEK293

cells [150, 151], ULK1 knock-out but not ULK2 blocks autophagy. Besides our experiment revealed that ULK1 expression was significantly decreased in starved cells ($p<0.05$, **fig. 19**). At first glance it appears aberrant, but Nazio et al. [154] and Allavena et al. [157] also noticed also downregulation of ULK1 levels after few hours of starvation. They considered that as a mechanism protecting cells from excessive autophagy.

MRT67307 sometimes decreased phospho-S6K1 expression in NIH 3T3, SMG-C6 and primary submandibular gland cells. The reason is not clear, but it is known that IKK2 inhibition favours S6K1 degradation [139]. According to Clark et al. [140], MRT67307 can inhibit IKKε but not IKK2. However, the concentration they tested was 10 µM whereas the working concentration used in this thesis was 0.072 mM.

In immortalised cells autophagy was sometimes significantly de-activated by MRT67307 (alone or combined with Torin 1) when compared to untreated cells. There could be many reasons: in many cells, basal autophagy is activated without stimuli [141] and is dependent of ULK1 and ULK2 [144, 145]. This can explain why LC3-I/LC3-II in MRT67307 (alone or combined with Torin 1) treated cells was stronger than in control cells. It was also demonstrated that ethanol could activate autophagy in many cells [142, 143]. A concentration as little as 50 mM was enough to activate autophagy in mouse astrocytes [142]. For disinfection, we sprayed multi-well plates with IMS 70% which contained ethanol: maybe ethanol vapour induced autophagy. Besides, Marino et al. [171] demonstrated that acidic pH could trigger autophagy in human melanoma cells. Since acidification occurs during cell culture, this could also be a possible explanation of autophagy activation in both NIH 3T3 and SMG-C6 control cells too. However, pH modulation of autophagy is cell type dependent, since Zhao et al. [172] noticed that in rat cardiomyocytes if pH was acidic autophagy was inhibited, while if pH was alkaline it was activated. Suk et al. [173] also observed an upregulation of autophagy in GFP-LC3 HeLa cells when they were subjected to alkaline stress.

In starved NIH 3T3 and SMG-C6 cells, despite the fact that autophagy was activated, mTORC1 was not totally inhibited in almost all experiments as weak phospho-S6K1 bands were detected. This is not aberrant as Pirkmajer et al. [152] who tested the effects of serum starvation on many cell lines (primary human myotubes, rat L6 myotubes, HEK293 cells) observed a decrease of phospho-S6K1 bands intensities but they did not disappear even after 24 hours starvation. Carroll et al. [118] who carried out experiments on senescent cells observed that mTOR was significantly activated when they were starved. They hypothesized that since primary cilias were

defective in these cells, growth factor signalling could not be inhibited. Moreover their autophagy was stronger than in young cells: this certainly provided a high amount of amino acids, and thus maintained mTOR activity. Chen et al. [153] who cultured CFP-LC3 NRK cells noticed a decrease of phospho-S6K1 expression and increase of autophagy up to 4 hours, then an increase of phospho-S6K1 and a decrease of autophagy up to 12 hours. Besides, the intracellular concentration of amino acids increased with time. They hypothesized that initial mTOR inhibition was due to the lack of growth factors provided by serum, leading to the activation of TSC which blocked mTOR and favoured autophagy. However, as autophagy enhanced amino acids uptake, intracellular level of amino acids increased and when it was strong enough mTOR was reactivated leading to a decrease of autophagy. Pan et al. [158] noticed that in TSC1 deficient bone marrow derived macrophages, mTOR, phospho-AMPKα and autophagy were strongly activated. Inhibition of mTOR by rapamycin decreased autophagy and phospho-AMPKα as well. Therefore, sustained activation of mTOR caused by TSC1 knock-out phosphorylated AMPKα, thus activating autophagy. However, TSC1 and TSC2 knock-out effects are cell type dependent. Di Nardo et al. [159] noticed that in mouse embryonic fibroblasts, mTOR activation led to decrease of LC3-II level in both TSC1 and TSC2 knock-out cells, whereas in TSC2 knock-out rat hippocampal neurons LC3-II expression increased. Nonetheless, LC3-II accumulation in neurons was not mTOR dependent as rapamycin administration had no effect, but was due to ULK1 phosphorylation at Ser555 by AMPK.

To sum up, experiments in the present study showed that ULK1 was essential for mTOR dependent autophagy in NIH 3T3 but ULK2 could take over if ULK1 was knocked-out, at least in NIH 3T3 cells. Therefore we confirmed what was admitted in the literature, and the drugs used were effective. A simultaneous activation of mTOR and autophagy was possible in both NIH 3T3 and SMG-C6 cells when they were serum deprived but as mTOR activity was weak, this activation was certainly due to the increase of intracellular amino acids produced by proteins degradations. Therefore what we observed was autophagy activation of mTOR but not the opposite. mTOR inhibition by Torin 1 did not upregulate autophagy, meaning that autophagy activation was mTOR independent. Concerning primary submandibular gland cells, autophagy activation was at least partly mTOR independent since Torin 1 could block mTOR but this inhibition did not activate autophagy. So there is probably no link between mTOR and autophagy in mouse submandibular gland, at least under certain conditions. The next step was to

irradiate mouse submandibular gland in order to see how mTOR and autophagy activation can influence salivary gland functions.

E. IRRADIATION EFFECTS ON MOUSE SALIVARY GLANDS

Introduction

Many researchers carried out experiments on irradiation effects on salivary glands. Following irradiation, two phases with different injuries can be observed: from day 0 to 60 is the acute phase characterised by a 50% reduction of saliva flow rate, a glandular atrophy and a fall of acinar cells number. Water and protein composition of saliva are modified as well [197]. From day 60 to 240 is the chronic phase characterised by a rise of fibrosis and dental caries, a fall of parenchymal cells number, blood vessel damage xerostomia, chronic inflammation and mucositis [8, 48]. Unfortunately most of experiments were performed on parotid glands. Morgan-Bathke et al. papers give details on mTOR and autophagy activation following irradiation [47, 48] on mouse parotid glands, but their papers do not mention if mTOR and autophagy can be activated beyond one week. The minimal dose which damage salivary glands remains unknown as well. Hence, this chapter is mainly dedicated on the damaging effects of different irradiation dose on mouse submandibular glands, on mTOR and autophagy activation and saliva flow.

Methods

For irradiation, we used a gamma irradiator Gp 1200. Mice were placed in a metal tube and were free to move inside. Firstly dose escalation study was carried out to find the minimal dose activating mTOR and autophagy. ICR mice were irradiated at 1, 3, 5, 7, 9 and 11 Gy (2 mice/dose) and their SMG were extracted 2 and 4 weeks later (1 mouse/dose sacrificed at each time point). Secondly, ICR and C57BL/6 mice were irradiated at 11 Gy and their SMG were extracted 3 hours, 1, 5 and 7 days later (1 mouse/strain sacrificed at each time point) since mTOR and autophagy seemed not to be activated in the dose escalation study. Thirdly irradiation effects on salivary gland function was evaluated. ICR mice were irradiated at 11 Gy. At different time points up to 60 days following irradiation, mice were anaesthetized in chamber with isoflurane. After few minutes, when mice were well anesthetized, 200 µL pilocarpine (0.1 mg/mL in saline) was intraperitoneally injected. After 5 to 10 minutes, once breathing rate was seen to increase, a piece of filter paper was put in their mouth during 5 minutes or 10 minutes. Then papers were retrieved and put into ice cooled tubes. As paper + tubes were pre-weighed, it was possible to weigh the amount of saliva retrieved. To eluate saliva, the base of tubes was cut and these tubes were put into new Eppendorf tubes.

Next 100 µL PBS was added to the papers and tubes were centrifuged. At the end we obtained a mixture of PBS + saliva.

In all experiments, extracted SMG (stored at -20°C) were put in 5% w/v of an ice-cold homogenization buffer containing 1% Triton X-100, 1 mM EDTA and a 1% v/v dilution of protease inhibitor cocktail set 1 (Merck Chemicals Ltd, Nottingham, UK) or RIPA buffer with the same protease inhibitor cocktail and homogenated with Ultra-Turrax TP18/10 or MP FastPrep-24. Next, samples were placed in Sigma 1-13 Centrifuge and centrifuged at 10000 rpm (~7043 g) and supernatants were collected. AQP5 expression, mTOR and autophagy activation were assessed by using Western blot (as described in page 72) and immunohistochemistry, H & E staining was used to evaluate irradiation induced damages. Coomassie and PAS staining were also performed on SMG homogenates to detect protein and mucin expression variations following irradiation respectively. Samples were mixed with DTT (reducing agent) and lithium dodecyl sulfate (anionic detergent for denaturing native proteins which can replace sodium dodecyl sulfate), boiled at 100 °C for 3 minutes. After having performed SDS-PAGE (NuPAGE Novex 4-12% Bis-Tris Gels), gels were coloured with Coomassie blue, and destained with 10% acetic acid. For PAS staining, gels were incubated in black trays containing periodic acid solution at 20 g/L for 15 minutes with gentle shaking. After washing with ultra-pure water (2 x 5 minutes), they were incubated in black trays containing Schiff's reagent for 90 minutes with gentle shaking, and then washed with Milli-Q water. Mice and SMG weights were also measured since both were supposed to decrease following irradiation.

Results

1. Dose escalation study (2 and 4 week endpoints)

As new users of the irradiator a dose escalation study was performed first in order to find the minimal dose which would damage the salivary glands. Two and four weeks were chosen as endpoints based on previous studies. Histology and immunohistochemistry were used to assess damage to the salivary glands. Whole body irradiation was used as the only irradiator available. Lead shielding of the rest of the body was not performed as used by other groups since it was not approved by the veterinary surgeon due to concerns regarding regulation of breathing and contamination. As well as damage salivary glands were also assessed biochemically for the activation

of mTOR pathway and any alteration in autophagy with a view to determining if, like the ligation model, mTOR and autophagy would be synchronously activated.

1.1. H & E staining

For morphological changes following irradiation, H & E staining was performed on ICR mice gland slices. Microscopic analysis (**fig. 27 a & b**) revealed that in 2 weeks glands, doses less than 5 Gy had no apparent effects. Greater than 5 Gy caused some significant changes such as infiltration of inflammatory cells, fibrosis and vacuolisation. These changes were more apparent with higher doses; however, damage could only be seen in some portions of tissue sections.

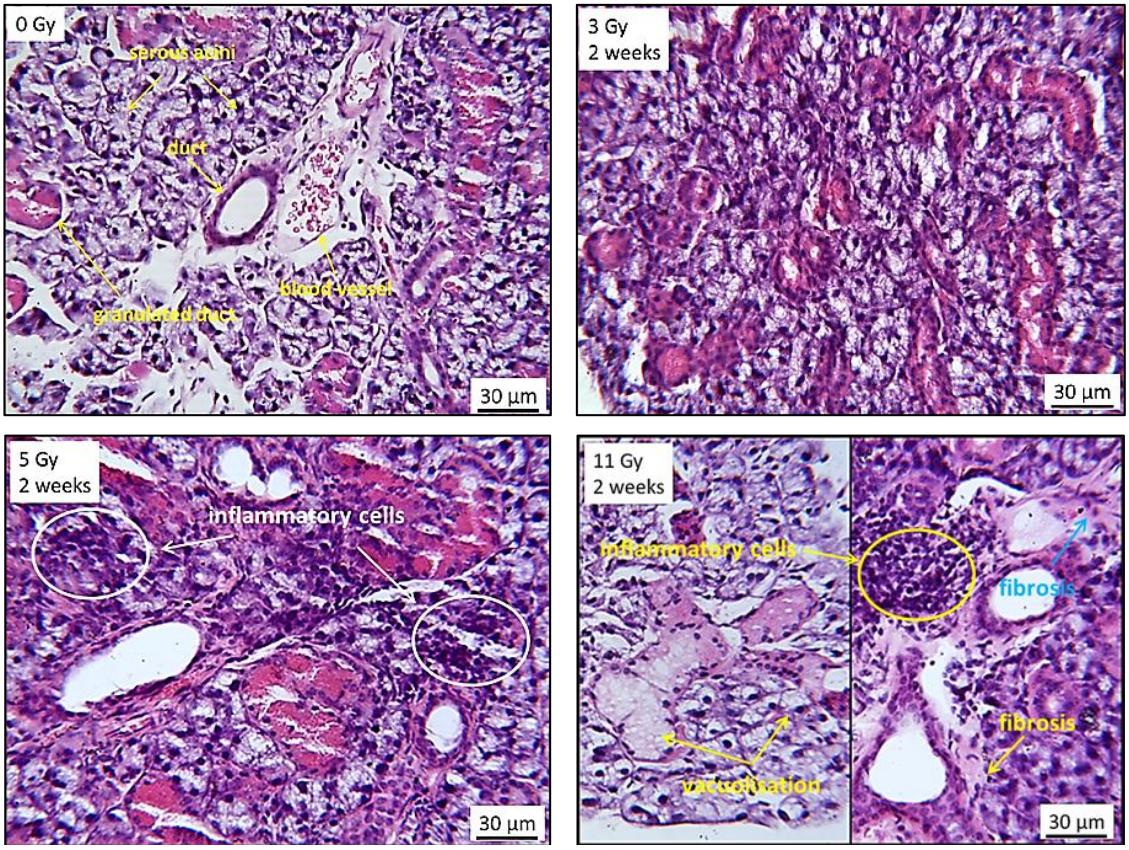

Fig. 27 a. H & E staining of ICR mice submandibular glands 2 weeks after irradiation. Doses less than 5 Gy had no effects. From 5 Gy, infiltration of inflammatory cells occurred. In addition fibrosis, vacuolisation of ductal and acinar cells also occurred.

Four weeks after irradiation glands appeared less damaged than at 2 weeks which suggests some recovery may have occurred. Generally there were fewer areas of damage and some gland sections appeared normal (**fig. 27 b**).

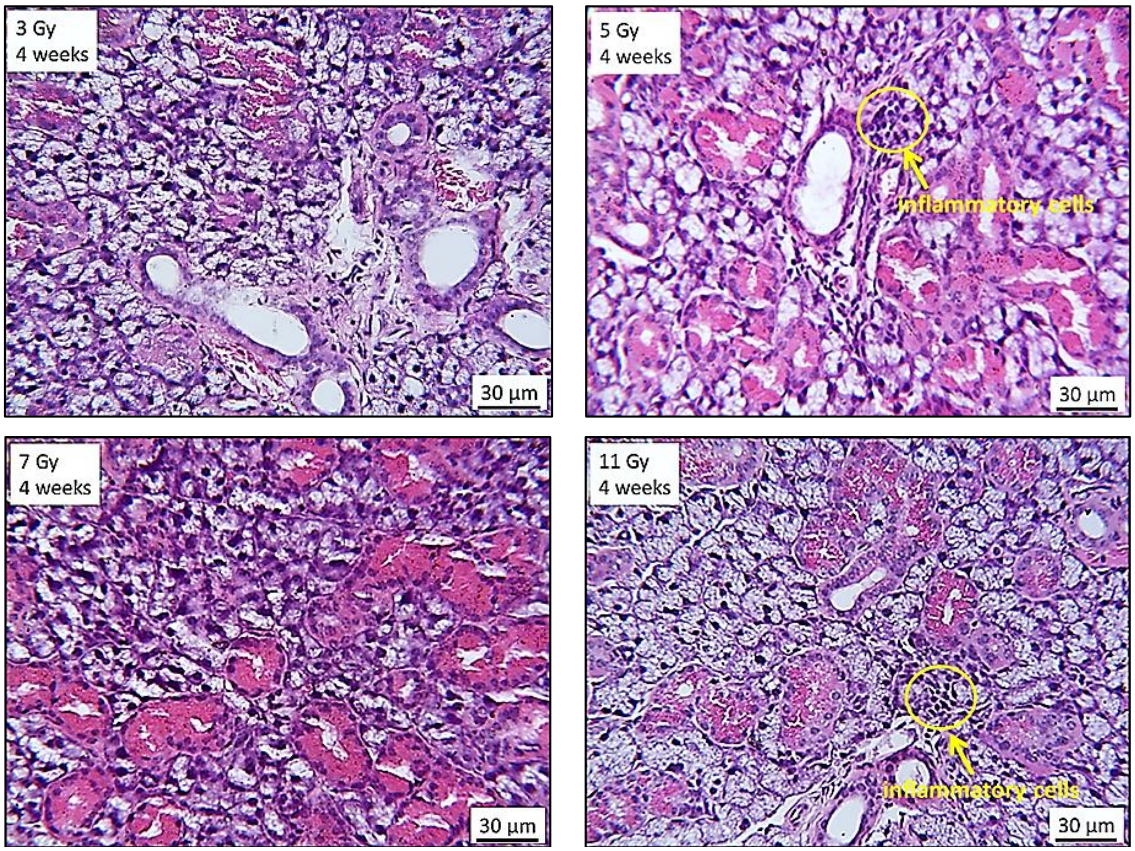

Fig. 27 b. H & E staining of ICR mice submandibular glands 4 weeks after irradiation. Doses less than 5 Gy had no effects. From 5 Gy, inflammatory cells could be observed but they were less numerous and the overall aspect is better compared to 2 weeks glands. Some heterogeneity occurred; the 7 Gy gland appeared normal, suggesting this mouse was less sensitive to IR and/or its healing capacity was stronger.

1.2. mTOR and autophagy activation studies

To determine if mTOR was activated by irradiation, western blot was performed using anti-phospho-4E-BP1 (Thr37/46) and anti-phospho-S6K1 (Ser240/244) antibodies. Concerning 4E-BP1, we can see several bands in the ligated sample (**fig. 28**) because 4E-BP1 can have 3 forms: α which is non-phosphorylated (non-activated) and its molecular weight is the smallest, β which is moderately phosphorylated and its molecular weight is intermediate, and γ which is hyperphosphorylated and its molecular weight is the greatest [128].

Concerning 4E-BP1 (**fig 28**), irradiated samples had only one band at the same level as the non-irradiated sample. The phospho-S6K1 blots show a few bands in irradiated (1 Gy 4 weeks, 5 Gy and 7 Gy 2 weeks) and none in non-irradiated glands (labelled "0"). A sample of previously ligated salivary gland was used as a positive control.

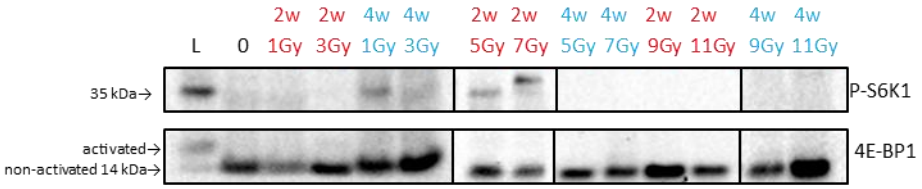

Fig. 28. Phospho-4E-BP1 (Thr37/46) and phospho-S6K1 (Ser240/244) western blots of irradiated ICR mice submandibular glands. Although S6K1 seemed to be activated in some irradiated samples. P-4E-BP-1: phospho-4E-BP1, P-S6K1: phospho-S6K1. 2w = 2 weeks, 4w = 4 weeks, L = ligated gland (4E-BP1 and S6K1 positive control), 0 = non-irradiated gland.

For autophagy activation detection, LC3 antibody was used to stain LC3-I and LC3-II to provide a ratio indicative of autophagy flux. Although LC3-II amount increases when autophagy is activated, observing only LC3-II band intensity is not accurate as LC3-II can be degraded by autophagy and the sensitivity of antibodies to LC3-II can be different than LC3-I [129].

Only a slight variation in LC3-I/LC3-II ratios occurred following 1 and 3 Gy irradiation compared to non-irradiated controls. In ligated gland sample, LC3-I band intensity was stronger than LC3-II (**fig. 29**). It is not surprising as when autophagy is activated, LC3-II can be strongly degraded by lysosome and we did not use lysosomal inhibitor [148]. However as presented in the next chapter our current understanding is that in the 2 week ligated gland autophagy is quiescent as inclusion of chloroquine did not alter the LC3-I/LC3-II ratio in ligated glands.

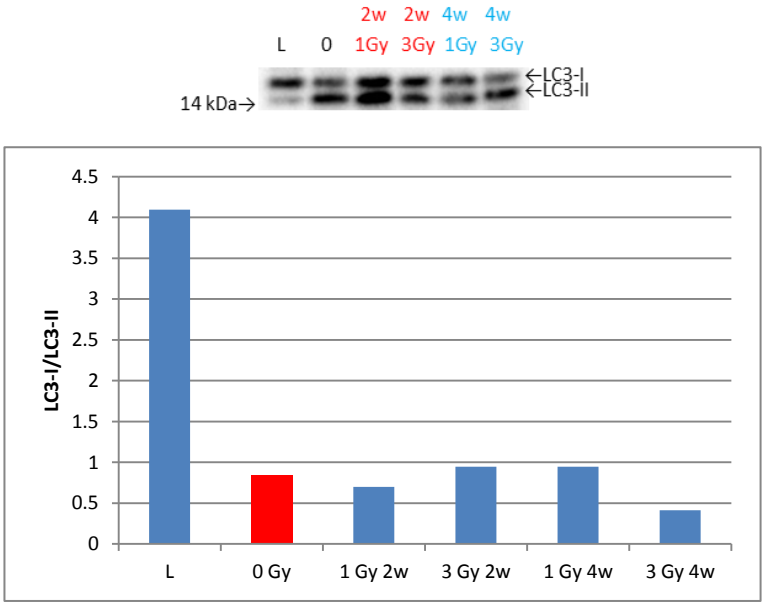

Fig. 29. LC3 western blot of 1 Gy and 3 Gy irradiated ICR mice submandibular glands. Autophagy was not activated in irradiated glands. 2w = 2 weeks, 4w = 4 weeks, L = ligated gland (autophagy positive control).

LC3 ratios of 5 to 11 Gy irradiated glands (**fig. 30**) suggested modest changes in flux that was probably not different to control samples. However not enough control samples were analysed for a statistical comparison.

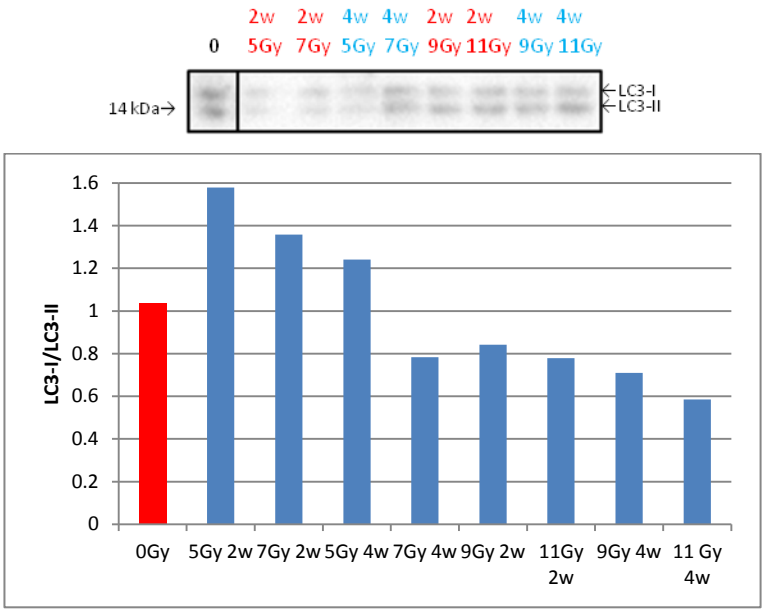

Fig. 30. LC3 western blot of 5 to 11 Gy irradiated ICR mice submandibular glands. No autophagy activation. 2w = 2 weeks, 4w = 4 weeks, L = ligated gland (autophagy positive control).

Immunohistochemical staining of submandibular glands was undertaken to confirm western blot results. Again anti-phospho-S6K1 (Ser240/244) antibody for mTOR activation, but anti-ATG5 antibody was chosen for autophagy activation since a previous study, Morgan-Bathke et al. [47], suggested it was more useful than LC3 antibody on tissue sections. Although some staining was observed in irradiated samples the same staining of granular tubular ducts also occurred in the non-irradiated and secondary only control (**fig. 31 a & b**).

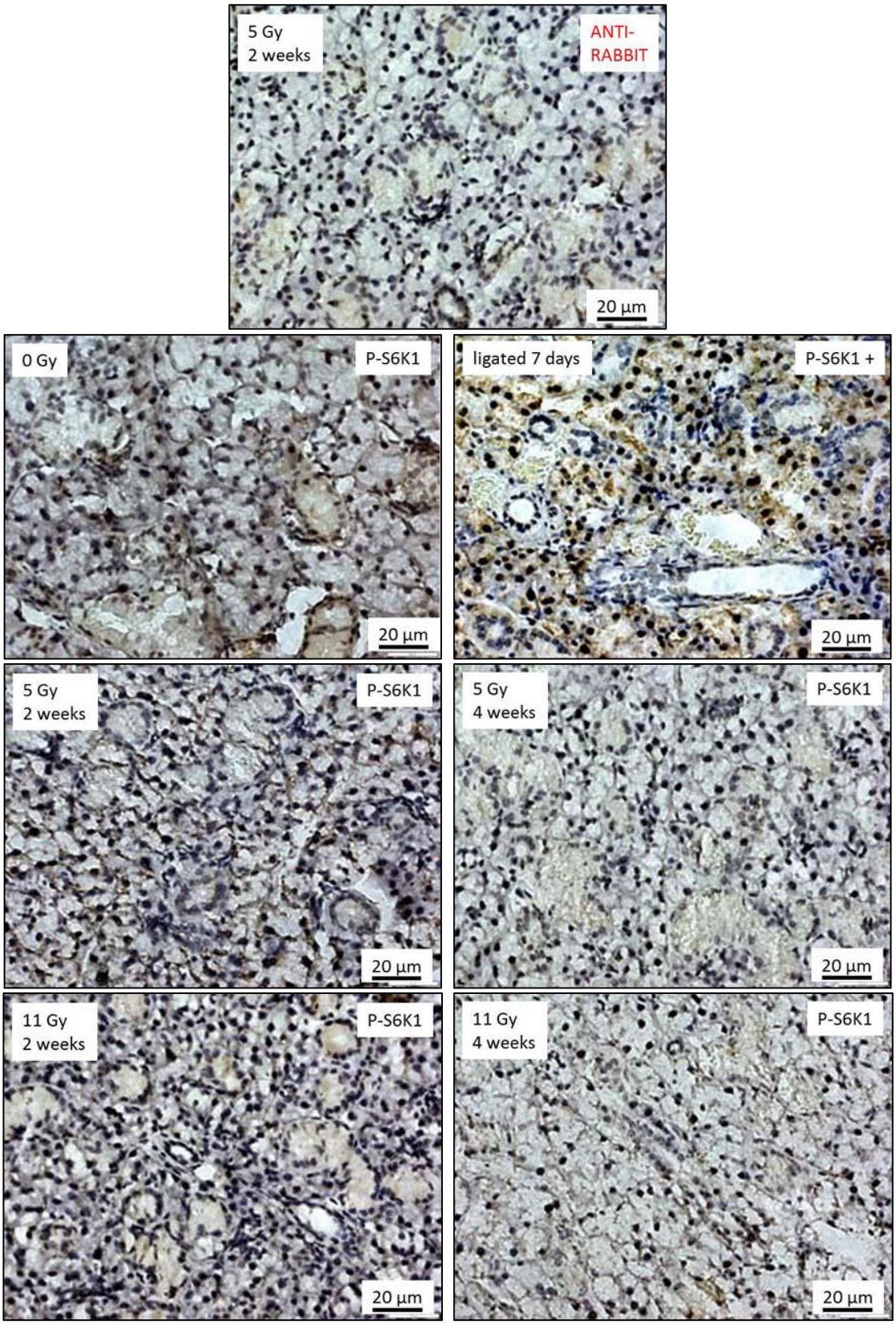

Fig. 31 a. Immunohistochemical staining of ICR mice submandibular glands using anti-phospho-S6K1 (Ser240/244) antibody. Occasional ductal staining occurred in all samples including non-irradiated glands and the secondary only control (anti-rabbit) and thus should be considered background staining. Ligated 7 days = positive control. Anti-rabbit = negative control.

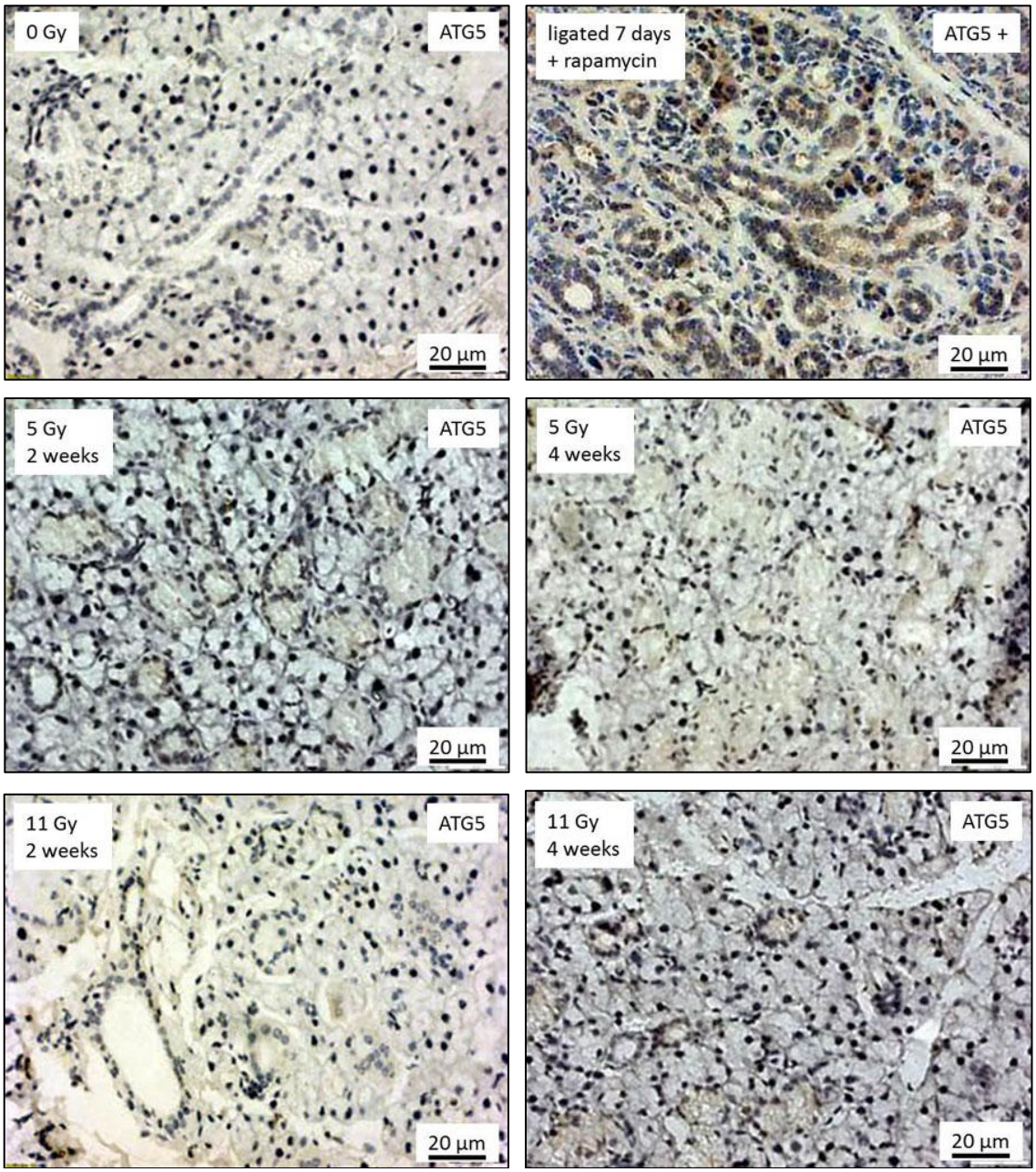

Fig. 31 b. Immunohistochemical staining of ICR mice submandibular glands using anti-ATG5 antibody. No irradiated sample showed autophagy activation. Ligated 7 days + rapamycin = positive control.

1.3. Aquaporin 5 expression in tissue sections

For an assessment of salivary secretory function AQP5 was studied. Initially western blots suggested that AQP5 was cleaved in all samples. To resolve this problem, samples of irradiated gland and muscle homogenates were prepared with or without DTT or boiling. However, in **figure 32**, all samples showed AQP5 was cleaved: no band at 28 kDa, whereas there were bands at ~20 kDa, ~10 kDa and 6 kDa.

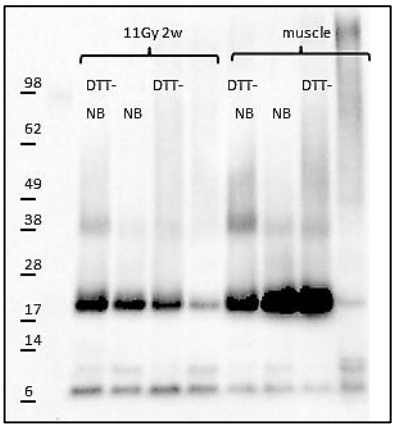

Fig. 32. AQP5 western blot of 11 Gy 2 weeks submandibular gland and muscle. In all samples AQP5 was cleaved, whether the sample was without DTT (DTT-) and/or not boiled (NB) as there were bands at ~20kDa, ~10 kDa and 6 kDa but not at 28 kDa.

In contrast, immunohistochemistry of AQP5 worked rather well. In non-irradiated glands (0 Gy **figure 33)**, apical staining of acinar cells was apparent (as previously reported). Furthermore in all samples, whatever the dose, this apical staining was apparent suggesting irradiation did not impair AQP5 expression.

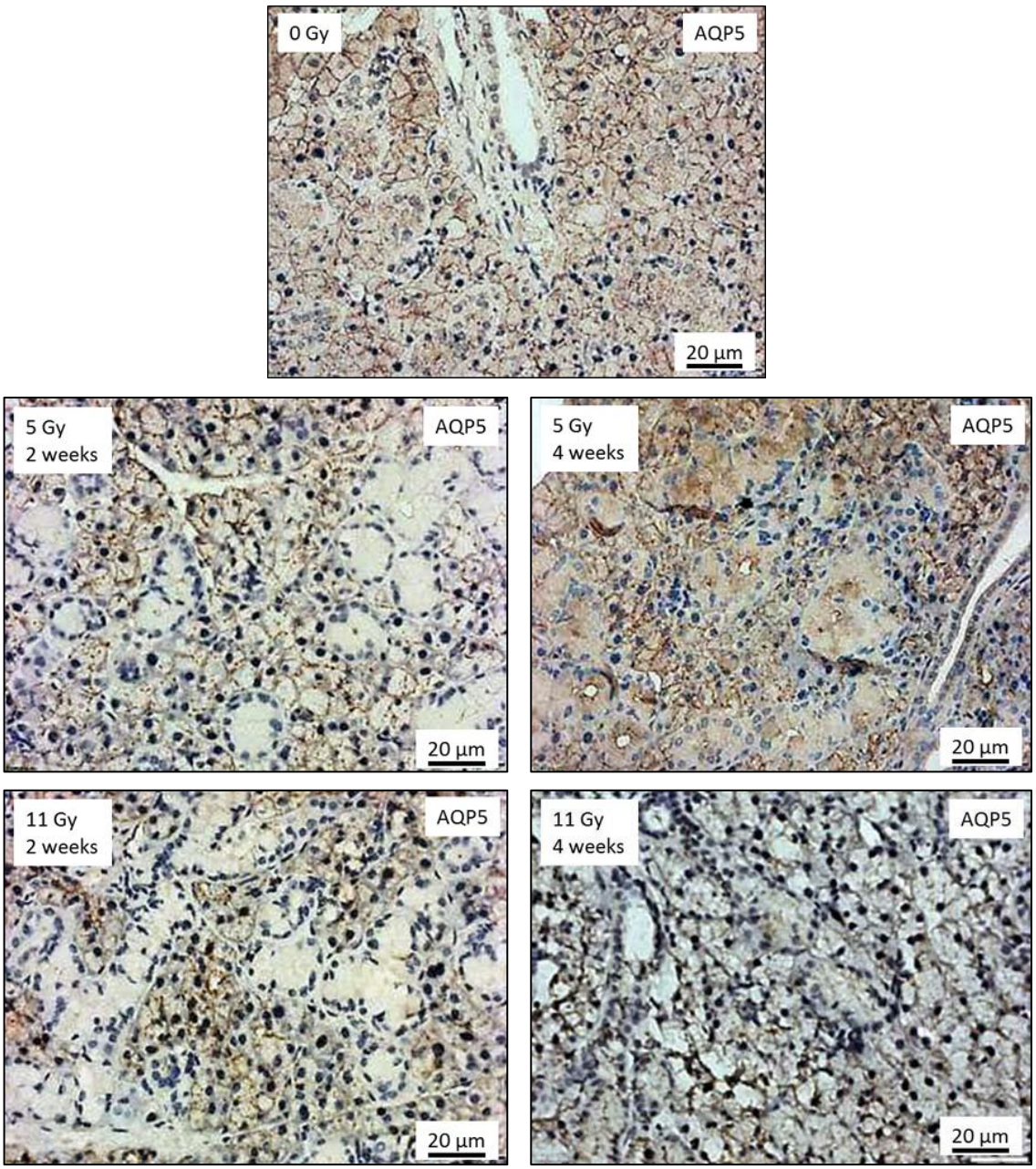

Fig. 33. Immunohistochemical staining of ICR mice submandibular glands using anti-AQP5. Whatever the dose and the time point, there was no decrease of AQP5 expression.

1.4. Coomassie blue and PAS staining

Coomassie staining did not show significant change in proteins expressions, and PAS staining revealed mucin bands intensities were rather similar whatever the irradiation dose and the extraction time (**fig. 34**). Therefore irradiation did not affect proteins and mucin synthesis.

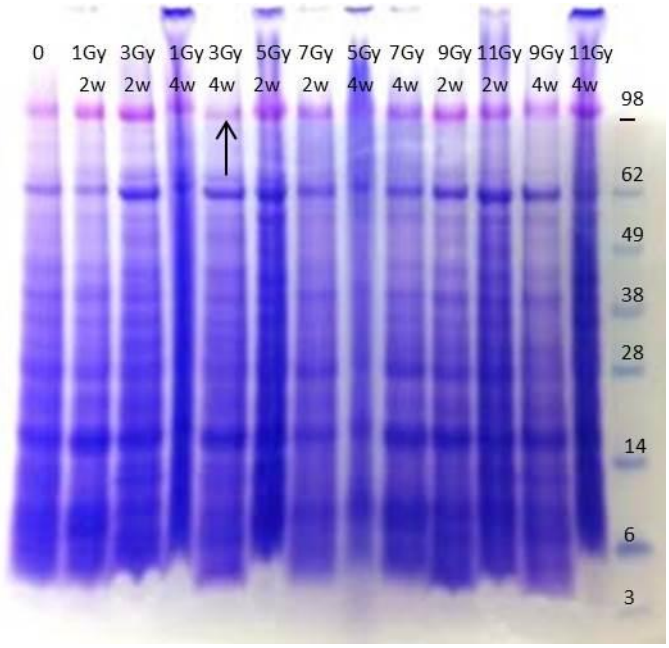

Fig. 34. Coomassie and PAS staining of submandibular glands homogenates. Proteins and mucin (arrow) bands intensities did not significantly change whatever the irradiation dose and the time of extraction. 0: non-irradiated gland; 2w: 2 weeks following irradiation; 4w: 4 weeks following irradiation.

2. Strain comparison study (0-7 days)

The results of the first dose escalation study suggested that whatever the dose, neither mTOR, nor autophagy was activated, 2 and 4 weeks after irradiation. This could be due to transient activation. Therefore, shorter time points using a single dose (11 Gy-maximum permitted dose) end-point study was performed. In addition, since other studies had suggested strain differences in radio-sensitivity [130, 137], ICR and C57BL/6 were chosen as a comparison (ICR had been used in the previous dose escalation study). They were irradiated at 11 Gy and glands were extracted 3 hours (D0), 1 day (D1), 5 days (D5) and 7 days (D7) following irradiation.

2.1. H & E staining

Except the ICR 0 Gy and D0 glands in which inflammatory cells were detected, no significant differences were observed between control glands and irradiated ones (**fig. 35**).

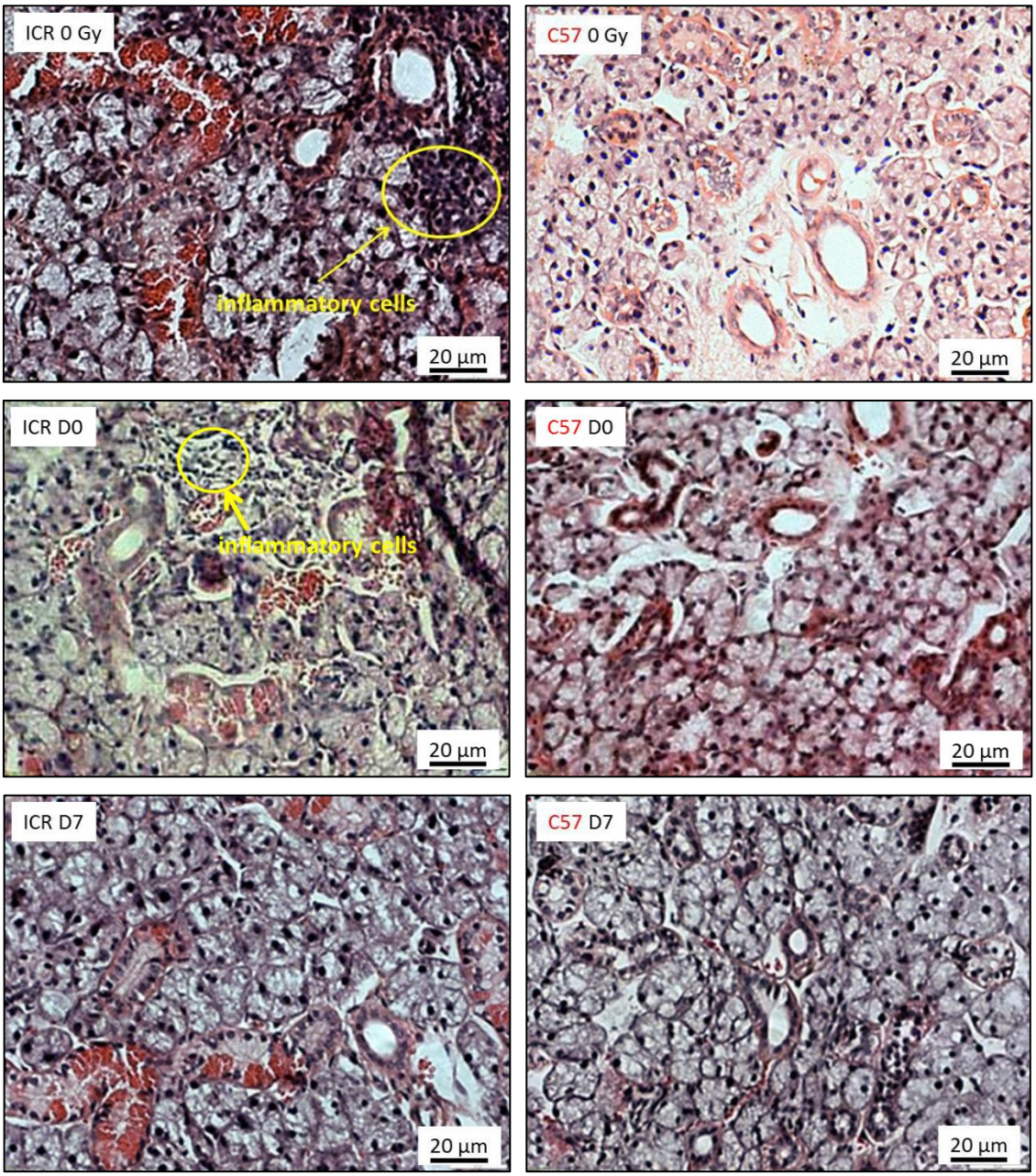

Fig. 35. H & E staining of ICR and C57BL/6 mice submandibular glands. No obvious changes occurred after irradiation except in ICR 0 Gy and D0 (3 hours) glands in which inflammatory cells could be seen.

2.2. mTOR and autophagy activation studies

Western blot showed that S6K1 was strongly phosphorylated at D5 and D7 in ICR mice. Concerning C57BL/6 mice, we could see a weak phosphorylation in 0 Gy, D0 (3 hours) and D1 glands, whereas in D5 and D7 glands, they were more strongly phosphorylated, so mTOR activation in D0 and D1 glands was probably not due to irradiation (**fig. 36 A & C**).

Concerning autophagy activity, we could see a variation of LC3-I/LC3-II value with time in both strains. In both ICR and C57BL/6, the ratios decreased at D0 and were

weaker than 0 Gy gland ratios. Then the ratios increased the next days for both strains and the values were similar to those of 0 Gy glands (**fig. 36 B**). This could mean that 3 hours after irradiation, autophagy was activated.

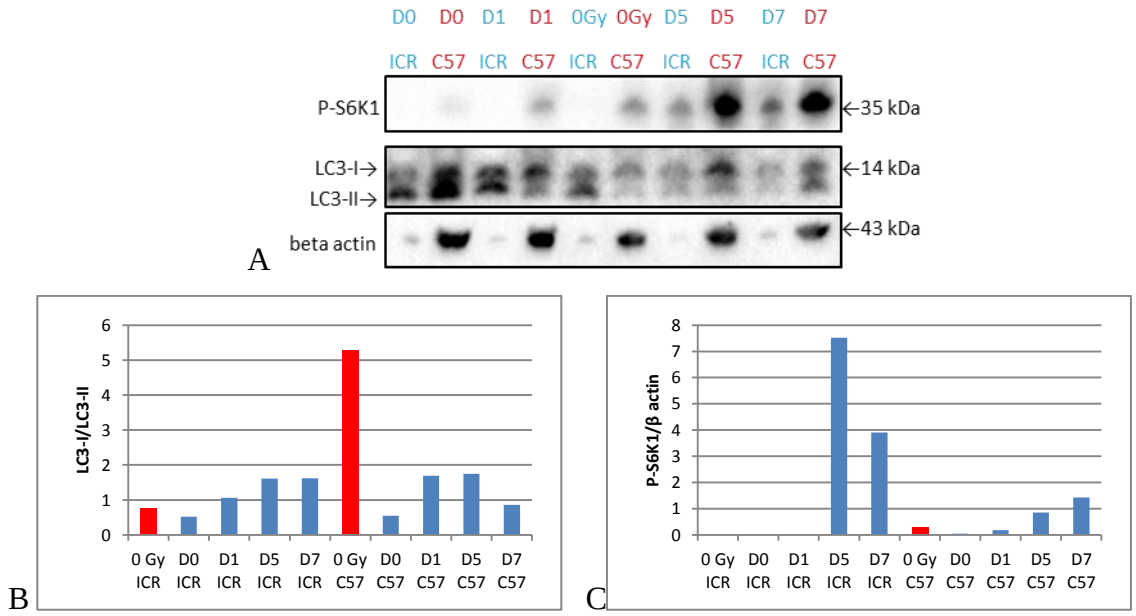

Fig. 36. LC3 and phospho-S6K1 (Ser240/244) western blots of ICR and C57BL/6 mice submandibular glands extracted 3 hours (D0), one day (D1), 5 days (D5), and 7 days (D7) after 11 Gy irradiation. S6K1 was lightly activated in the non-irradiated gland of the C57BL/6 mouse. At D5 and D7, it was strongly activated in both C57BL/6 and ICR mice (A & C). Concerning LC3, LC3-I/LC3-II ratio seems to show that autophagy was activated at D0 in both strains as the ratios decrease after irradiation and then increase again from D1 to D7 in both strains (B). P-S6K1: phospho-S6K1

Immunohistochemistry showed that S6K1 activation was weak in D0 glands, whereas in D7 glands the staining seemed to be stronger in both strains (**fig. 37 a**). Concerning autophagy, ATG5 seemed to be slightly positive in ICR D0 gland (**fig. 37 b**).

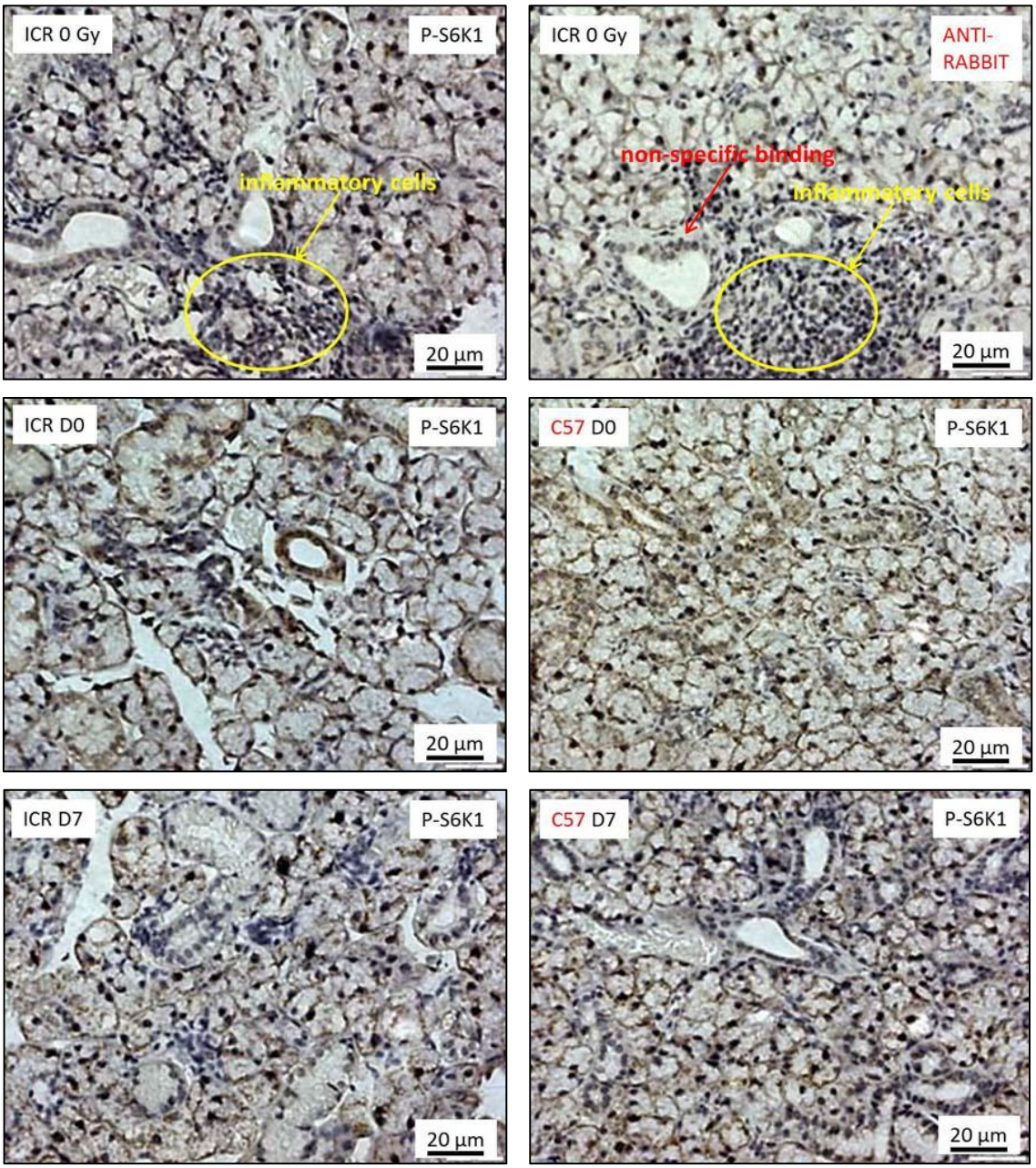

Fig. 37 a. Immunohistochemical staining of ICR and C57BL/6 mice submandibular glands using anti-phospho-S6K1 (Ser240/244). In both strains, S6K1 phosphorylation was weak at D0 (3 hours), whereas it seemed to be stronger at D7 and mostly located in the acinar, rather than ductal cells (which had non-specific binding).

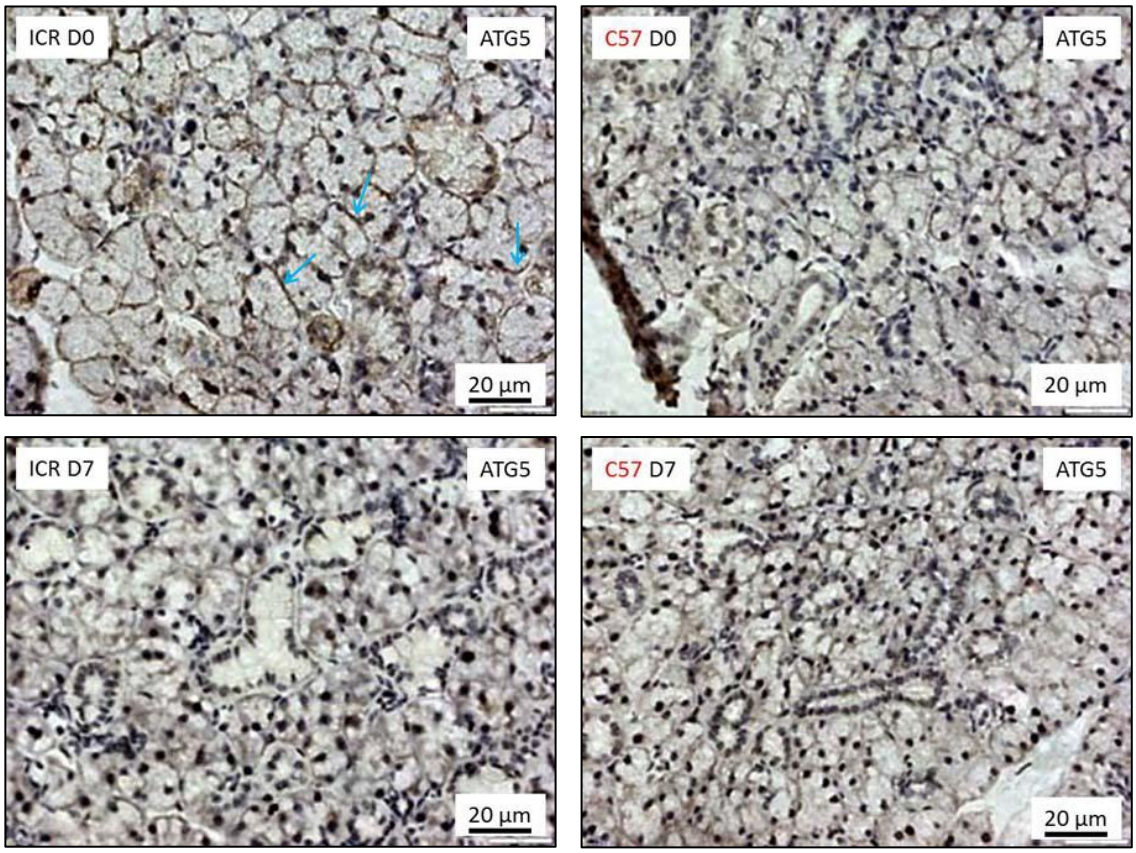

Fig. 37 b. Immunohistochemical staining of ICR and C57BL/6 mice submandibular glands using anti-ATG5. Only ICR D0 (3 hours) gland seemed to be positive in basolateral areas of acinar cells (blue arrows).

2.3.Aquaporin 5 expression in tissue sections

It was difficult to get clear staining with anti-AQP5 antibodies in these samples. The usual apical staining of the acinar cells was not readily apparent. Irradiation may have affected AQP5 localisation and expression in both strains (**fig. 38**).

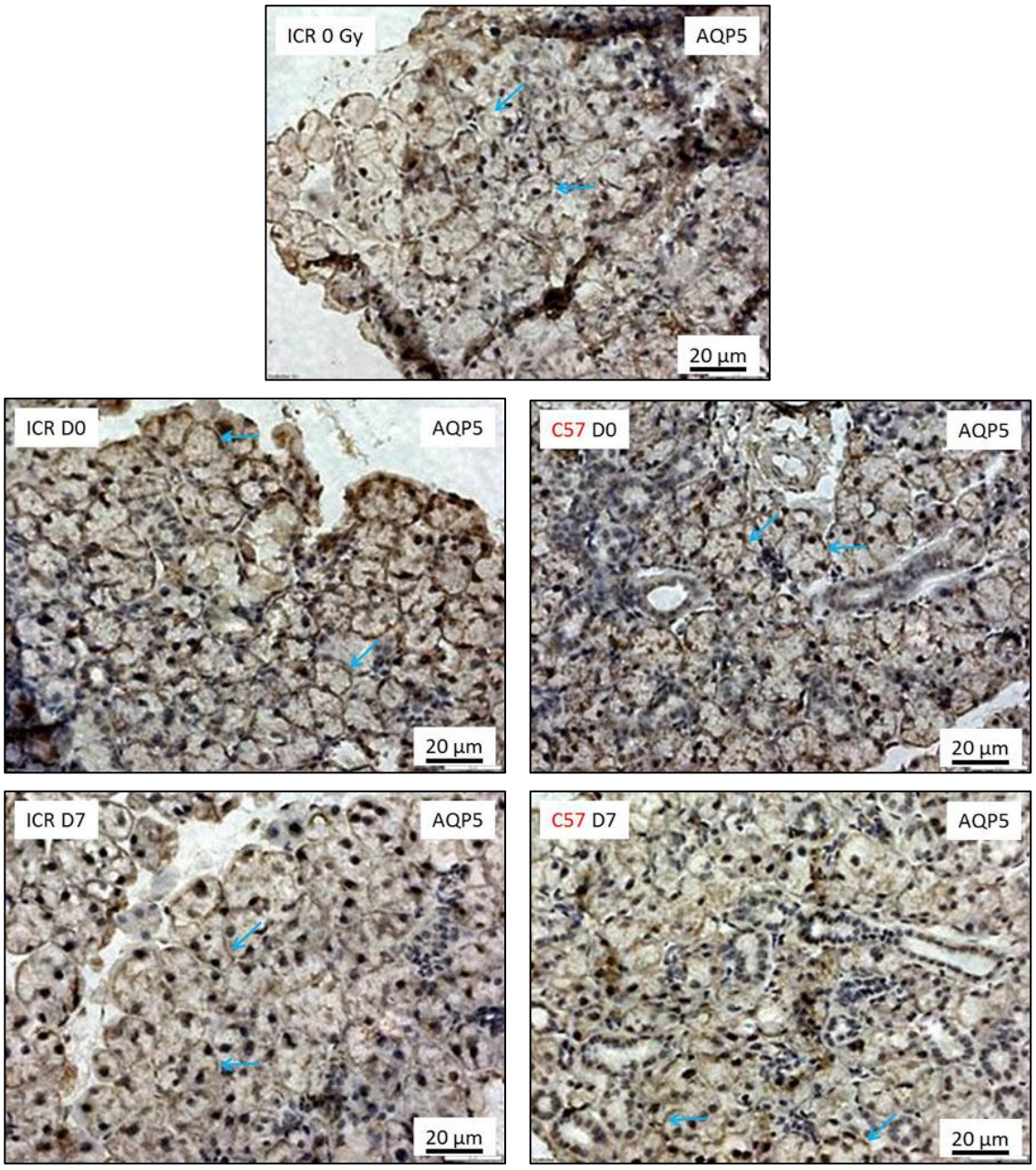

Fig. 38. Immunohistochemical staining of ICR and C57BL/6 mice submandibular glands using anti-AQP5. Whatever the time point and strain, there was no decrease of AQP5 expression (blue arrows).

3. Functional study of irradiation (pilocarpine stimulated saliva flow studies)

The previous study suggested some disruption in the secretory machinery so a further study was used to assess saliva secretion using a recovery method to enable repeated collections from 10 ICR mice over time. Mice were randomly divided into 2 cages (5 per cage), one mouse was not irradiated in each cage, whereas the others were all irradiated at 11 Gy. Saliva was collected under gaseous anaesthesia by I.P. pilocarpine stimulation from day 4 to day 60 following irradiation. Before irradiation, day 0 salivary flow was collected from all mice; cage 1 mice saliva samples were collected once (1

mouse was not collected), and cage 2 mice twice before irradiation (14 saliva samples collected in total). Saliva was collected for either 5 minutes from day 0 to day 46, or 10 minutes until day 60. Collection was done twice a week, but to avoid stressing too much mice, only one cage mice received injection at each time. **Figure 39** shows the pilocarpine-stimulated saliva flows before and after irradiation. Saliva flow seemed to decrease from day 0 to 10, then increased until day 24, and decreased again until day 46. Saliva flow slightly increased from day 47 to 60 but it could be partly due to the fact that saliva was collected during 10 minutes instead of 5 minutes, although flows are shown as per minute of stimulation.

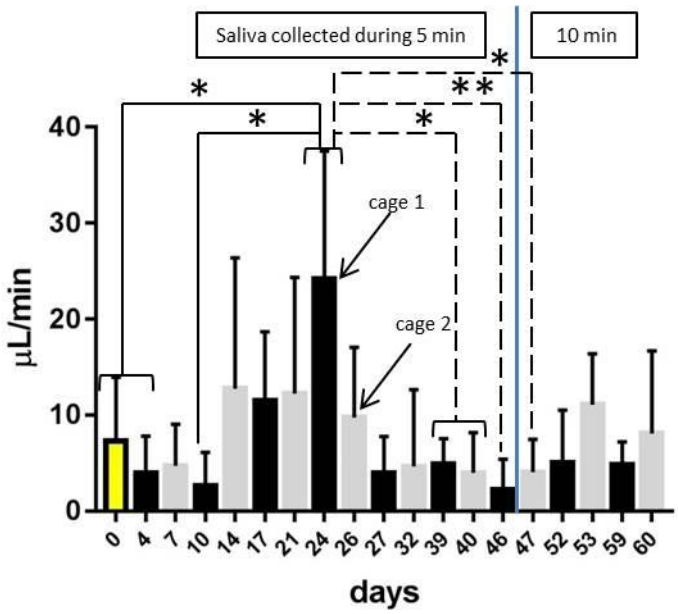

Fig. 39. Pilocarpine-stimulated salivary flow following 11 Gy irradiation. Saliva collected from all animals before irradiation: yellow column; cage 1 irradiated mice: black columns; cage 2 irradiated mice: grey columns. Saliva was collected twice a week but to avoid stressing too much mice, only one cage mice received injection at each time. Error bar: SD, n = 4 (14 for day 0). Significant differences (*$p<0.05$, **$p<0.01$) were determined using a One-way ANOVA followed by a post-hoc Tukey multiple comparisons test.

Concerning body weight, **figure 40** showed no significant variation of weights with time in both cage 1 and 2 mice.

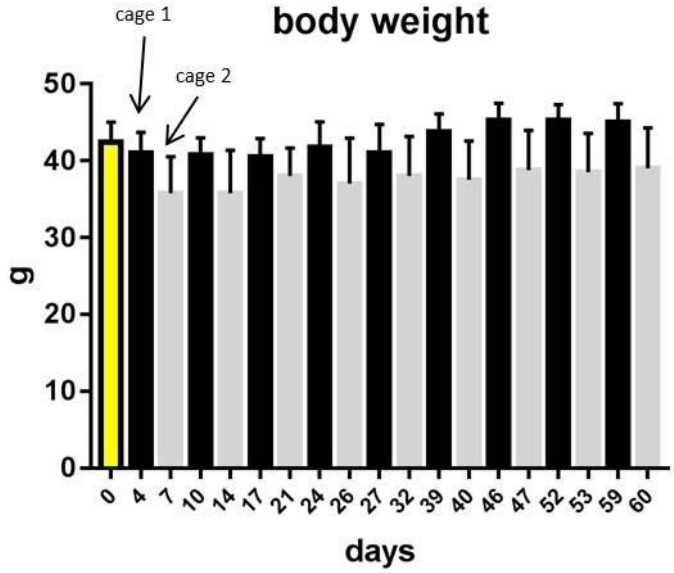

Fig. 40. Body weight following 11 Gy irradiation. Cage 1 mice before irradiation: yellow column; cage 1 irradiated mice: black columns; cage 2 irradiated mice: grey columns. Mouse weights were relatively stable in both cages and increased with time consistant with normal growth rates. Error bar: SD, n = 4 (n = 5 in day 0). One-way ANOVA followed by a post-hoc Tukey multiple comparisons test.

Submandibular glands were extracted 63 days after irradiation. There was no significant difference in weight between irradiated and control glands (**fig. 41**).

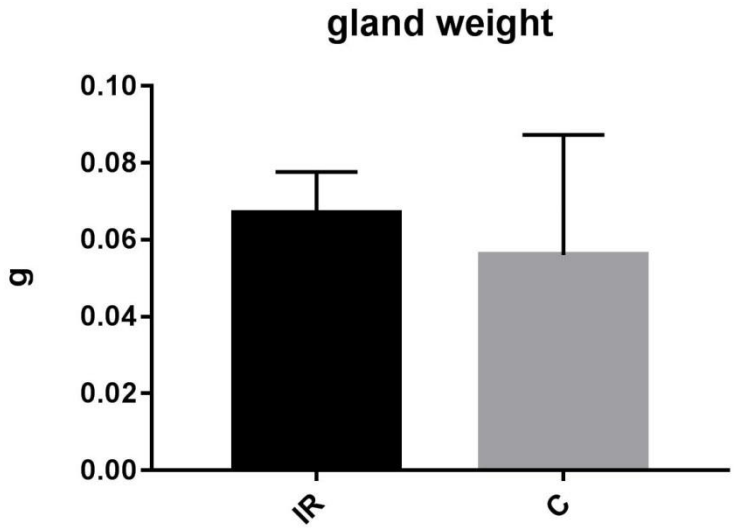

Fig. 41. Submandibular gland weight of irradiated (IR) and control (C) mice. Glands were extracted 63 days following irradiation. Irradiated glands weights were similar to control glands. Error bar: SD, n = 16 for IR, n = 4 for C. Unpaired Student's t test.

Biochemical assessment of autophagy showed a strong LC3-II band intensity in both irradiated and non-irradiated samples (**fig. 42 A**). For that reason, LC3-I/LC3-II ratios were less than 0.5 in all samples including non-irradiated ones, and their values were rather similar (**fig. 42 B**). When compared with normal (non-irradiated and non-pilocarpine treated) submandibular glands, there was a statistically significant difference, so autophagy was activated in all pilocarpine treated submandibular glands (**fig. 42 C**). Unfortunately we did not keep tissue samples to carry out H & E staining.

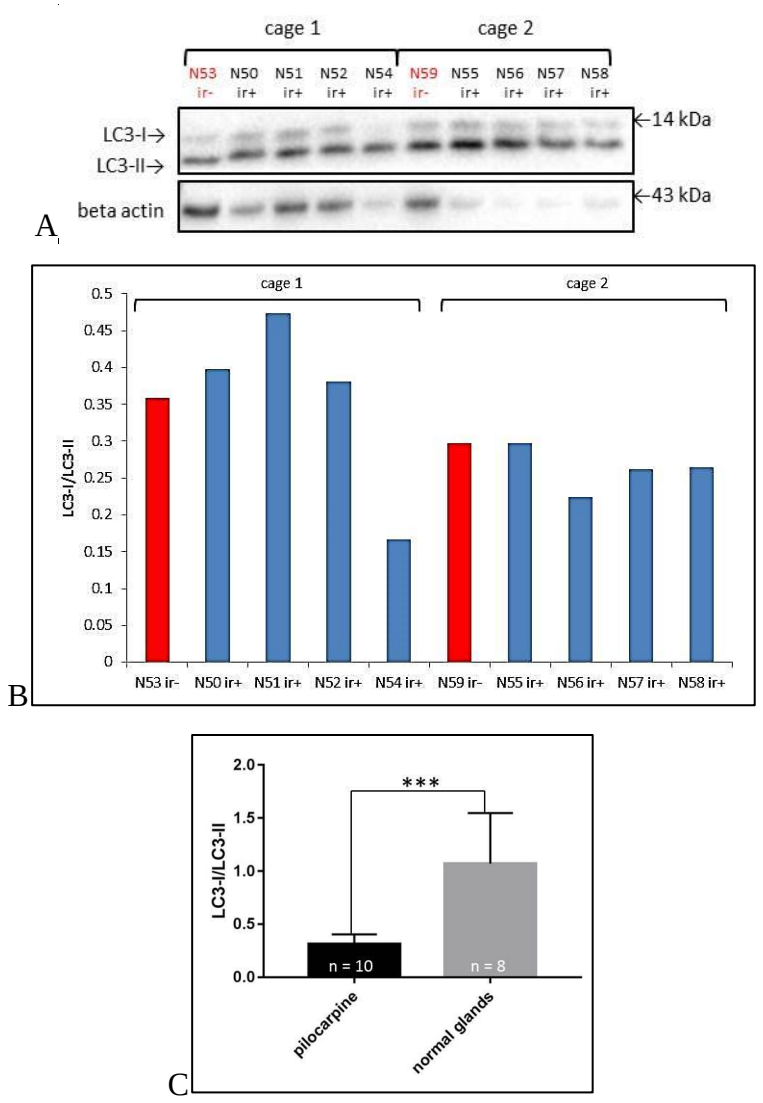

Fig. 42. Autophagy activation study of pilocarpine treated submandibular glands. Western blot clearly showed a strong LC3-II band intensity (A) and LC3-I/LC3-II ratios were less than 0.5 in both irradiated (ir+) and non-irradiated (ir-) ones (B). The comparison of LC3-I/LC3-II ratios between pilocarpine treated glands (ir+ and ir-) and normal glands (non-irradiated and non-pilocarpine treated) showed a statistically significant difference (C). Error bars: SD, n = 10 for pilocarpine treated glands, n = 8 for normal glands. Significant difference (***$p<0.001$) was determined using an unpaired Student's t test.

Discussion

Histological analysis revealed that irradiation did not induce significant morphological changes during the first week. Two weeks later, inflammation (glands were rich in blood vessels), fibrosis, and vacuolisation could be observed in some tissue sections if irradiation was ≥ 5 Gy. From their study, Muhvic-Urek et al. [131], who irradiated (head and neck) C57BL/6 mice and extracted submandibular glands, observed acinar atrophy. Acinar cells number decreased and strong vacuolization was noticed. They irradiated mice at 7.5 and 15 Gy, but glands were extracted 40 and 90 days after irradiation. They also noticed that damages increased when irradiation was stronger (degeneration of granular duct cells and small oedema in 15 Gy irradiated glands). In comparison, our mice were not as damaged which could be due to the fact that our mice were not immobilized. They could move and sometimes were not in the area were the beam was at its maximum intensity. The type of irradiator used in the present study was designed to irradiate blood bags so maximum beam strength occurred approx. 10 cm from the bottom of the loading vessel. Thus the mice probably received only 50% of the dose, which means that even at 11 Gy, the maximum permitted dose, they received around 6 Gy only. Coomassie and PAS staining did not reveal any significant change in proteins and mucin expressions in irradiated glands whatever the irradiation dose and the time of extraction. This does not match Lin et al. results [160], since they noticed a strong decrease of 23.5 kDa band and a decrease of mucin band 24 and 48 hours after 30 Gy whole body irradiation of C57BL/6 mice. Our mice clearly did not receive sufficient radiation dose to inflict significant damages.

Despite this, the low dose of irradiation activated mTOR at day 5 and day 7 in both ICR and C57BL/6 since phospho-S6K1 was positive in both western blot and immunohistochemistry. Whereas autophagy, seemed to be activated at day 0 (3 hours) samples in both strains since western blot showed that LC3-I/LC3-II ratios decreased 3 hours after irradiation and immunohistochemistry was slightly ATG5 positive. These results are similar to those of Morgan-Bathke et al. who noticed a weak activation of autophagy 8 hours [47] and a strong activation of mTOR 4 and 5 days [48] after irradiation in mice parotid glands. Concerning mTOR, it is not clear how irradiation activates it. However, it is known that when skin cells are irradiated by UV, although some cells undergo apoptosis, mTOR is also activated in order to inhibit apoptosis and to repair damaged DNA, thus ensuring cell survival [135]. Ligation of submandibular gland, leads to gland atrophy and strong loss of acinar cells by apoptosis, but also

activates mTOR as well. This activation seems to favour remaining acinar cells to survive [44]. So mTOR activation after ionizing irradiation could be a survival process. Besides, Bralic et al. [136] who irradiated C57BL/6 mice at 7.5 and 15 Gy (head and neck) noticed an increase of apoptotic index which peaked 3 days following irradiation in acinar and ductal cells, and an upregulation of proliferative index of submandibular gland cells (acinar and ductal cells) from day 3 to day 6 following irradiation. After 6 days, the index decreased and became almost similar to non-irradiated gland cells. Therefore mTOR activation following irradiation could be explained by the increased mitosis.

AQP5 expression to assess saliva secretory function has been used before by western blots but AQP5 was cleaved for a reason that was not clear. Li et al. [84] who irradiated Wistar rats at 15 Gy (head and neck) noticed a significant decrease of AQP5 expression in submandibular glands at day 3 (60 ± 9% of those of non-irradiated) and day 30 (44 ± 2%) post-irradiation with Western blotting. Even immunohistochemistry showed a clear decrease of AQP5 expression at both day 3 and day 30. Choi et al. [133] found similar results on 10 Gy (head and neck) irradiated Sprague-Dawley rats. Immunohistochemical analysis revealed 60% loss of AQP5 in submandibular glands 5 days after irradiation and even 90% 20 to 90 days following irradiation. In our study a loss of typical apical staining of acinar cells in the first week post-irradiation suggested some disruption of the secretory capacity, however the results are far from conclusive.

Stimulated salivary flow experiment showed that even though the variations were not always statistically significant, the flow decreased from day 0 (non-irradiated) to 10, then increased and peaked at day 24 ($p<0.05$ compared to 0 Gy), and decreased again until day 46 ($p<0.01$ compared to day 24). The transient increase of saliva flow from day 14 to day 24 might be due to acinar cell proliferation to replace damaged or dead cells. As mentioned above, Bralic et al. [136] noticed an increase of proliferative index which peaked 6 days after irradiation. Our saliva flow result is different to those mentioned in other papers. Lin et al. [160] who irradiated C57BL/6 mice at 30 Gy (whole body) uncovered that 24 hours after irradiation, the lag time for the secretion of saliva (after pilocarpine injection) increased 3 folds and the flow rate decreased by more than half. No saliva secretion could be obtained 6 days following irradiation. Takakura et al. [83] who irradiated ICR mice at 15 Gy observed a decrease (almost 50%) of saliva flow (saliva collected for 15 minutes after pilocarpine injection) from 1 day after irradiation and the flow remained almost similar until day 28. Li et al. [84] who irradiated Wistar rats at 15 Gy (salivary glands targeted) noticed a strong decrease of

saliva flow (saliva collected for 20 minutes after pilocarpine injection) on day 3 (68 ± 6% of the mean value for controls) and day 30 (62 ± 6%) following irradiation. For their study, Morgan-Bathke et al. [47] irradiated $Atg5^{+/+}$; AQP5 male and female mice at 5 Gy (head and neck). Male mice showed a 12% decrease of saliva flow rate (saliva collected for 5 minutes after carbachol injection) at day 3, 17% decrease at day 14, and a modest improvement of salivary flow rate at day 30 after irradiation. Concerning female mice, they noticed a 17% decrease at day 3, 19% decrease at day 14, and 20% decrease at day 30. In another experiment [48], they irradiated FVB mice at 5 Gy (head and neck) and observed a decreased salivary flow rate (saliva collected for 5 minutes after carbachol injection) at day 3, 30, 60 and 90 following irradiation. It is not clear why our results are so different, but it could be due to the lower doses supplied. Indeed in our preliminary work, 2 weeks after 11 Gy (true dose 50% less) irradiation, submandibular glands seemed to be rather in good condition since damages were observed only in some portions of tissue sections, and glands looked almost normal 4 weeks following irradiation. It is also interesting to mention Takeda et al. paper [134], as they irradiated ICR mice at 15 Gy and some of them were given nitric oxide inhibitor at different concentrations. They noticed that 1 week after irradiation, saliva flow was similar in all mice 5 minutes after pilocarpine injection and there was no significant difference between non-irradiated, irradiated and irradiated + nitric oxide inhibitor. However, saliva flow became strong 10 minutes after pilocarpine injection and a significant difference between the groups were noticed. The flow reached a peak 15 minutes after pilocarpine injection, whereas at 20 minutes it began to decrease. Maybe we should have collected saliva during 15 minutes following pilocarpine injection. Our assessment of autophagy was also variable. Western blot analysis revealed that autophagy was variable in non-irradiated submandibular glands (ranging from 0.5 to 1.0 in different experiments). The reasons for such variation are unclear but an effect of pilocarpine stimulation was noticed. According to Cao et al. [191], excessive pilocarpine injection elicits status epilepticus which induces autophagy, so it is perhaps not surprising that autophagy was activated in our mice, even with a lower dose.

Irradiation is known to decrease mouse and salivary glands weights. Kamiya et al. [137] who irradiated C57BL/6, ICR and ICR-nu/nu mice at 25 Gy (submandibular glands targeted) noticed a decrease of body weights from 1 week after irradiation. The decrease was maximal at 2 weeks (35 to 40 % lower than control mice), then mice regained weight beyond 3 weeks. Bralic et al. [136] who irradiated male C57BL/6 mice at 7.5 and 15 Gy (head and neck) observed a weight loss in both doses up to 3 weeks.

Then 7.5 Gy irradiated mice regained weights whereas 15 Gy irradiated mice weights continued to decrease until 6 weeks. For their part, O'Connell et al. [138] irradiated Wistar rats at 10 Gy (parotid and submandibular glands targeted) and noticed that irradiated rats weights were significantly lower than control rats 3 months following irradiation. Submandibular gland weights of irradiated rats were also lower than those of control rats. Our results are not similar as there were no significant decrease of mice and submandibular glands weights. As we have already mentioned, our mice which were supposed to receive 11 Gy probably received only 50% of the expected dose. So irradiation dose was not strong enough to induce mouse and submandibular gland weight decrease.

Despite the fact that Kamiya et al. who irradiated ICR, ICR-nu/nu and C57/BL/6 mice noticed strain-specific responses [137], no difference could be observed in our mice. However, they irradiated their mice at 25 Gy, whereas our mice probably received around 6 Gy (instead of 11 Gy). We suppose that the irradiation dose was not strong enough to see any difference between ICR and C57/BL6 mice.

To sum up, our experiments showed that low dose irradiation caused minimal damages to submandibular glands and after a slight decrease in salivary secretion a slight increased occurred. Autophagy was activated for only few hours after irradiation certainly to degrade damaged cell components. Concerning mTOR, it was transiently activated from 5 to 7 days following irradiation probably to inhibit apoptosis and favour mitosis but at 14 days it was switched off. On the other hand a temporary increase of saliva flow was observed from day 14 to 24. This was probably due to acinar cells proliferation, which means that mTOR was certainly activated beyond 14 days. Therefore a transient activation of autophagy followed by mTOR activation is beneficial to salivary gland functions. Despite the fact that these findings were interesting, they did not confirm or refute the apparent lack of link between mTOR and autophagy observed in SMG-C6 cells and primary submandibular gland cells. For that reason, it was necessary to carry out experiments on ligated submandibular glands in which both mTOR and autophagy were known to be activated 3 days following ligation and beyond [44].

F. EFFECTS OF AUTOPHAGY INHIBITOR ON LIGATED SALIVARY GLANDS

Introduction

It was known that normally mTOR and autophagy were inactive in salivary glands. However, ligation experience showed an activation of both mTOR and autophagy at day 3 and beyond [44]. At first glance it looked aberrant since mTOR activation was supposed to lead to ULK1 inhibition and autophagy [91]. However it was demonstrated that mTOR and ULK1 independent autophagy could occur as well [63]: this might explain why autophagy was activated in ligated submandibular glands despite the fact that mTOR was activated at the same time. To verify this hypothesis, it was necessary to administrate the ULK1 inhibitor MRT67307 to ligated mice submandibular glands to see if it could block autophagy. Besides it was demonstrated that inhibition of autophagy could protect neural stem and progenitor cells in the brain of irradiated mice pups [146]. Therefore it was interesting to see if autophagy inhibition could have protective effects on ligated submandibular glands. We also decided to test the effect of chloroquine which was known to inhibit autophagy, even though some papers described it as being able to induce autophagy in vivo [111, 112].

Methods

To ligate submandibular gland duct, ICR mice were anesthesized by ip injection of xylazine (5 mg/kg)/ketamine (25 mg/kg). Then mice were put on a controlled heating pad to avoid body temperature decrease. Pedal reflex was used to assess the depth of anesthezia. While mice were maintained lying on their back, the midline of the neck skin was incised (~0.5 cm long), the fat tissue surrounding the left submandibular gland was removed, then the gland duct was ligated by using a 6-0 Ethicon suture. Next the neck was sutured and the mice were put in a cage placed in a warm room and received 10 mg/kg buprenorphine (analgesic) in order to recover from anaesthesia. To decrease the risk of infection, aseptic conditions were carried out during the surgical procedure.

Chloroquine (10 mg/kg) was intraperitoneally injected in mice immediately after ligation, and SMG were extracted 1 week later. The protocol was similar with MRT67307 (100 µL and 200 µL of 1 mM MRT67307) but mice were daily injected and SMG were retrieved 3 days following ligation. Autophagy and mTOR activities were assessed by using Western blot (as described at page 72). To see if chloroquine and MRT67307 could at least delay SMG atrophy, H & E staining was carried out (as decribed in page 91) and glands weights were measured as well.

Results

1. Chloroquine injection

Since Rao et al. [147] injected chloroquine 10 mg/kg once a week in NOD/SCID mice (in order to treat triple-negative breast cancer cells), we decided to inject the same dose in 3 control ICR mice. No toxicity was observed so chloroquine injections were given to mice with one ligated submandibular gland which was extracted 7 days later as previously described.

1.1. H & E staining

H & E staining showed that ligated glands from chloroquine-injected animals were atrophic as acinar cells were shrunken and duct lumens were dilated, whereas contralateral glands looked normal (**fig. 43**).

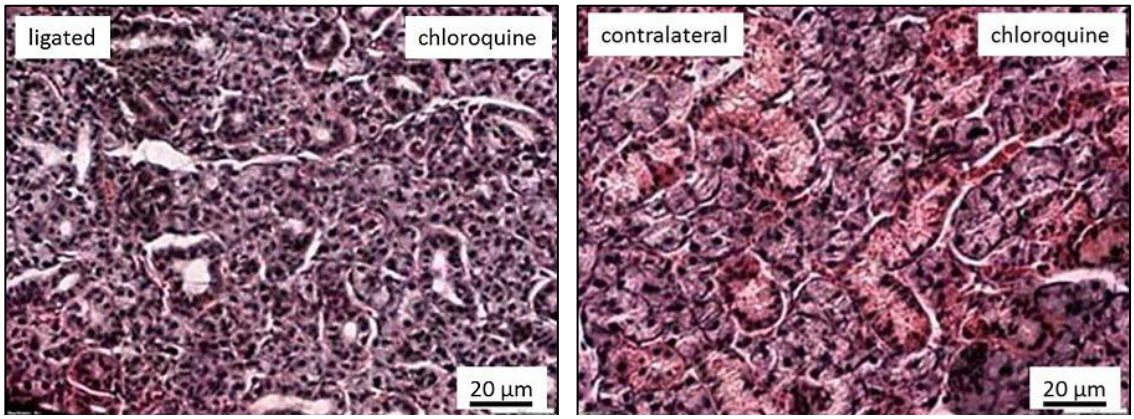

Fig. 43. H & E staining of ligated and contralateral submandibular glands extracted 7 days after chloroquine injection. Contralateral glands looked normal whereas ligated glands showed shrunken acinar cells and dilated duct lumens which are features of glandular atrophy.

All glands were weighed (the weights of glands without chloroquine are those of Bozorgi's experiment [45]). No significant difference could be seen between contralateral + chloroquine and contralateral, control + chloroquine and control glands. Concerning ligated + chloroquine glands, they were heavier than ligated glands and slightly lighter (although not statistically significant) than control and contralateral glands with or without chloroquine (**fig. 44**).

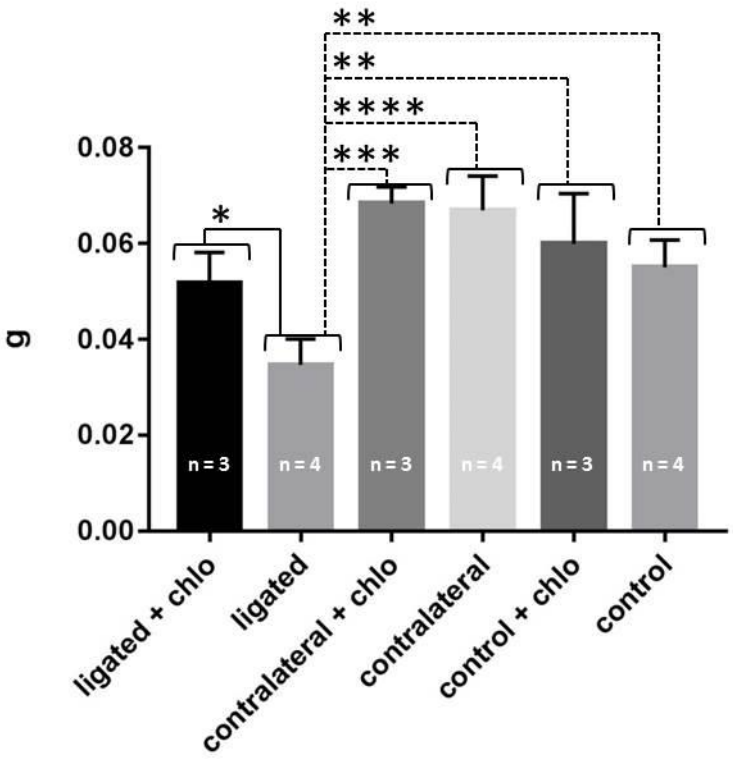

Fig. 44. Mean weights of ligated, contralateral and control glands with and without chloroquine. Chloroquine treated ligated glands were heavier than ligated only glands. Error bar: SD. Significant difference (*p<0.05) was determined by using one-way ANOVA followed by a post-hoc Tukey multiple comparisons test.

1.2. mTOR and autophagy activation studies

The effect of chloroquine injection on LC3-I/LC3-II ratio was assessed in ligated, ligated + chloroquine and control + chloroquine samples. As expected, LC3-I/LC3-II ratio of ligated submandibular gland + chloroquine was slightly weaker than ligated only submandibular gland, though the difference was not statistically significant (**fig. 45**).

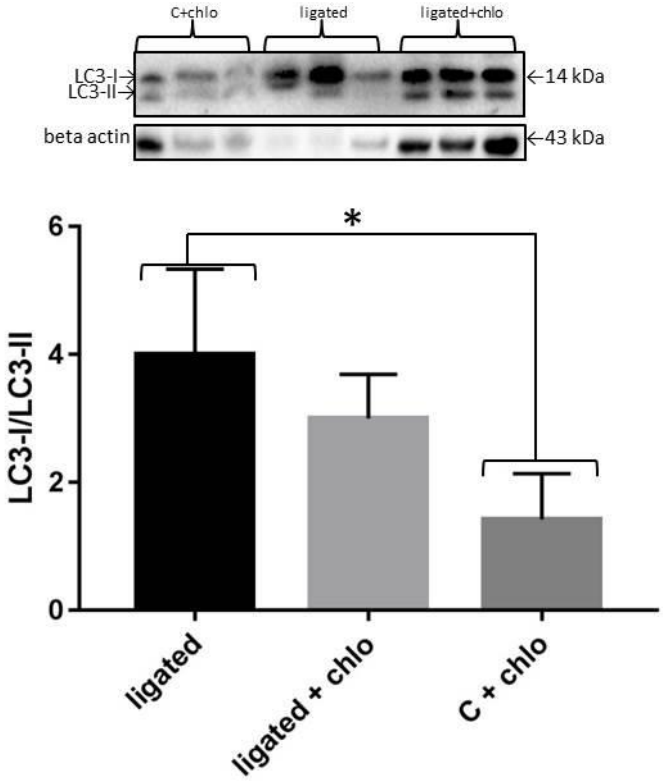

Fig. 45. Comparison of LC3-I/LC3-II ratios between ligated and ligated + chloroquine submandibular glands, 7 days after chloroquine injection. Although not statistically significant, LC3-I/LC3-II ratio of ligated submandibular gland + chloroquine was slightly weaker than ligated only submandibular gland, which means that chloroquine had partially inhibited LC3-II degradation. Error bar: SD, n = 3. Significant difference (*$p<0.05$) was determined by using one-way ANOVA followed by a post-hoc Tukey multiple comparisons test.

S6K1 was phosphorylated in ligated and contralateral glands and surprisingly in one of the control glands as well- but this is likely to be an anomaly as all control glands have previously tested negative for phospho-S6K1. All previous ligated glands were mTOR positive so it appears that chloroquine did not affect mTOR processes. Concerning autophagy, LC3-I/LC3-II ratios were not statistically different between ligated with or without chloroquine: chloroquine possibly decreased autophagic flux, since LC3-II bands intensities were not particularly high (**fig. 46**).

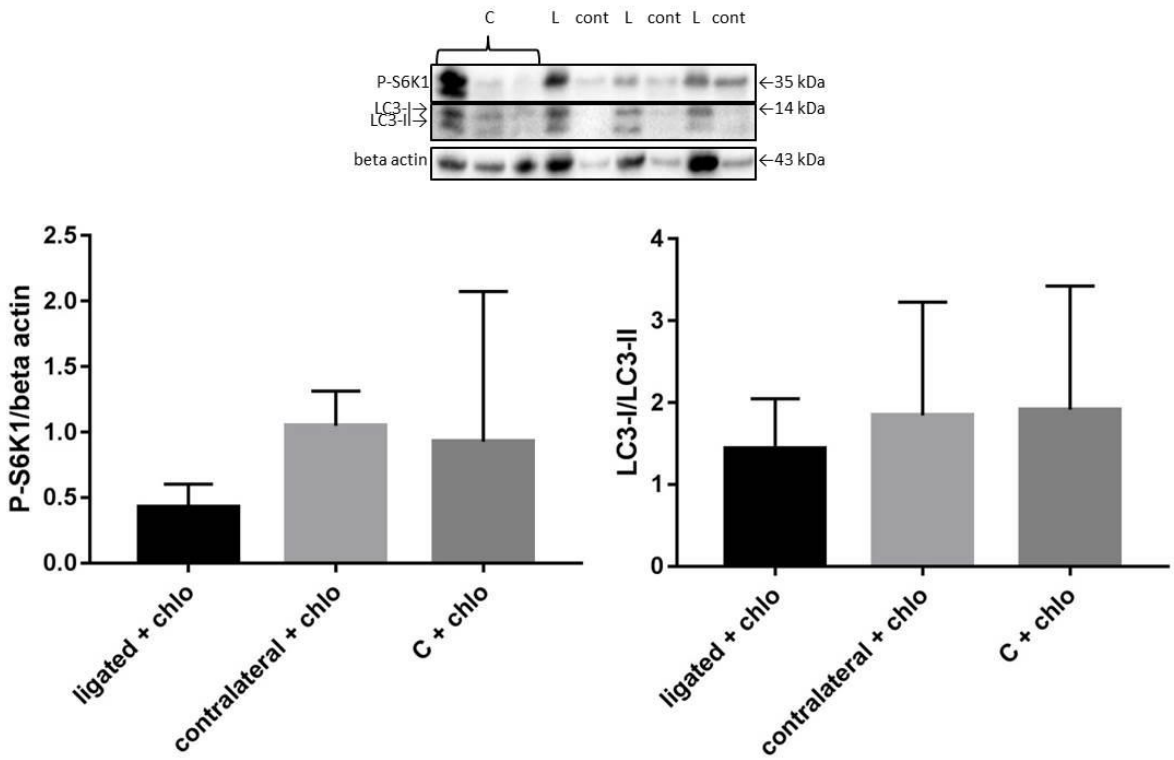

Fig. 46. Phospho-S6K1 (Ser240/244) and LC3 western blots of submandibular glands extracted 7 days after chloroquine injection. No significant difference could be noticed between control (C), ligated (L), and contralateral (cont) glands. P-S6K1: phospho-S6K1. Error bar: SD, n = 3. Statistical analysis was carried out by using one-way ANOVA followed by a post-hoc Tukey multiple comparisons test.

It is worth mentioning that during our preliminary work on irradiated submandibular glands (without drug injection), contralateral glands were not similar to glands from untreated animals and tended to behave like ligated glands as LC3-I band intensity was significantly stronger than LC3-II (**fig. 47**).

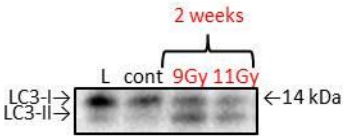

Fig. 47. Earlier work on irradiated salivary glands showing autophagy activation in both ligated (L) and contralateral (cont) glands.

2. MRT67307 injection

The first *in vitro* study of ULK1 inhibitor MRT67307 has only recently been reported and its effects *in vivo* unknown. Intraperitoneal injections of 100 µL of 1 mM MRT67307 solution were given daily in 2 ICR mice (mouse 1 and 2) weighing around

30 g. The first injection was done on the same day as left submandibular glands were ligated. Then mice continued to receive 1 injection per day. Glands were extracted 3 days after ligation. In a second experiment the dose was doubled by injecting 200 µL in 2 other ligated ICR mice (mouse 3 and 4).

2.1. H & E staining

Like chloroquine, MRT67307 did not prevent gland atrophy whatever the dose, as acinar cells were shrunken and duct lumens were dilated too. Contralateral glands looked normal (**fig. 48**).

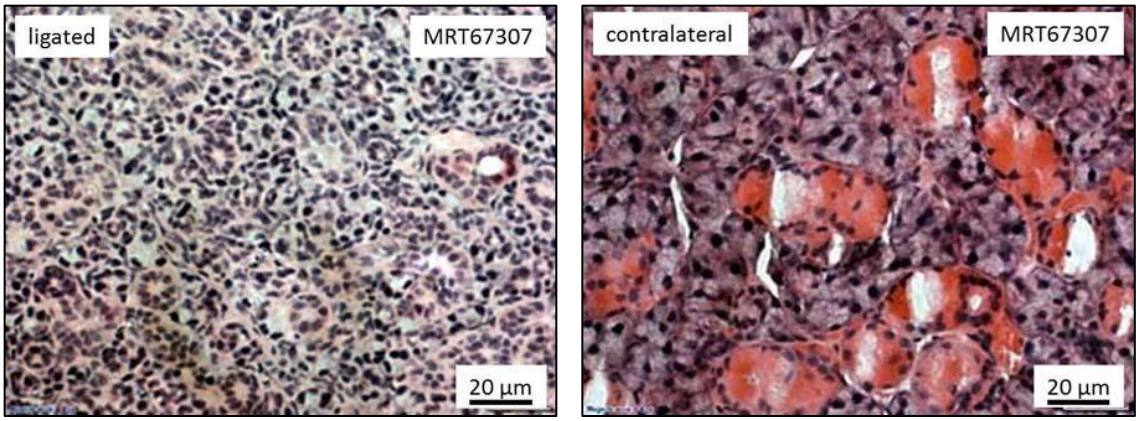

Fig. 48. H & E staining of ligated and contralateral submandibular glands extracted 3 days after ligation and receiving daily injection of 100 µL of MRT67307 at 1 mM. Contralateral glands looked normal whereas ligated glands showed shrunken acinar cells and dilated duct lumens like in chloroquine treated mice.

Concerning gland weights, whatever the dose ligated glands were lighter than contralateral glands like chloroquine injected mice (**table 2**), so the ligation procedure worked. Like in chloroquine injection experiment, MRT67307 treated ligated glands were heavier than ligated only glands (0.035+/- 0.003g, Bozorgi et al., 2014 [45]).

	ligated (g)	contralateral (g)
mouse 1 (100 µL)	0.0638	0.0644
mouse 2 (100 µL)	0.0551	0.0798
mouse 3 (200 µL)	0.0680	0.0920
mouse 4 (200 µL)	0.0530	0.0580

Table 2. Submandibular glands weights.

2.2. mTOR and autophagy activation studies

As for the chloroquine experiment, we used phospho-S6K1 (Ser240/244), phospho-4E-BP1 (Thr 37/46) and LC3 antibodies to study mTOR and autophagy. In ligated glands, whatever the dose, mTOR was clearly activated as both S6K1 and 4E-BP1 were phosphorylated. Concerning autophagy, in both 100 µL and 200 µL injected mice, only LC3-I were observable (**fig. 49 a**, **49 b**).

In contralateral glands, in 100 µL injected mice, no phospho-S6K1 band appeared, and only one 4E-BP1 band could be observed. On the other hand, in 200 µL injected mice, phospho-S6K1 bands were clearly observable, and only one 4E-BP1 band could be seen. mTOR was probably activated in both 100 µL and 200 µL, and not different to ligation in the absence of drug treatment. Concerning autophagy both LC3-I and LC3-II bands could be seen in 100 µL injected mice, whereas only LC3-I bands were apparent in 200 µL injected mice (**fig. 49 a**, **49 b**). However when we prepared a new blot with ligated, ligated + 200 µL MRT67307 and control glands, LC3-II bands clearly appeared, and although it was not possible to perform statistical analysis, LC3-I/LC3-II ratio of ligated MRT67307 treated gland was similar to ligated only, so there was no autophagy inhibition (**fig. 49 c**).

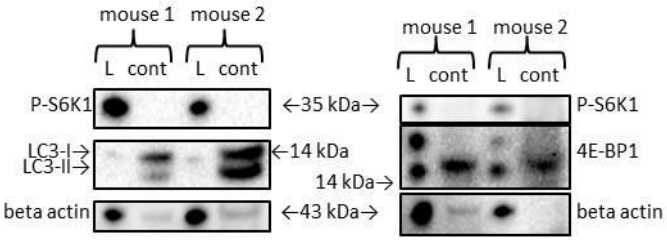

Fig. 49 a. Phospho-S6K1 (Ser240/244), phospho-4E-BP1 (Thr 37/46) and LC3 western blots of submandibular glands extracted 3 days after ligation and receiving daily injection of 100 µL of MRT67307 at 1 mM. L: ligated gland, cont: contralateral gland, P-S6K1: phospho-S6K1.

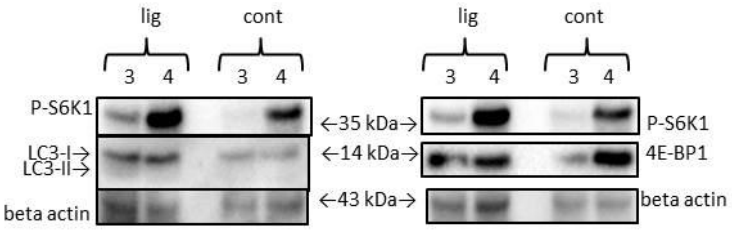

Fig. 49 b. Phospho-S6K1 (Ser240/244), phospho-4E-BP1 (Thr 37/46) and LC3 western blots of submandibular glands extracted 3 days after ligation and receiving daily injection of 200 µL of MRT67307 at 1 mM. lig: ligated gland, cont: contralateral gland, P-S6K1: phospho-S6K1.

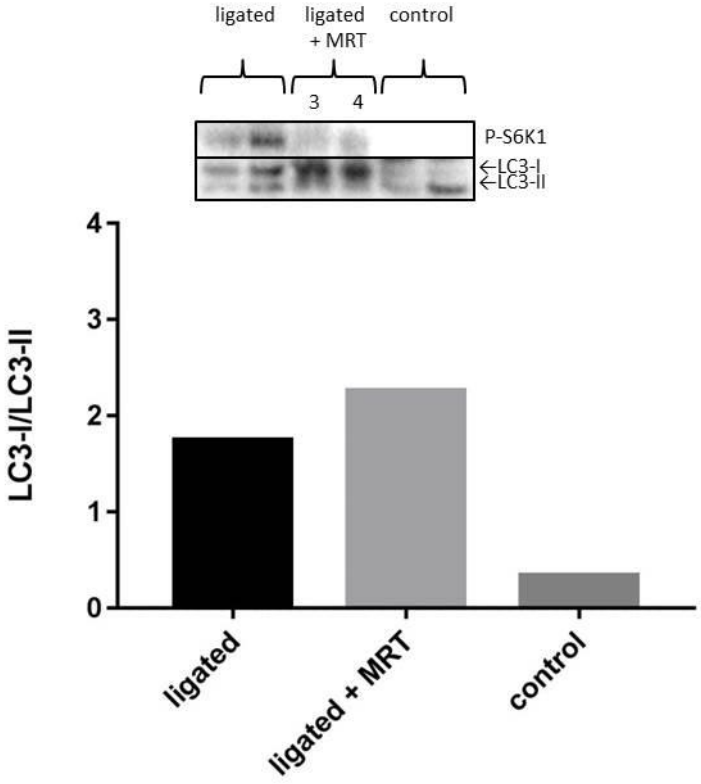

Fig. 49 c. New blot showing ligated only, ligated + 200 µL MRT67307 and control submandibular glands. LC3-II bands appeared in ligated + MRT67307 and LC3-I/LC3-II ratios between ligated and ligated + MRT were similar, so autophagy was not inhibited by MRT67307. P-S6K1: phospho-S6K1. 3 and 4: mouse 3 and 4.

Discussion

Chloroquine injection did not prevent gland atrophy as glands weights were decreased, acinar cells were shrunken and duct lumens were dilated. However, ligated chloroquine treated glands were heavier than those of ligated only glands of Bozorgi's experiment [45], so glands atrophy was slightly delayed. Therefore, chloroquine injection had probably little beneficial effect. Morgan-Bathke et al. [48] found similar results on irradiated salivary glands: injection of hydroxychloroquine did not improve salivary gland function. Our experiment revealed that S6K1 was phosphorylated in all samples including contralateral glands. Hu et al. [149] demonstrated that chloroquine could increase mTOR and phospho-mTOR protein levels in osteoclasts and this increase was due to the inhibition of their degradation. This could have also favoured the apparition of phospho-S6K1 bands. Concerning autophagy, LC3-I/LC3-II ratios of ligated + chloroquine submandibular glands were slightly weaker than ligated only submandibular glands, even if the difference was not statistically significant. Therefore chloroquine had partially blocked LC3-II degradation. A more concentrated chloroquine solution is required to significantly inhibit LC3-II degradation.

Whatever the dose, MRT67307 injection failed to prevent gland atrophy too. 100 µL injection of MRT67307 had no effect on autophagy since LC3-I and LC3-II bands were clearly seen in contralateral glands. Concerning the ligated glands, the lack of LC3-II bands was certainly due to a problem of the blot since if LC3-I bands appeared, they were barely observable. Autophagy seemed to be deactivated in 200 µL injected submandibular glands by inhibiting ULK1 and ULK2, since this dose inhibited the appearance of LC3-II bands. However the new blot showed that LC3-II was not absent and moreover LC3-I/LC3-II ratio of ligated + 200 µL MRT67307 was similar to ligated only, which means that even at 200 µL autophagy was not inhibited. Since mTOR was still active, autophagy does not account for atrophic process in ligated glands. Regarding glands weights, ligated MRT67307 treated glands weights were higher than those of ligated only glands of Bozorgi's experiment [45], so atrophy was slightly delayed.

Contralateral glands behaved like ligated glands since mTOR and autophagy were both activated. In fact this phenomenon has already been observed by Walker et al. [163]. They observed a proliferation of ductal and acinar cells in the contralateral parotid glands of rats. This is consistent with mTOR activation observed in our mice contralateral submandibular glands. Unfortunately, they did not report if autophagy was

activated. Neither chloroquine, nor MRT67307 had any effect on contralateral and control glands weights.

Even if autophagy inhibition by MRT67307 has little beneficial effects, it did not necessarily mean that blocking autophagy would not help gland regeneration. As gland atrophy following ligation is due to acinar cells apoptosis [155], and since autophagy can activate apoptosis [68], inhibition of autophagy could help maintaining gland weight by inhibiting apoptosis. Wang et al. [146] noticed that Atg7 knock-out newborn mice neural stem and progenitor cells did not undergo apoptosis after irradiation. Inouye et al. [156] uncovered that if newborn mice received cycloheximide injection 1 hour after irradiation, cell death in the external granular layer was inhibited up to 6 hours following irradiation, whereas if mice received a second injection 6 hours after irradiation, no apoptosis occurred until 15 hours following irradiation.

To sum up, experiments in this chapter revealed that autophagy in mouse submandibular gland was mTOR and ULK1 independent since MRT67307 failed to inhibit autophagy. This was probably the first time that MRT67307 was used in vivo and no paper mentions mTOR independent activation of autophagy in salivary glands, so we got novel data. Although it was not possible to carry out statistical analysis, inhibition of autophagy by chloroquine, if it did not preserve gland morphology, delayed salivary gland atrophy. MRT67307 seemed to have delayed too, although it did not inhibit autophagy.

G. DISCUSSION

NIH 3T3 cells experiments results match well what is generally known. It is well known that mTORC1 inhibition leads to ULK1 activation triggering autophagy [46, 53, 54, 55], starvation activates AMPK which in turn activates ULK1 and inhibits mTORC1 as well [23, 26], and if ULK1 is knock-out ULK2 can ensure autophagy activation [57]. MRT67307 was efficient to block autophagy since it inhibited both ULK1 and ULK2, even if starvation and Torin 1 blocked mTORC1 (**fig. 50**). A synchronous activation of autophagy and inhibition of mTORC1 occurred in starved cells. It was probably an autophagy activation of mTORC1, since it was demonstrated that serum starved cells degraded proteins which provided amino acids which activated mTORC1 [153] and inhibition of autophagy decreased mTORC1 activity [167]. Nonetheless, it was proved that mTORC1 activation of autophagy could occur, but only when TSC1 or TSC2 was inhibited. The likely mechanism is that if TSC1 or TSC2 is inhibited, mTORC1 is constantly activated, thus favouring protein, lipid or glycolytic metabolism, generating energetic stress, which in turn activates AMPK leading to autophagy activation [158, 159].

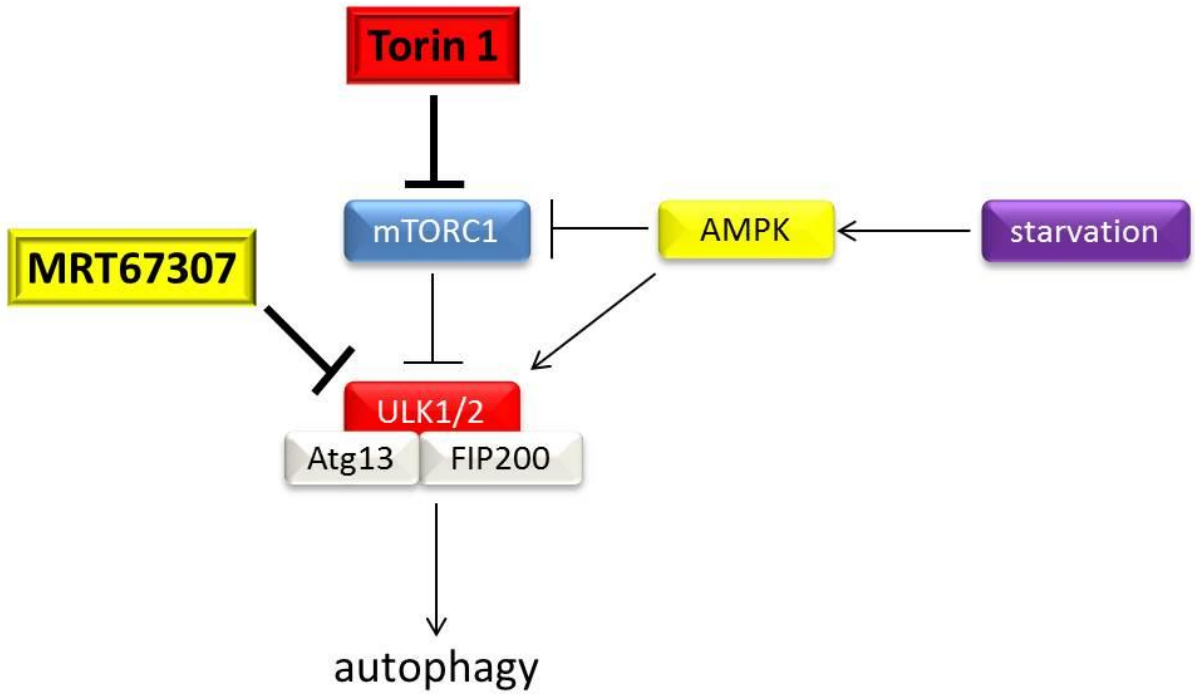

Fig. 50. Effects of Torin 1 and MRT67307 on NIH 3T3 cells. Torin 1 and starvation can both inhibit mTORC1, leading to ULK1 and ULK2 activation which in turn trigger autophagy. However, administration of MRT67307 cancels Torin 1 and starvation induced autophagy by inhibiting both ULK1 and ULK2.

Although ULK1 and ULK2 are highly involved in autophagy activation in many cells, they are not absolutely necessary. Cheong et al. [164] demonstrated in mouse embryonic fibroblasts that if ULK1/2 double knock-out cells could not induce autophagy after serum starvation, they were able to activate autophagy in response to glucose starvation. They uncovered that under glucose starvation, cells catabolized amino acids which produced ammonia which in turn activated autophagy without inhibiting mTORC1. However, ammonia effects can vary depending on cell types. In rat hepatocytes [165] and bovine embryonic smooth muscle cells [166] ammonia decreases autophagy whereas in human breast cancer cells MCF-7, ammonia activates mTORC2 which in turn activates mTORC1 [119].

In control cells, autophagy was sometimes activated despite the fact that mTOR was significantly activated. mTOR independent autophagy could have occurred [39, 58, 61, 63]. Another possibility is that even though the effect of pH on autophagy is cell type dependent [171, 172, 173], acidification of the medium could have favoured autophagy activation as well.

Results in SMG-C6 and primary submandibular gland cells were different, since mTOR inhibition by Torin 1 did not upregulate autophagy, meaning that autophagy activation was probably mTOR and ULK independent in mouse submandibular gland.

Concerning submandibular glands, they were rather radioresistant since even though an irradiation dose (likely dose 50% less) of 5 Gy could be enough to notice an infiltration of inflammatory cells, 11 Gy (likely dose 50% less) was required to inflict significant damages, and even at this dose glands recovered well 4 weeks following irradiation. Moreover AQP5 expression and mucin production seemed not to be affected. These results were logical since submandibular glands are more radioresistant than parotid glands which contain only radiosensitive serous acini whereas submandibular glands contain both serous acini and the radio-resistant mucous acini [3].

11 Gy irradiation experiment (true dose less than 50%) showed mTORC1 activation 5 and 7 days after irradiation whereas autophagy was activated 3 hours after irradiation. This suggested that firstly autophagy was activated in order to repair irradiation induced damages [194] but it also favoured apoptosis in some cells, and secondly mTORC1 was activated to ensure cell survival and mitosis to replace dead cells. This hypothesis is supported by the fact that it was demonstrated that autophagy induced by irradiation could favour apoptosis in malignant glioma cells [161]. On the other hand, Wu et al. [162] who carried out targeted cytoplasmic irradiation of human

small airway epithelial cells noticed a protective effect of autophagy since inhibition of autophagy by chloroquine and 3-methyladenine DNA repair was delayed and cell viability decreased. The activation of autophagy, which occurred 30 minutes after irradiation, was correlated with AMPK activation and mTORC1 inhibition at the same time point. This AMPK activation was possibly due to mitochondrial dysfunction induced by irradiation, since Zhao et al. [186] demonstrated in human HaCaT keratinocytes that following UV irradiation, mitochondria were damaged leading to activation of AMPK which in turn triggered autophagy, promoting cell survival. Bralic et al. [136] observed in C57BL/6 mice an increase of proliferative index of submandibular gland cells from day 3 to day 6 after irradiation and decreased beyond. Mitosis clearly occurred from day 3 to day 6 and probably beyond. This is consistent with mTORC1 activation noticed from day 5 to 7 in our mice and from day 4 to 5 in Morgan Bathke et al. experiment [48]. mTORC1 activation also ensured cell survival [44, 135]. However, the irradiation activation of mTORC1 could also favour cellular senescence since irradiation induces oxidative stress in mitochondria [176] and it was demonstrated that increase of ROS in mitochondria activated mTORC1 leading to senescence, whereas blocking mTORC1 by rapamycin or administration of mitochondrial ROS scavengers inhibited senescence activation [177]. ROS can also favour apoptosis since administration of antioxidants blocks it [179, 187]. Activation of mTORC1 and autophagy by ROS is dose dependent, since it was demonstrated in cardiac fibroblasts that S6K1 was phosphorylated when H_2O_2 concentration was $\leq$ 600 µM, whereas at 800 µM AMPK was significantly activated thus decreasing S6K1 phosphorylation [177]. However, no paper mentions AMPK activation in irradiated salivary glands. Besides ROS is also known to induce ER stress activating autophagy [209]. The same phenomenon could occur in salivary glands. Since MRT67307 did not block autophagy in Torin 1 treated and starved SMG-C6 cells and primary submandibular gland, ROS triggers autophagy without activating ULK1 and ULK2, so irradiation induced autophagy is probably mTOR and ULK independent. **Figure 51** shows the likely effects of irradiation on salivary glands.

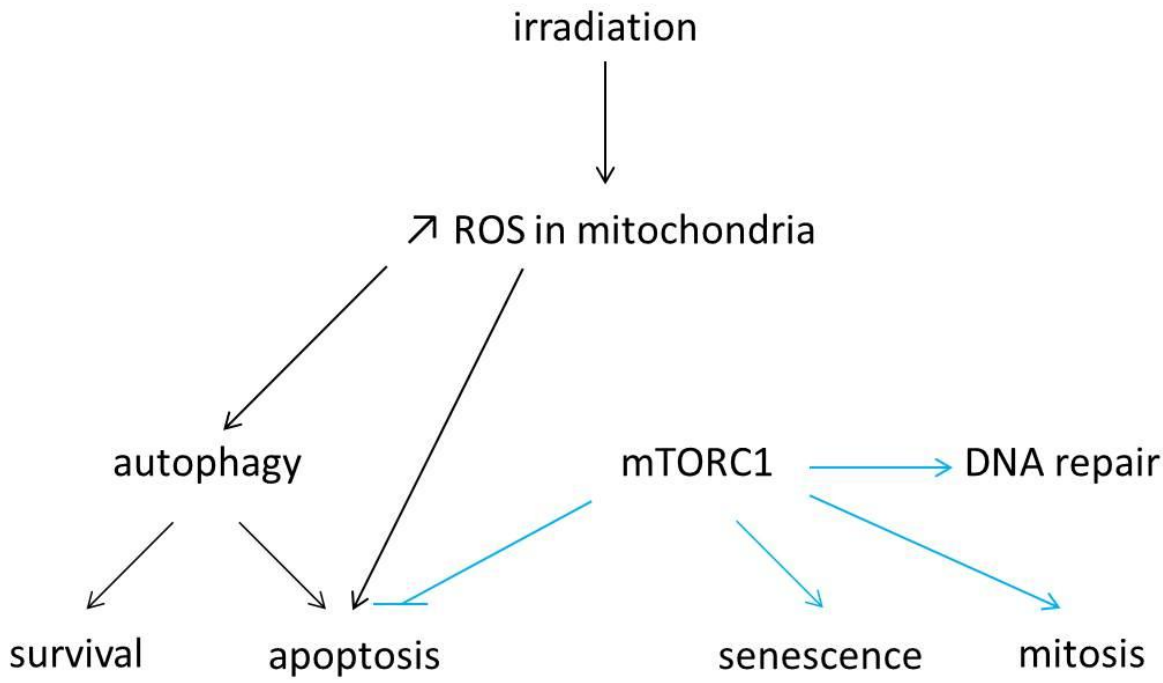

Fig. 51. Likely effects of irradiation on salivary glands. Irradiation transiently increases ROS in mitochondria triggering autophagy (without activating ULK) which can be pro-survival but can also be pro-apoptotic. ROS could also activate apoptosis without autophagic activation as well. A few days later, as ROS concentration decreases, autophagy is reduced. Then mTORC1 becomes activated to trigger mitosis to replace dead cells, ensuring DNA repair and blocking apoptosis or favouring senescence.

It is worth mentioning that ULK1 and ULK2 are also involved in neural growth and this growth is autophagy independent. They can also hasten apoptosis when cells accumulate a high amount of ROS [193]. Maybe irradiation induced apoptosis is partially due to ULK1 and ULK2 involvement.

Concerning saliva flow experiments, we did not see any statistically significant decrease of saliva flow during the first week. However, we observed an increase of stimulated saliva flow from day 14 to 24, and then it decreased to become normal. Maybe this phenomenon was due to the fact that following irradiation new acinar cells were produced in order to replace dead ones, and since there was an excessive proliferation of acinar cells, those which were damaged but still functional were eliminated. No paper mentions this transient increase of saliva flow following irradiation, so this finding is novel.

Ligated submandibular gland experiments showed that chloroquine and MRT67307 injections had no beneficial effect, except the fact that they slightly decreased glands atrophy. It is hard to make any definitive conclusion at the moment,

but the injected doses were probably not correct, at least for chloroquine. In chloroquine injected glands (control, ligated and contralateral), we expected LC3-II bands were going to increase since chloroquine was known to block LC3-II degradation by raising lysosomal pH [168], but we did not notice any spectacular increase of LC3-II bands intensities, so autophagy inhibition was weak. The dose was probably not strong enough. Indeed, Adelusi et al. [188] who also intraperitoneally injected 10 mg/kg of chloroquine in rats noticed that in many tissues chloroquine was weakly eliminated 1 week after injection (**fig. 52**).

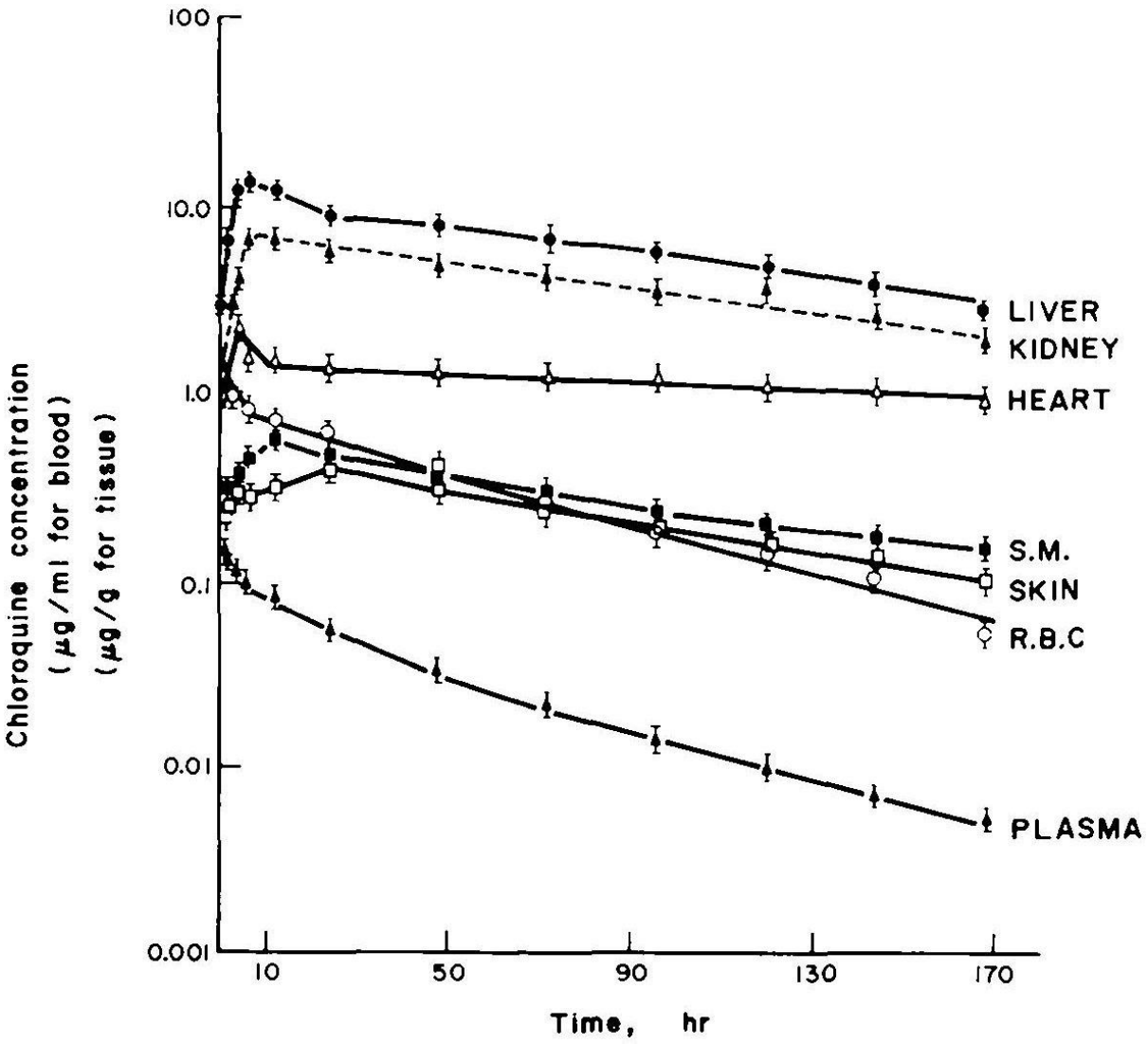

Fig. 52. Concentration time curve for chloroquine in rat different tissues following a single intraperitoneal injection (10 mg/kg). One point: mean ± SE. SM: skeletal muscle; RBC: red blood cell [188].

Concerning MRT67307, 100 µL and even 200 µL injections were inefficient to inhibit autophagy, which means that autophagy is ULK independent. However, we cannot exclude that autophagy is partly ULK dependent. To verify this hypothesise, the

use of MRT68921 known to inhibit more potently ULK1 (IC_{50} = 2.9 nM instead of 45 nM) and ULK2 (IC_{50} = 1.1 nm instead of 38 nM) than MRT67307 [70] should be more efficient to block autophagy. There is at least one paper mentioning the effects of autophagy inhibition on ligated submandibular gland. Lin et al. [169] tested the effects of Atg5 knock-out in ligated mouse submandibular glands. They uncovered that Atg5 knock-out delayed acinar cells apoptosis which was beneficial. On the other hand, senescence in ductal cells (probably due to the lack of clearance mechanism) was strongly activated in both Atg5 knock-out and control ligated glands after 3 days ligation, but after 7 days ligation Atg5 knock-out ligated glands was stronger than ligated control glands. So Atg5 knock-out favoured senescence, which was detrimental. Besides, Atg5 knock-out ligated glands weights were slightly higher than those of ligated control glands 3 days after ligation, whereas no difference could be observed 7 days after ligation. Therefore the effects of autophagy inhibition by knocking-out Atg5 is similar to those of inhibition of mTOR by rapamycin since administration of the latter maintains ligated glands weights up to 3 days whereas 7 days after ligation they are atrophic like the ligated only glands [45]. Maybe autophagy inhibition by chloroquine and MRT67307 had similar effects. It is tempting to say that Atg5 is more important than ULK1 in autophagy induction, but it is not the case. Indeed, Cemma et al. [24] noticed that in Atg5 knock-out mouse embryonic fibroblasts and bone marrow derived macrophages, phagosome maturation occurred. For their part, Arakawa et al. [170] uncovered that in Atg5 deficient mouse embryonic fibroblasts, autophagic structures (such as autophagosomes and autolysosomes) formed after administration of etoposide (inducer of DNA strand breaks). On the other hand, silencing ULK1 or FIP200 (forms a complex with ULK1) in Atg5 deficient mouse embryonic fibroblasts led to a decrease of autophagic membranes formation. The role of this Atg5 independent autophagy is not clearly defined at the moment but it was found that during reticulocytes maturation, mitochondria were eliminated by this type of autophagy, while conventional autophagy is involved in elimination of ribosomes and endoplasmic reticulum. Therefore it seems that Atg5 independent autophagy and conventional autophagy do not play the same role within the same cell. In fact, the importance of ULK and Atg proteins is probably cell type dependent. Indeed, Alers et al. [174] who cultured DT40 cells (chicken lymphoblasts), noticed that ULK1 and ULK2 double knock-out did not inhibit starvation induced autophagy, whereas Atg13 knock-out did it. They also observed that Atg13 function depended on FIP200 binding.

Despite the fact that we could not uncover why in ligated submandibular glands both mTOR and autophagy were activated, the likely reason is that many reactions take place simultaneously. Ligation persistently stresses submandibular gland cells, notably acinar cells, thus activating autophagy which in turn activates apoptosis [68]. However, mTOR activation also occurs in many cells as some acinar cells try to resist apoptosis [44]. Moreover, ductal cells [155, 163] and probably acinar cells [95] undergo mitosis, which necessitate mTOR activation as well. Besides it is known that ROS is generated in duct ligated liver [178, 183] and mitochondria themselves generate ROS [178], so mitochondria in ligated salivary glands probably generate ROS, leading to mTORC1 activation which in turn favours cellular senescence [177] but autophagy activation as well [162]. It was also demonstrated in rat alveolar epithelial cells that administration of rapamycin prior to hypoxia-reoxygenation (favours ROS production) decreased endoplasmic reticulum stress [180]. Moreover Lemer et al. [181] noticed that in WI-38 cells (human diploid fibroblasts) administration of rapamycin decreased ROS levels within cells, cells were more resistant to exogenous H_2O_2 exposure, and their lifespan increased. These effects were due to strong autophagic flux which favoured clearance of depolarized mitochondria. For their part Miwa et al. [185] observed in mouse brain neurons that mTOR inhibition by rapamycin increased accumulation of TERT (telomerase reverse transcriptase) in mitochondria and decreased mitochondrial ROS release, while in TERT knock-out brain neurons rapamycin administration had no effect on this ROS release. Therefore, the beneficial effect of rapamycin administration on ligated salivary glands [45] could partly be due to the fact that since mTORC1 is inhibited, TERT accumulates into mitochondria, and autophagy activation leads to clearance of depolarized mitochondria, hence decreasing oxidative stress and blocking apoptosis. Therefore ROS produced during ligation activates autophagy, even if mTORC1 is activated suggesting autophagy is mainly mTOR independent. **Figure 53** illustrates the likely effects of ligation and administration of rapamycin on salivary glands.

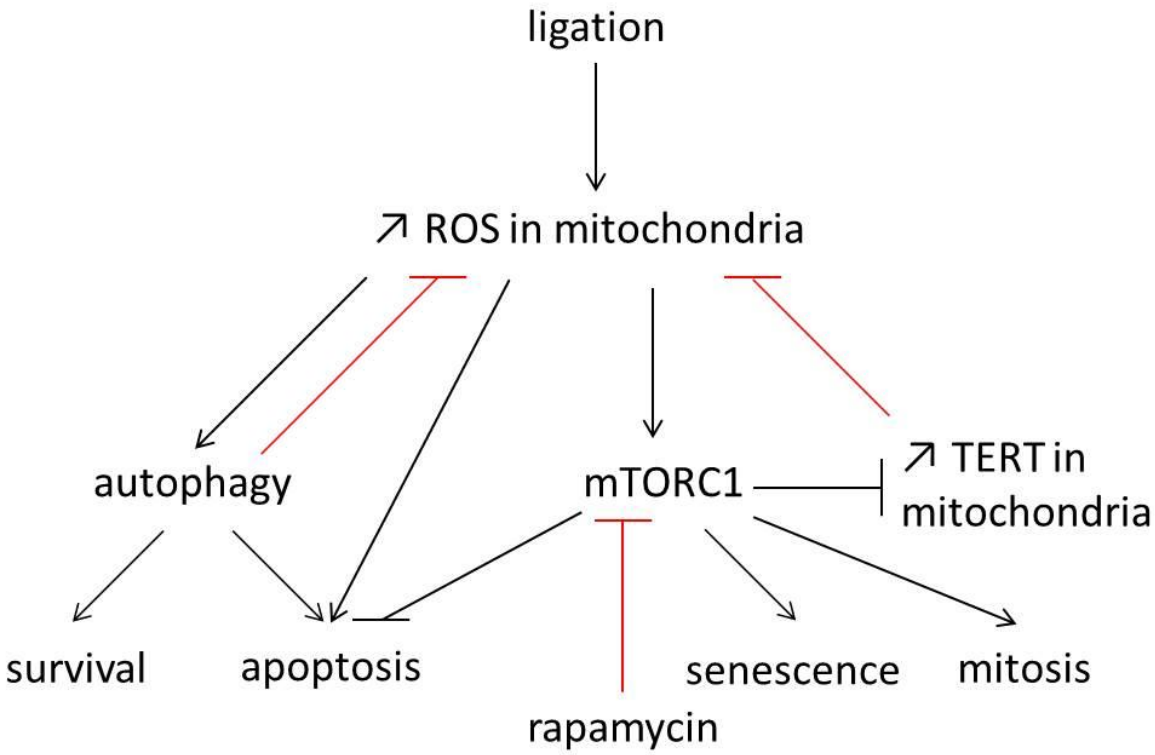

Fig. 53. Likely effects of ligation and administration of rapamycin on salivary glands. Ligation increases cellular stress, especially by increasing mitochondrial ROS production which in turn activates mTORC1, autophagy and apoptosis. Even though autophagy can have protective effects, its activation could favour apoptosis. mTORC1 activation probably increases oxidative stress leading to apoptosis by inhibiting TERT accumulation in mitochondria. Concerning autophagy, ROS activates autophagy even if mTORC1 is activated, permitting mTOR independent autophagy. If rapamycin is immediately administrated following ligation, oxidative stress is decreased since TERT can accumulate in mitochondria and autophagy can eliminate depolarized mitochondria, favouring survival.

ROS and mitochondria are certainly key components of autophagy activation and apoptosis. In mammalian cells oxidized proteins can be eliminated by chaperone-mediated autophagy, and mildly stressed lysosomes are prone to bind and internalize more substrates by chaperone-mediated autophagy, which is pro-survival. In plant cells, macroautophagy is activated to degrade oxidized proteins, which is pro-survival as well. During starvation, H_2O_2 is accumulated in mitochondria and it oxidizes Atg4 which in turn cleaves the C-terminus of Atg8 (LC3 in mammalian cells) which is required for autophagosome maturation. In sympathetic neurons, the lack of nerve growth factor favours accumulation of ROS in mitochondria, oxidizing their lipids and causing loss of cardiolipin, leading to autophagic cell death. Administration of rapamycin to *Saccharomyces cerevisiae* promotes ROS production in mitochondria, oxidizing their lipids and leading to autophagic cell death as well [182]. Besides mitochondria can

release ROS into cytosol favouring more ROS production leading to stronger mitochondrial and cellular damages [184].

This study provided new data concerning mTOR and autophagy activation in salivary glands. Firstly inhibition of both ULK1 and ULK2 by MRT67307 on SMG-C6 cells and mouse primary submandibular gland cells revealed that autophagy was mainly mTOR independent in these cells. Secondly irradiation experiments showed that irradiation could transiently increase saliva flow, probably due to acinar cell mitosis and mTOR activation. Thirdly we carried out the first in vivo experiment using MRT67307 and we uncovered that autophagy activation in mouse ligated submandibular gland was mainly mTOR independent, confirming the results obtained on SMG-C6 cells and mouse primary submandibular gland.

FUTURE WORKS

Despite the fact that we obtained some interesting results in this PhD work, it will be necessary to continue experiments in order to better understand the mechanisms of salivary gland atrophy and the treatment to improve their regeneration in both irradiated and ligated glands.

To verify if MRT67307 was not strong enough to strongly block autophagy, MRT68921 which is more potent [70] will be tested. If this compound can strongly decrease autophagy, then it would mean that ULK1 and ULK2 are significantly involved in submandibular gland autophagy. It would also be interesting to inject both MRT68921 and Torin 1 (simultaneously or not) and see if this combination can be beneficial. It will also be necessary to carry out western blot to see the phosphorylation status of ULK1 and ULK2.

If Torin 1 and/or MRT68921 injections can protect salivary glands from irradiation, it will be necessary to verify if saliva flow is improved. Nonetheless, it will be necessary to improve our technique in order to collect saliva more efficiently.

Administration of MRT67307 clearly blocked autophagy in NIH 3T3. However, this compound inhibits both ULK1 and ULK2, so we could not know which one was the most important in autophagy activation. It will be necessary to knock out ULK1 only and ULK2 only to find the answer. It will also be interesting to knock-out both to see if SMG-C6 can activate autophagy without them.

Since irradiation and probably ligation of salivary glands generate ROS in mitochondria, administration of mitochondrial ROS scavengers should have protective effects.

Western blot did not work as AQP5 was cleaved, so it was not possible to see if irradiation modified its expression. By carrying out RT-PCR, there should be fewer problems.

Injection of pilocarpine triggered autophagy in submandibular glands. It could be interesting to see if administration of this drug to SMG-C6 will have the same effect.

Recently an ULK1 activator known as LYN-1604 was discovered [192]. This drug should be tested in vitro to see if its effect is stronger compared to inhibition by MRT67307 and MRT68921. It should also be injected in rodents in order to trigger autophagy in salivary glands.

BIBLIOGRAPHY

1. Redman RS. **On approaches to the functional restoration of salivary glands damaged by radiation therapy for head and neck cancer, with a review of related aspects of salivary gland morphology and development.** Biotech. Histochem. 2008, 83 (3), 103-130.

2. Nanduri LSY, Maimets M, Pringle SA,van der Zwaag M, van Os RP, Coppes RP. **Regeneration of irradiated salivary glands with stem cell marker expressing cells.** Radiother Oncol 2011, 99 (3), 367-372.

3. Abok K, Brunk U, Jung B, Ericsson J. **Morphologic and histochemical studies on the differing radiosensitivity of ductural and acinar cells of the rat submandibular gland.** Virchows Arch. B Cell Pathol. including molecular pathology 1984, 45 (4), 443-460.

4. Cherry CP, Gluckman A. **Injury and repair following irradiation of salivary glands in male rats.** Br. J. Radiol. 1959, 32 (381), 596-608.

5. Nagler RM. **The enigmatic mechanism of irradiation-induced damage to the major salivary glands.** Oral Diseases 2002, 8, 141-146.

6. Coppes RP, Zeilstra LJW, Kampinga HH, Konings AWT. **Early to late sparing of radiation damage to the parotid gland by adrenergic and muscarinic receptor agonists.** Br. J. Cancer 2001, 85 (7), 1055-1063.

7. Peter B, Van Waarde MAWH, Vissink A,'s-Gravenmade EJ, Konings AWT. **The role of secretory granules in radiation-induced dysfunction of rat salivary glands.** Radiation Research 1995, 141 (2), 176-182.

8. Valdez IH, Atkinson JC, Ship JA, Fox PC. **Major salivary gland function in patients with radiation-induced xerostomia: flow rates and sialochemistry.** Int J Radiation Oncol Biol Physiol 1992, 25 (1), 41-47.

9. Chomette G, Auriol M, Vaillant JM, Bertrand JC, Chenal C. **Effects of irradiation on the submandibular gland of the rat. An enzyme histochemical and ultrastructural study.** Virchows Arch. (Pathol. Anat.) 1981, 391 (3), 291-299.

10. Mandel SJ, Mandel L. **Radioactive iodine and the salivary glands.** Thyroid 2003, 13 (3), 265-271.

11. Valdez IH, Atkinson JC, Ship JA, Fox PC. **Major salivary gland function in patients with radiation-induced xerostomia: flow rates and sialochemistry.** Int. J. Radiation Oncol. Biol. Physiol. 1992, 25 (1), 41-47.

12. Heylmann D, Rödel F, Kindler T, Kaina B. **Radiation sensitivity of human and murine peripheral blood lymphocytes, stem and progenitor cells.** Biochim. Biophys. Acta 2014, 1846 (1), 121-129.

13. Wang Y, Schulte BA, LaRue AC, Ogawa M, Zhou D. **Total body irradiation selectively induces murine hematopoietic stem cell senescence.** Blood 2006, 107 (1), 358-366.

14. Grande T, Gaitán S, Tejero C, Bueren JA. **Residual haematopoieteic damage in adult and 8 day-old mice exposed to 7 Gy of X-rays.** Int. J. Radiat. Biol. 1993, 63 (1), 59-67.

15. Vávrová J, Sinkorová Z, Rezáčová M, Tichý A, Filip S, Mokrý J, Lukášová E. **Irradiated stem cells and ageing of the haematopoietic system.** Radiat. Environ. Biophys. 2012, 51 (2), 205-213.

16. Simonnet AJ, Nehmé J, Vaigot P, Barroca V, Leboulch P, Tronik-Le Roux D. **Phenotypic and functional changes induced in haematopoietic stem/progenitor cells after gamma-ray radiation exposure.** Stem cells 2009, 1400-1409.

17. Wang Y, Liu L, Pazhanisamy SK, Li H, Meng A, Zhou D. **Total body irradiation causes residual bone marrow injury by induction of persistent oxidative stress in murine hematopoietic stem cells.** Free Radic. Biol. Med. 2010, 48 (2), 348-356.

18. Ban N, Kai M. **Implication of replicative stress-related stem cell ageing in radiation-induced murine leukaemia.** Br. J. Cancer 2009, 101 (2), 363-371.

19. Yamauchi M, Otsuka K, Kondo H, Hamada N, Tomita M, Takahashi M, Nakasono S, Iwasaki T, Yoshida K. **A novel in vitro survival assay of small intestinal stem cells after exposure to ionizing radiation.** J. Radiat. Res. 2014, 55 (2), 381-390.

20. Li T, Li L, Li F, Liu Y. **X-ray irradiation accelerates senescence in hippocampal neural stem/progenitor cells via caspase-1 activation.** Neurosci. Lett. 2015, 585, 60-65.

21. Schneider L, Pellegatta S, Favaro R, Pisati F, Roncaglia P, Testa G, Nicolis SK, Finocchiaro G, D'Adda di Fagagna F. **DNA damage in mammalian neural stem cells leads to astrocytic differentiation mediated by BMP2 signaling through JAK-STAT.** Stem Cell Reports 2013, 1 (2), 123-138.

22. Semont A, Nowak EB, Silva Lages C, Mathieru C, Mouthon MA, May E, Allemand I, Millet P, Boussin FD. **Involvement of p53 and fas/CD95 in murine neural progenitor cell response to ionizing irradiation.** Oncogene 2004, 23 (52), 8497-8508.

23. Yamahara K, Yasuda M, Kume S, Koya D, Maegawa H, Uzu T. **The role of autophagy in the pathogenesis of diabetic nephropathy.** Journal of Diabetes Research 2013, Vol. 2013, article ID 193757.

24. Cemma M, Grinstein S, Brumell JH. **Autophagy proteins are not universally required for phagosome maturation.** Autophagy 2016, Vol. 12, No. 9

25. Su W, Chen Y, Zeng W, Liu W, Sun H. **Involvement of Wnt signalling in the injury of murine mesenchymal stem cells exposed to X-radiation.** Int. J. Radiat. Biol. 2012, 88 (9), 635-641.

26. Jung CH, Ro S-H, Cao J, Otto NM, Kim D-H. **mTOR regulation of autophagy.** FEBS Lett. 2010. 584 (7), 1287-1295.

27. AlQurashi N, Hashimi SM, Wei MQ. **Chemical inhibitors and microRNAs (miRNA) targeting the mammalian target of rapamycin (mTOR) pathway: potential for novel anticancer therapeutics.** Int. J. Sci. 2013, 14 (2), 3874-3900.

28. Magnuson B, Ekim B, Fingar DC. **Regulation and function of ribosomal protein S6 kinase (S6K) within mTOR signalling networks.** Biochem. J. 2012, 441 (1), 1-21.

29. Dann SG, Selvaraj A, Thomas G. **mTOR complex 1-S6K1 signaling: at the crossraods of obesity, diabetes and cancer.** TRENDS Mol. Med. 2007, 13 (6), 252-259.

30. Huang S, Bjornsti M-A, Houghton PJ. **Rapamycins: mechanism of action and cellular resistance.** Cancer Biol. Ther. 2003, 2 (3), 222-232.

31. Wullschleger S, Loewith R, Hall MN. **TOR signaling in growth and metabolism.** Cell 2006, 124 (3), 471-484.

32. Yoshida S, Hong S, Suzuki T, Nada S, Mannan AM, Wang J, Okada M, Guan K-L, Inoki K. **Redox regulates mammalian target of rapamycin complex 1 (mTORC1) activity by modulating the TSC1/TSC2-Rheb GTPase pathway.** J. Biol. Chem. 2011, 286 (37), 32651-32660.

33. Kim D-H, Sarbassov Dos D, Ali SM, King JE, Latek RR, Erdjument-Bromage H, Tempst P, Sabatini DM. **mTOR interacts with raptor to form a nutrient-sensitive complex that signals to the cell growth machinery.** Cell 2002, 110 (2), 163-175.

34. Hay N, Sonenberg N. **Upstream and downstream of mTOR.** Genes Dev. 2004, 18 (16), 1926-1945.

35. Nicklin P, Bergman P, Zhang B, Triantafellow E, Wang H, Nyfeler B, Yang H, Hild M, Kung C, Wilson C, Myer VE, MacKeigan JP, Porter JA, Wang YK, Cantley LC, Finan PM, Murphy LO. **Bidirectional transport of amino acids regulates mTOR and autophagy.** Cell 2009, 136 (3), 521-534.

36. Carrera AC. **TOR signaling in mammals.** Journal of Cell Science 2004, Sep 15, 117 (Pt 20), 4615-4616.

37. Feldman ME, Apsel B, Uotila A, Loewith R, Knight ZA, Ruggero D, Shokat KM. **Active-site inhibitors of mTOR target rapamycin-resistant outputs of mTORC1 and mTORC2.** PLOS Biology 2009, 7 (2), 371-383.

38. Sarbassov DD, Guertin DA, Ali SM, Sabatini DM. **Phosphorylation and regulation of Akt/PKB by the rictor-mTOR complex.** Science 2005, 307 (5712), 1098-1101.

39. DeBosch BJ, Heitmeier MR, Mayer AL, Higgins CB, Crowley JR, Kraft TE, Chi M, Newberry EP, Chen Z, Finck BN, Davidson NO, Yarasheski KE, Hruz PW, Moley KH. **Trehalose inhibits solute carrier 2A (SLC2A) proteins to induce autophagy and prevent hepatic steatosis.** Sci Signal 2016, Feb 23; 9 (416): ra21.

40. Frias MA, Thoreen CC, Jaffe JD, Schroder W, Sculley T, Carr SA, Sabatini DM. **mSin1 is necessary for Akt/PKB phosphorylation, and its isoforms define three distinct mTORC2s.** Curr. Biol. 2006, 16 (18), 1865-1870.

41. Yuan R, Kay A, Berg WJ, Lebwohl D. **Targeting tumorigenesis: development and use of mTOR inhibitors in cancer therapy.** J. Hematol. Oncol. 2009, 2 (45)

42. Faivre S, Kroemer G, Raymond E. **Current development of mTOR inhibitors as anticancer agents.** Nat. Rev. Drug Discov. 2006, 5 (8), 671-688.

43. Hai B, Yang Z, Shangguan L, Zhao Y, Boyer A, Liu F. **Concurrent transient activation of Wnt/β-catenin pathway prevents radiation damage to salivary glands.** Int. J. Radiat. Oncol. Biol. Phys. 2012, 83 (1), e109-e116.

44. Silver N, Proctor GB, Arno M, Carpenter GH. **Activation of mTOR coincides with autophagy during ligation-induced atrophy in the rat submandibular gland.** Cell Death and Disease 2010, Vol. 1, e14; doi: 10.1038/cddis.2009.12.

45. Bozorgi SS, Proctor GB, Carpenter GH. **Rapamycin delays salivary gland atrophy following ductal ligation.** Cell Death and Disease 2014, Vol. 5, e1146.

46. Maiuri MC, Zalckvar E, Kimchi A, Kroeme G. **Self-eating and self-killing: crosstalk between autophagy and apoptosis.** Nat. Rev. Mol. Cell Biol. 2007, 8 (9), 741-752.

47. Morgan-Bathke M, Hill GA, Harris ZI, Lin HH, Chibly AM, Klein RR, Burd R, Ann DK, Limesand KH. **Autophagy correlates with maintenance of salivary gland function following radiation.** Sci. Rep. 2014, 4.

48. Morgan-Bathke M, Harris ZI, Arnett DG, Klein RR, Burd R, Ann DK, Limesand KH. **The rapalogue, CCI-779, improves salivary gland function following radiation.** PLoS One 2014, 9 (12).

49. Zhang B, Su YP, Ai GP, Liu XH, Wang FC, Cheng TM. **Differentially expressed proteins of gamma-ray irradiated mouse intestinal epithelial cells by two-dimensional electrophoresis and MALDI-TOF mass spectrometry.** World J. Gastroenterol. 2003, 9 (12), 2726-2731.

50. Bannik K, Rössier U, Faus-Kessier T, Gomolka M, Hornhardt S, Dalke C, Klymenko O, Rosemann M, Trott KR, Atkinson M, Kulka U, Graw J. **Are mouse lens epithelial cells more sensitive to γ-irradiation than lymphocytes?** Radiat. Environ. Biophys. 2013, 52, 279-286.

51. Knox SM, Lombaert IMA, Haddox CL, Abrams SR, Cotrim A, Wilson AJ, Hoffman MP. **Parasympathetic stimulation improves epithelial organ regeneration.** Nat. Commun. 2013, 4:1494.

52. Chibly AM, Querin L, Harris Z, Limesand KH. **Label-retaining cells in the adult murine salivary glands possess characteristics of adult progenitor cells.** PLoS One 2014, 9 (9).

53. Mizushima N, Levine B. **Autophagy in mammalian development and differentiation.** Nat. Cell Biol. 2010, 12 (9), 823-830.

54. Ding WX, Yin XM. **Mitophagy: mechanisms, pathological roles, and analysis.** Biol. Chem. 2012, 393 (7), 547-564.

55. Schneider JL, Cuervo AM. **Autophagy and human disease: emerging themes.** Curr. Opin. Genet. Dev. 2014, 26, 16-23.

56. Petherick KJ, Conway OJL, Mpamhanga C, Osborne SA, Kamal A, Saxty B, Ganley IG. **Pharmacological inhibition of ULK1 kinase blocks mammalian target of rapamycin (mTOR)-dependant autophagy.** J. Biol. Chem. 2015, 290 (18), 11376-11183.

57. Kundu M, Lindsten T, Yang CY, Wu J, Zhao F, Zhang J, Selak MA, Ney PA, Thompson CB. **Ulk1 plays a critical role in the autophagic clearance of mitochondria and ribosomes during reticulocyte maturation.** Blood 2008, 112 (4), 1493-1502.

58. Codogno P, Mehrpour M, Proikas-Cezanne T. **Canonical and non-canonical autophagy: variations on a common theme of self-eating?** Nat. Rev. Mol. Cell Rev. 2012, 13 (1), 7-12.

59. Hu YY, Zhou CH, Dou WH, Tang W, Hu CY, Hu DM, Feng H, Wang JZ, Qian MJ, Cheng GL, Wang SF. **Improved autophagic flux is correlated with mTOR activation in the later recovery stage of experimental acute pancreatitis.** Pancreatology 2015, 15 (5), 470-477.

60. Hać A, Domachowska A, Narajczyk M, Cyske K, Pawlik A, Herman-Antosiewicz A. **S6K1 controls autophagosome maturation in autophagy induced by sulforaphane or serum deprivation.** Eur. J. Cell Bio. 2015, 94 (10), 470-481.

61. Kang YL, Saleem MA, Chan KW, Yung BYM, Law HKW. **Trehalose, an mTOR independent autophagy inducer, alleviates human podocyte injury after puromycin aminonucleoside treatment.** PLoS One 2014, 9 (11).

62. Tang H, Inoki K, Lee M, Wright E, Khuong A, Khuong A, Sugiarto S, Garner M, Paik J, DePinho RO, Goldman D, Guan KL, Shrager JB. **mTORC1 promotes denervation-induced muscle atrophy through a mechanism involving the activation of FoxO and E3 ubiquitin ligases.** Sci. Signal. 2014, 7 (314).

63. Manzoni C, Mamais A, Roosen DA, Dihanich S, Soutar MP, Plun-Favreau H, Bandopadhyay R, Hardy J, Tooze SA, Cookson MR, Lewis PA. **mTOR independent regulation of macroautophagy by Leucine Rich Repeat Kinase 2 via Beclin-1.** Sci. Rep. 2016, 6, 635106.

64. Giménez-Xavier P, Roser F, Platini F, Pérez R, Ambrosio S. **LC3-I conversion to LC3-II does not necessarily result in complete autophagy.** Int. J. Mol. Med. 2008, 22 (6), 781-785.

65. Mizushima N, Komatsu M. **Autophagy: Renovation of Cells and Tissues.** Cell 2011, 147 (4), 728-741.

66. Li WW, Li J, Bao JK. **Microautophagy: lesser-known self-eating.** Cell. Mol. Life Sci. 2012, 69 (7), 1125-1136.

67. Encyclopaedia Britannica 2010.

68. Mariño G, Niso-Santano M, Baehrecke EH, Kroemer G. **Self-consumption: the interplay of autophagy and apoptosis.** Nat. Rev. Mol. Cell Biol. 2014, 15 (2), 81-94.

69. Yin Y, Dang W, Zhou X, Xu L, Wang W, Cao W, Chen S, Su J, Cai X, Xiao S, Peppelenbosch MP, Pan Q. **PI3K-Akt-mTOR axis sustains rotavirus infection via the 4E-BP1 mediated autophagy pathway and represents an antiviral target.** Virulence 2017, Vol. 0, No. 0, 1-16.

70. Petherick KJ, Conway OJL, Mpamhanga C, Osborne SA, Kamal A, Saxty B, Ganley IG. **Pharmacological inhibition of ULK1 kinase blocks mammalian target of rapamycin (mTOR)-dependent autophagy.** J. Biol. Chem. 2015, 290 (18), 11376-11383.

71. Leontieva OV, Demidenko ZN, Blagosklonny MV. **Dual mTORC1/C2 inhibitors suppress cellular geroconversion (a senescence program).** Oncotarget 2015, Jul 27.

72. Guertin DA, Sabatini D. **The pharmacology of mTOR inhibition.** Cancer 2009, 2 (67).

73. Christy B, Demaria M, Campisi J, Huang J, Jones D, Dodds SG, Williams C, Hubbard G, Livi CB, Gao X, Weintraub S, Curiel T, Sharp ZD, Hasty P. **p53 and rapamycin are additive.** Oncotarget 2015, 6 (18).

74. Egan DF, Chun MGH, Vamos M, Zou H, Rong J, Miller CJ, Lou HJ, Raveendra-Panickar D, Yang CC, Sheffler DJ, Teriete P, Asara JM, Turk BE, Cosford NDP, Shaw RJ. **Small molecule inhibition of the autophagy kinase ULK1 and identification of ULK1 substrates.** Mol. Cell 2014, 59 (2), 285-297.

75. Yang YP, Hu LF, Zheng HF, Mao CJ, Hu WD, Xiong KP, Wang F, Liu CF**. Application and interpretation of current autophagy inhibitors and activators.** Acta Pharmacol. Sin. 2013, 34 (5), 625-635.

76. Berkovitz, BKB, Holland GR, Moxham BJ. **Oral Anatomy, Histology and Embryology.** 4th Edition 2009, Mosby Elsevier.

77. Osborn JW, Armstrong WG, Speirs RL. **Anatomy, Biochemistry and Physiology.** Oxford; Boston: Blackwell Scientific Publications, 1982.

78. Ekström J, Khosravani N, Castagnola M, Messana I. **Saliva and the Control of Its Secretion.** Dysphasia, Medical Radiology. Diagnostic Imaging, DOI: 10.1007/174_2011_481, Ekberg (ed.), Springer-Verlag Berlin Heidelberg 2012.

79. Delporte C, Steinfeld S. **Distribution and roles of aquaporins in salivary glands.** Biochim. Biophys. Acta 2006, 1758 (8), 1061-1070.

80. Delporte C. **Role of aquaporins in saliva secretion.** OA Biochemistry 2013 Sep 01; 1 (2): 14.

81. Larsen HS, Huus A-K, Galtung HK. **Aquaporin expression patterns in the developing mouse salivary glands.** Eur J Oral Sci 2009, 117 (6), 655-662.

82. Horsefield R, Nordén K, Fellert M, Backmart A, Törnroth-Horsefield S, Terwisscha van Scheltinga AC, Kvassman J, Kjellbom P, Johanson U, Neutze R. **High-resolution x-ray structure of human aquaporin 5.** PNAS 2008, 105 (36).

83.Takakura K, Takaki S, Takeda I, Hanaue N, Kizu Y, Tonogi M, Yamane GY. **Effect of cevimeline on radiation-induced salivary gland dysfunction and AQP5 in submandibular gland in mice.** Bull. Tokyo Dent. Coll. 2007, 48 (2), 47-56.

84. Li Z, Zhao D, Gong B, Xu Y, Sun H, Yang B, Zhao X. **Decreased saliva secretion and down-regulation of AQP5 in submandibular gland in irradiated rats.** Radiat Res 2006, 165 (6), 678-687.

85. Yao C, Purwanti N, Karabasil M R, Azlina A, Javkhlan P, Hasegawa T, Akamatsu T, Hosoi T, Ozawa K, Hosoi K. **Potential down-regulation of salivary gland AQP5 by LPS via cross-coupling of NF-κB and p-c-Jun/c-Fos.** Am J Pathol 2010, 177 (2), 724-734.

86. Segal K, MD, Lisnyansky I, MD, Nageris B, MD, Feinmesser R, MD. **Parasympathetic innervation of the salivary glands.** Operative Techniques in Otolaryngology-Head and Neck Surgery 1996, Vol. 7, Issue 4, 333-338.

87. Tabak LA, Levine MJ, Mandel ID, Ellison SA. **Role of salivary mucins in the protection of the oral cavity.** J. Oral Pathol. 1982, 11 (1): 1-17.

88. Slomiany BL, Murty VLN, Piotrowski J, Slomiany A. **Salivary mucins in oral Mucosal defense.** Gen. Pharmac. 1996, 27 (5), 761-777.

89. Liu B, Lague JR, Nunes DP, Toselli P, Oppenheim FG, Soares RV, Troxler RF, Offner GD. **Expression of membrane-associated mucins MUC1 and MUC4 in major human salivary glands.** J. Histochem. Cytochem. 2002, 50 (6), 811-820.

90. Gibbins HL, Proctor GB, Yakubov GE, Wilson S, Carpenter GH. **Concentration of salivary protective proteins within the bound oral mucosal pellicle.** Oral Dis. 2014, 20 (7), 707-713.

91. Fan XY, Tian C, Wang H, Xu Y, Ren K, Zhang BY, Gao C, Shi Q, Meng G, Zhang LB, Zhao YJ, Shao QX, Dong XP. **Activation of the AMPK-ULK1 pathway plays an important role in autophagy during prion infection.** Sci. Rep. 2015, 5: 14728

92. Siddiqui SJ. **Sialolithiasis: an unusually large submandibular salivary stone.** Br. Dent. J. 2002, 193 (2), 89-91.

93. Coppes RP, Stokman MA. **Stem cells and the repair of radiation-induced salivary gland damage.** Oral Dis. 2011, 17 (2), 145-153.

94. Pringle S, Van Os R, Coppes RP. **Concise review: adult salivary gland stem cells and a potential therapy for xerostomia.** Stem Cells 2013, 31 (4), 613-619.

95. Aure MH, Konieczny SF, Ovitt CE. **Salivary gland homeostasis is maintained through acinar cell self-duplication.** Dev. Cell 2015, 33 (2), 231-237.

96. Fallahi B, Beiki D, Abedi SM, Saghari M, Fard-Esfahani A, Akhzari F, Mokarami B, Eftekhari M. **Does vitamin E protect salivary glands from I-131 radiation damage in patients with thyroid cancer?** Nucl. Med. Commun. 2013, 34 (8), 777-786.

97. Babicová A, Havlínová Z, Hroch M, Řezáčová M, Pejchal J, Vávrová J, Chládek J. **In vivo study of radioprotective effect of NO-synthase inhibitors and acetyl-L-carnitine.** Physiol. Res. 2013, 62 (6), 701-710.

98. Üçüncü H, Ertekin MV, Yörük Ö, Sezen O, Özkan A, Erdoğan F, Kiziltunç A, Gündoğdu C. J. **Vitamin E and L-carnitine, separately or in combination, in the prevention of radiation-induced oral mucositis and myelosuppression: a controlled study in a rat model.** Radiat. Res. 2006, 47 (1), 91-102.

99. Yamada T, Ryo K, Tai Y, Tamaki Y, Inoue H, Mishima K, Tsubota K, Saito I. **Evaluation of therapeutic effects of astaxanthin on impairments in salivary secretion.** J. Clin. Biochm. Nutr. 2010, 47 (2), 130-137.

100. Şimşek G, Gürocak Ş, Karadağ N, Karabulut AB, Demirtaş E, Karataş E. **Protective effects of resveratrol on salivary gland damage induced by total body irradiation in rats.** Laryngoscope 2012, 122 (12), 2743-2748.

101. Funegård U, Johansson I, Malmer B, Henriksson R, Ericson T. **Can α-tocopherol and β-carotene supplementation reduce adverse radiation effects on salivary glands?** Eur. J Cancer 1995, 31A (13-14), 2347-2353.

102. Sumita Y, Liu Y, Khalili S, Maria OM, Xia D, Key S, Cotrim AP, Mezey E, Tran SD. **Bone marrow-derived cells rescue salivary gland function in mice with head and neck irradiation.** Int. J. Biochem. Cell Biol. 2011, 43 (1), 80-87.

103. Schwarz S, Huss R, Schulz-Siegmund M, Vogel B, Brandau S, Lang S, Rotter N. **Bone marrow-derived mesenchymal stem cells migrate to healthy and damaged salivary glands following stem cell infusion.** Int. J. Oral Sci. 2014, 6 (3), 1-8.

104. Wang Z, Ju Z, He L, Li Z, Liu Y, Liu B. **Intraglandular transplantation of adipose-derived stem cells for the alleviation of irradiation-induced parotid gland damage in miniature pigs.** J. Oral Maxillofac. Surg. 2017, 75 (8), 1784-1790.

105. Nanduri LSY, Maimets M, Pringle SA, van der Zwaag M, van Os RP, Coppes RP. **Regeneration of irradiated salivary glands with stem cell marker expressing cells.** Radiother. Oncol. 2011, 99 (3), 367-372.

106. Feng J, van der Zwaag M, Stokman MA, van Os R, Coppes RP. **Isolation and characterization of human salivary gland cells for stem cell transplantation to reduce radiation-induced hyposalivation.** Radiother. Oncol. 2009, 92 (3), 466-471.

107. Andreadis D, Bakopoulou A, Leyhausen G, Epivatianos A, Volk J, Markopoulos A, Geurtsen W. **Minor salivary glands of the lips: a novel, easily accessible source of potential stem/progenitor cells.** Clin. Oral Invets. 2014, 18 (3), 847-856.

108. Ono H, Obana A, Usami Y, Sakai M, Nohara K, Egusa H, Sakai T. **Regenerating salivary glands in the microenvironment of induced pluripotent stem cells.** Biomed. Res. Int. 2015, 2015: 293570.

109. Fang D, Hu S, Liu Y, Quan VH, Seuntjens J, Tran SD. **Identification of the active components in bone marrow soup: a mitigator against irradiation-injury to salivary glands.** Sci. Rep. 2015, 5.

110. Amano O, Mizobe K, Bando Y, Sakiyama K. **Anatomy and histology of rodent and human major salivary glands.** Acta Histochem. Cytochem. 2012, 45 (5), 241-250.

111. Gray RH, Sokol M, Brabec RK, Brabec MJ. **Characterization of chloroquine-induced autophagic vacuoles isolated from rat liver.** Exp. Mol. Pathol. 1981, 34 (1), 72-86

112. Ramser B, Kokot A, Metze D, Weiβ N, Luger TA, Böhm M. **Hydroxychloroquine modulates metabolic activity and proliferation and induces autophagic cell death of human dermal fibrosis.** J. Invest. Dermatol. 2009, 129 (10), 2419-2426.

113. Zhu Z, Pang B, Iglesias-Bartolome R, Wu X, Hu L, Zhang C, Wang J, Gutkind JS, Wang S. **Prevention of irradiation-induced salivary hypofunction by rapamycin in swine parotid glands.** Oncotarget 2016, 7 (15), 20271-20281.

114. Park D, Jeong H, Lee MN, Koh A, Kwon O, Yang YR, Noh J, Suh PG, Park H, Ryu SH. **Resveratrol induces autophagy by directly inhibiting mTOR through ATP competition.** Sci. Rep. 2016, 6: 21772.

115. Pringle S, Maimets M, Van der Zwaag M, Stokman MA, van Gosliga D, Zwart E, Witjes MJH, de Haan G, van Os R, Coppes RP. **Human salivary gland stem cells functionally restore radiation damaged salivary glands.** Stem cells 2016, 34 (3), 640-652.

116. Takahashi A, Inoue H, Mishima K, Ide F, Nakayama R, Hasaka A, Ryo K, Ito Y, Sakurai T, Hasegawa Y, Saito I. **Evaluation of the effects of quercetin on damaged salivary secretion.** PLoS ONE 2015, 10 (1).

117. Choi JS, Shin HS, An HY, Kim YM, Lim JY. **Radioprotective effects of keratinocyte growth factor-1 against irradiation-induced salivary gland hypofunction.** Oncotarget 2017, 8 (8), 13496-13508.

118. Carroll B, Nelson G, Rabanal-Ruiz Y, Kucheryavenko O, Dunhill-Turner NA, Chesterman CC, Zahari Q, Zhang T, Conduit SE, Mitchell CA, Maddocks ODK, Lovat P, von Zglinicki T, Korolchuk VI. **Persistent mTORC1 signaling in cell senescence results from defects in amino acid and growth factor sensing.** J. Cell Biol. 2017, 216 (7), 1949-1957.

119. Mehri A, Delrée P, Marini AM. **The metabolic waste ammonium regulates mTORC2 and mTORC1 signaling.** Sci. Rep. 2017, 7: 44602.

120. Knox SM, Lombaert IMA, Haddox CL, Abrams SR, Cotrim A, Wilson AJ, Hoffman MP. **Parasympathetic stimulation improves epithelial organ regeneration.** Nat. Commun. 2013, 4:1494.

121. Subhashree M, Venkateswarlu R, Karthik K, Shangamithra V, Venkatachalam P. **DNA damage and the bystander response in tumor and normal cells exposed to X-rays.** Mutat. Res. 2017, 821, 20-27.

122. Kobayashi F, Matsuzaka K, Inoue T. **The effects of basic fibroblast growth factor on regeneration in a surgical wound model of rat submandibular glands.** International Journal of Health Science 2006, 8, 16-23.

123. Li X, Xu Y, Hong Y, Li W, Wang G. **Effects of basic fibroblast growth factor on radiation-induced proliferation inhibition and apoptosis in thymocytes and splenocytes.** International Journal of Health Science 2006, 52 (6), 655-659.

124. Kinoshita N, Tsuda M, Hamuy R, Nakashima M, Nakamura-Kurashige T, Matsuu-Matsuyama M, Hirano A, Akita S. **The usefulness of basic fibroblast growth factor for radiation-exposed tissue.** Wound Repair Regen. 2012, 20 (1), 91-102.

125. Matsuu-Matsuyama M, Nakashima M, Shichijo K, Okaichi K, Nakayama T, Sekine I. **Basic fibroblast growth factor suppresses radiation-induced apoptosis and TP53 pathway in rat small intestine.** Radiat. Res. 2010, 174 (1), 52-61.

126. Marmary Y, Adar R, Gaska S, Wygoda A, Maly A, Cohen J, Eliashar R, Mizrachi L, Orfaig-Geva C, Baum BJ, Rose-John S, Galun E, Axelrod JH. **Radiation-induced loss of salivary gland hypofunction is driven by cellular senescence and prevented by IL-6 modulation.** Cancer Res. 2016, 76 (5), 1170-1180.

127. Ogawa M, Tsuji T. **Reconstitution of a bioengineered salivary gland using a three-dimensional cell manipulation method.** Curr. Protoc. Cell Biol. 2015, 66: 19, 17, 1-13.

128. Sikalidis AK, Mazor KM, Kang M, Liu H, Stipanuk MH**. Total 4EBP1 is elevated in liver of rats in response to low sulfur amino acid intake.** J Amino Acids vol. 2013, Article ID 864757, 11 pages, 2013. doi:10.1155/2013/864757.

129. Mizushima N, Yoshimori T. **How to interpret LC3 immunoblotting.** Autophagy 2007, Nov-Dec; 3 (6): 542-545.

130. Malashenko AM, Beskova TB, Pomerantseva MD, Ramaiya LK. **Comparison of three inbred mouse strains with respect to general and genetic radiosensitivity.** Journal of Genetics (2003) 39: 1052. doi:10.1023/A:1025731319338.

131. Muhvic-Urek M, Bralic M, Curic S, Pezelj-Ribaric S, Borcic J, Tomac J. **Imbalance between apoptosis and proliferation causes late radiation damage of salivary gland mouse.** Physiol. Res. 2006, 55 (1), 89-95.

132. Thoreen CC, Kang SA,Chnag JW, Liu Q, Zhang J, Gao Y, Reichling LJ, Sim T, Sabatini DM, Gray NS. **An ATP-conpetitive Mammalian Target of Rapamycin Inhibitor Reveals Rapamycin-resistant Functions of mTORC1.** J Biol Chem 2009, 284 (12), 8023-32.

133. Choi JH, Wu HG, Jung KC, Lee SH, Kwon EK. **Apoptosis and expression of AQP5 and TGF-β in the irradiated rat submandibular gland.** Cancer Res. Treat. 2009, 41 (3), 145-154.

134. Takeda I, Kizu Y, Yoshitaka O, Saito I, Yamana GY. **Possible role of nitric oxide in radiation-induced salivary gland dysfunction.** Radiat. Res. 2003, 159 (4), 465-470.

135. Strozyk E, Kulms D. **The role of AKT/mTOR pathway in response to UV-irradiation: implication in skin carcinogenesis by regulation of apoptosis, autophagy and senescence.** Int. J. Mol. Sci. 2013, 14 (8), 15260-15285.

136. Bralic M, Muhvic-Urek M, Stemberga V, Golemac M, Jurkovic S, Borcic J, Braut A, Tomac J. **Cell death and cell proliferation in mouse submandibular gland during early post-irradiation phase.** Acta Med. Okayama 2005, 59 (4), 153-159.

137. Kamiya M, Kawase T, Hayame K, Tsuchimochi M, Okuda K, Yoshie H. **X-ray-induced damage to the submandibular salivary glands in mice: an analysis of strain-specific responses.** Biores. Open Acess 2015, 4 (1), 307-318.

138. O'Connell AC, Redman RS, Evans RL, Ambudkar IS. **Radiation-induced progressive decrease in fluid secretion in rat submandibular glands is related to decreased acinar volume and not impaired calcium signaling.** Radiat. Res. 1999, 151 (2), 150-158.

139. Zhang J, Gao Z, Ye J. **Phosphorylation and degradation of S6K1 (p70S6K1) in response to persistent JNK1 activation.** Bioch. Biophys. Acta. 2013, 1832 (12), 1980-1988.

140. Clark K, Peggie M, Plater L, Sorcek RJ, Young ERR, Madwed JB, Hough J, McIver EG, Cohen P. **Novel cross-talk within the IKK family controls innate immunity.** Biochem. J. 2011, 434 (1), 93-104.

141. Musiwaro P, Smith M, Manifava M, Walker SA, Ktistakis NT. **Characteristics and requirements of basal autophagy in HEK 293 cells.** Autophagy 2013, 9 (9), 1407-1417.

142. Pla A, Pascual M, Guerri C. **Autophagy constitutes a protective mechanism against ethanol toxicity in mouse astrocytes and neurons.** PLoS One 2016, 11 (4), e0153097

143. Chang W, Bai J, Tian S, Ma M, Li W, Yin Y, Deng R, Cui J, Li J, W G, Zhang P, Tao K. **Autophagy protects gastric mucosal epithelial cells from ethanol-induced oxidative damage via mTOR signalling pathway.** Exp. Biol. Med. (Maywwod) 2017, 242 (10), 1025-1033.

144. Papinski D, Kraft C. **Regulation of autophagy by signalling through the Atg1/ULK1 complex.** J. Mol. Biol. 2016, 428 (9 Pt A), 1725-1741.

145. Ro SH, Jung CH, Hahn WS, Xu X, Kim YM, Yun YS, Park JM, Kim KH, Seo M, Ha TY, Arriaga EA, Bernlohr DA, Kim DH. **Distinct functions of Ulk1 and Ulk1 in the regulation of lipid metabolism in adipocytes.** Autophagy 2013, 9 (12), 2103-2114.

146. Wang Y, Zhou K, Li Tao, Xu Y, Xie C, Sun Y, Zhang Y, Rodriguez J, Blomgren K, Zhu C. **Inhibition of autophagy prevents irradiation-induced neural stem and progenitor cell death in the juvenile mouse brain.** Cell Death Dis. 2017, 8 (3), e2694.

147. Rao R, Balusu R, Fiskus W, Mudunuru U, Venkannagari S, Chauchan L, Smith JE, Hembruff SL, Ha K, Atadja P, Bhalla KN. **Combination of pan-histone deacetylase inhibitor and autophagy inhibitor exerts superior efficacy against triple-negative human breast cancer cells.** Mol. Cancer Ther. 2012, 11 (4), 973-983.

148. Barth S, Glick D, Macleod KF. **Autophagy: assays and artifacts.** J. Pathol. 2010, 221 (2), 117-124.

149. Hu Y, Carraro-Lacroix LR, Wang A, Owen C, Bajenova E, Corey PN, Brumell JH, Voronov I. **Lysosomal pH plays a key role in regulation of mTOR activity in osteoclasts.** J, Cell. Bio. Biochem. 2016, 117 (2), 413-425.

150. Young ARJ, Chan EYW, Hu XW, Köchl R, Crawshaw SG, High S, Hailey DW, Lippincott-Schwartz J, Tooze SA. **Starvation and ULK1-dependent cycling of mammalian Atg9 between the TGN and endosomes.** J. Cell Sci. 2006, 119 (Pt 18), 3888-3900.

151. Chan EYW, Kir S, Tooze S. siRNA screening of the kinome identifies **ULK1 as a multidomain modulator of autophagy.** J. Biol. Chem. 2007, 282 (35), 25464-25474.

152. Pirkmajer S, Chibalin AV. **Serum starvation: caveat emptor.** Am. J. Physiol. Cell Physiol. 2011, 301 (2), C272-C279.

153. Chen R, Zou Y, Mao D, Sun D, Gao G, Shi X, Liu X, Zhu C, Yang M, Ye W, Hao Q, Li R, Yu L. **The general amino acid control pathway regulates mTOR and autophagy during serum/glutamine starvation.** J. Cell Biol. 2014, 206 (2), 173-182.

154. Nazio F, Cecconi F. **Autophagy up and down by outsmarting the incredible ULK.** Autophagy 2017, 13 (5), 967-968.

155. Takahashi S, Nakamura S, Suzuki R, Islam N, Domon T, Yamamoto T, Wakita M. **Apoptosis and mitosis of parenchymal cells in the duct-ligated rat submandibular gland.** Tissue & Cell 1998, 32 (6), 457-463.

156. Inouye M, Tamaru M, Kameyama Y. **Effect of cycloheximide and actinomycin D on radiation-induced apoptotic cell death in the developing mouse cerebellum.** Int. J. Radiat. Biol. 1992, 61 (5), 669-674.

157. Allavena G, Boyd C, Oo KS, Maellaro E, Zhivotovsky B, Kaminskyy VO. **Suppressed translation and ULK1 degradation as potential mechanisms of autophagy limitation under prolonged starvation.** Autophagy 2016, 12 (11), 2085-2097.

158. Pan H, Zhong XP, Lee S. **Sustained activation of mTORC1 in macrophages increases AMPKα-dependent autophagy to maintain cellular homeostasis.** BMC Biochem. 2016, 17 (1), 14.

159. Di Nardo A, Wertz MH, Kwiatkowski E, Tsai PT, Leech JD, Greene-Colozzi E, Goto J, Dilsiz P, Talos DM, Clish CB, Kwiatkowski DJ, Sahin M. **Neuronal Tsc1/2 complex controls autophagy through AMPK-dependent regulation of ULK1.** Hum. Mol. Gen. 2014, 23 (14), 3865-3874.

160. Lin AL, Johnson DA, Wu Y, Wong G, Ebersole JL, Yeh CK. **Measuring short-term γ-irradiation on mouse salivary gland function using a new saliva collection device.** Arch. Oral Biol. 2001, 46 (11), 1085-1089.

161. Jo GH, Bögler O, Chwae YJ, Yoo H, Lee SH, Park JB, Kim YJ, Kim JH, Gwak HS. **Radiation-induced autophagy contributes to cell death and induces apoptosis partly in malignant glioma cells.** Cancer Res. Treat. 2015, 47 (2), 221-241.

162. Wu J, Zhang B, Wuu YR, Davidson MM, Hei TK**. Targeted cytoplasmic irradiation and autophagy.** Mutat. Res. 2017, S0027-5107 (16) 30147-6.

163. Walker NI, Gobé GC. **Cell death and cell proliferation during atrophy of the rat parotid gland induced by duct obstruction.** J. Pathol. 1987, 153 (4), 333-344.

164. Cheong H, Lindsten T, Wu J, Lu C, Thompson CB. **Ammonia-induced autophagy is independent of ULK1/ULK2 kinases.** PNAS 2011, 108 (27), 11121-11126.

165. Seglen PO, Reith A. **Ammonia inhibition of protein degradation in isolated rat hepatocytes.** Exp. Cell Res. 1976, 100 (2), 276-280.

166. Bates PJ, Coetzee GA, Van der Westhuyzen DR. **The degradation of endogenous and exogenous proteins in cultured smooth cells.** Biochim. Biophys. Acta 1982, 719 (2), 377-387.

167. Beugnet A, Tee AR, Taylor PM, Proud CG. **Regulation of targets of mTOR (mammalian target of rapamycin) signalling by intracellular amino acid availability.** Biochem. J. 2003, 372 (Pt 2), 555-566.

168. Mizushima N, Yoshimori T, Levine B. **Methods in mammalian autophagy research.** Cell 2010, 140 (3), 313-326.

169. Lin HH, Lin SM, Chung Y, Vonderfecht S, Camden JM, Flodby P, Borok Z, Limesand KH, Mizushima N, Ann DK. **Dynamic involvement of ATG5 in cellular stress responses.** Cell Death Dis. 2014, 5, e1478.

170. Arakawa S, Honda S, Yamaguchi H, Shimizu S. **Molecular mechanisms and physiological roles of ATG5/ATG7-independent alternative autophagy.** Proc. Jpn. Acad. Ser B Phys. Biol. Sci. 2017, 93 (6), 378-385.

171. Marino ML, Pellegrini P, Di Lernia G, Djavaheri-Mergny M, Brnjic S, Zhang X, Hägg M, Linder S, Fais S, Codogno P, De Milito A. **Autophagy is a protective mechanism for human melanoma under acidic stress.** J. Biol. Chem. 2012, 287 (36), 30664-30676.

172. Zhao L, Cui L, Jiang X, Zhang J, Zhu M, Jia J, Zhang Q, Zhang J, Zhang D, Huang Y. **Extracellular pH regulates autophagy via the AMPK-ULK1 pathway in rat cardiomyocytes.** FEBS Lett. 2016, 590 (18), 3202-3212.

173. Suk J, Kwak SS, Lee JH, Choi JH, Lee SH, Lee DH, Byun B, Lee GH, Joe CO. **Alkaline stress-induced autophagy is mediated by mTORC1 inactivation.** J. Cell. Biochem. 2011, 112 (9), 2566-2573.

174. Alers S, Löffler AS, Paasch F, Dieterle AM, Keppeler H, Lauber K, Campbell DG, Fehrenbacher B, Schaller M, Wesselborg S, Stork B. **Atg13 and FIP200 act independently of Ulk1 and Ulk2 in autophagy induction.** Autophagy 2011, 7 (12), 1424-1433.

175. Schneyer CA, Hall HD. **Parasympathetic regulation of mitosis induced in rat parotid by dietary change.** Am. J. Physiol. 1975, 229 (6), 1614-1617.

176. Kam WWY, Banati RB. **Effects of ionizing radiation on mitochondria.** Free Radic. Biol. Med. 2013, 65, 607-619.

177. Nacarelli T, Azar A, Sell C. **Mitochondrial stress induces cellular senescence in an mTORC1-dependent manner.** Free Radic. Biol. Med. 2016, 95 133-154.

178. Shen K, Feng X, Su R, Xie H, Zhou L, Zheng S. **Epigallocatechin 3-gallate ameliorates bile duct ligation induced liver injury in mice by modulation of mitochondrial oxidative stress and inflammation.** PLoS One 2015, 10 (5), e0126278.

179. Matés JM, Sánchez-Jiménez FM. **Role of reactive oxygen species in apoptosis: implications for cancer therapy.** Int. J. Biochem. Cell Biol. 2000, 32 (2), 157-170

180. Fan T, Chen L, Huang Z, Wang W, Zhang B, Xu Y, Mao Z, Hu H, Geng Q. **Autophagy activation by rapamycin before hypoxia-reoxygenation reduces endoplasmic reticulum stress in alveolar epithelial cells.** Cell. Physiol. Biochem. 2017, 41 (1), 79-90.

181. Lerner C, Bitto A, Pulliam D, Nacarelli T, Konigsberg M, Van Remmen H, Torres C, Sell C. **Reduced mammalian target of rapamycin activity facilitates mitochondrial retrograde signalling and increases life span in normal human fibroblasts.** Aging Cell. 2013, 12 (6), 966-977.

182. Scherz-Shouval R, Elazar Z. **ROS, mitochondria and the regulation of autophagy.** Trends Cell Biol. 2007, 17 (9), 422-427.

183. Wei D, Liao S, Wang J, Yang M, Kong L. **Cholestatic liver injury model of bile duct ligation and the protection of Huang-Lian-Jie-Du decoction by NMR** metabolic profiling. RSC Advances 2015, 5 (81), 66200-66211.

184. Zorov DB, Juhaszova M, Sollott SJ. **Mitochondrial ROS-induced ROS release: an update and review.** Biochim. Biophys. Acta 2006, 1757 (5-6), 509-517.

185. Miwa S, Saretzki G. **Telomerase and mTOR in the brain: the mitochondria connection.** Neural Regen. Res. 2017, 12 (3), 358-361.

186. Zhao B, Qiang L, Joseph J, Kalyanaraman B, Viollet B, He YY. **Mitochondrial dysfunction activates the AMPK signalling and autophagy to promote cell survival.** Genes & Diseases 2016, 3 (1), 82-87.

187. Simon HU, Haj-Yehia A, Levi-Schaffer. **Role of reactive oxygen species (ROS) in apoptosis induction.** Apoptosis 2000, 5 (5), 415-418.

188. Adelusi SA, Salako LA. **Kinetics of the distribution and elimination of chloroquine in the rat.** Gen. Pharmacol. 1982, 13 (5), 433-437.

189. Kim J, Kundu M, Viollet B, Guan KL. **AMPK and mTOR regulate autophagy through direct phosphorylation of Ulk1.** Nat. Cell Biol. 2011, 13 (2), 132-141.

190. Carpenter GH, Proctor GB, Ebersole LE, Garrett JR. **Secretion of IgA by rat parotid and submandibular cells in response to autonomimetic stimulation in vitro.** Int. Immunopharmacol. 2004, 4 (8), 1005-1014.

191. Cao L, Xu J, Lin Y, Zhao X, Liu X, Chi Z. **Autophagy is upregulated in rats with status epilepticus and partly inhibited by Vitamin E.** Biochem. Biophys. Res. Comm. 2009, 379 (4),949-953.

192. Zhang L, Fu L, Zhang S, Zhang J, Zhao Y, Zheng Y, He G, Yang S, Ouyang L, Liu B. **Discovery of a small molecule targeting ULK1-modulated cell death of triple negative breast cancer in vitro and in vivo.** Chem. Sci. 2017, 8 (4), 2687-2701.

193. Wang B, Kundu M. **Canonical and noncanonical functions of ULK/Atg1.** Curr. Opin. Cell Biol. 2017, 45, 47-54.

194. Eliopoulos AG, Havaki S, Gorgoulis VG. **DNA damage response and autophagy: a meaningful partnership.** Front. Genet. 2016, 7: 204.

195. Lombaert IMA. **Regeneration of irradiated salivary glands by stem cell therapy.** Doctoral dissertation, University of Groningen 2008.

196. Araujo MVT, Spadella MA, Chies AB, Arruda GV, Santos T de M, Cavariani MM, Domeniconi RF. **Effect of low radiation dose on the expression and location of aquaporins in rat submandibular gland.** Tissue Cell 2018, 53, 104-110.

197. Limesand KH, Said S, Anderson SM. **Suppression of radiation-induced salivary gland dysfunction by IGF-1.** PLoS One 2009, 4 (3), e4663.

198. Li Y, Taylor JM, Ten Haken RK, Eisbruch A. **The impact of dose on parotid salivary recovery in head and neck cancer patients treated with radiation therapy.** Int J Radiat Oncol Biol Phys 2007, 67 (3), 660-669.

199. Grundmann O, Mitchell GC, Limesand KH. **Sensitivity of salivary glands to**

radiation: from animal models to therapies. J Dent Res 2009, 88 (10), 894-903.

200. Vissink A, Jansma J, Spikjervet FK, Burlage FR, Coppes RP. **Oral sequelae of head and neck radiotherapy.** Crit Rev Oral Biol Med 2003, 14 (3): 199-212.

201. Cotroneo E, Proctor GB, Paterson KL, Carpenter GH. **Early markers of regeneration following ductal ligation in the rat submandibular gland.** Cell Tissue Res 2008, 332 (2), 227-235.

202. Watanabe H, Takahashi H, Hata-Kawakami M, Tanaka A. **Expression of c-kit and cytokeratin 5 in the submandibular gland after release of long-term ligation of the main excretory duct in mice.** Acta Histochemi Cytochem 2017, 50 (3), 111-118.

203. Leibiger C, Kosyakova N, Mkrtchyan H, Glei M, Trifonov V, Liehr T. **First Molecular Cytogenetic High Resolution Characterization of the NIH 3T3 Cell Line by Murine Multicolor Banding.** J Histochem Cytochem 2013, 61 (4), 306-312.

204. Lam RK, Han W, Yu KN. **Unirradiated cells rescue cells exposed to ionizing radiation: Activation of NF- κB pathway in irradiated cells.** Mutat Res 2015, 782, 23-33.

205. Gonçalves Fonseca A, Leiros Sena Fernandes Ribeiro Dantas, Morais Fernandes Jùlia, Zucolotto SM, Antoninni Neves Lima A, Lira Soares LA, Oliveira Rocha HA, Araùjo Moura Lemos TM. **In vivo and in vitro toxicity evaluation of hydroethanolic extract of Kalanchoe brasiliensis (Crassulaceae) leaves.** J Toxicol 2018, 2018, 6849765, doi.org/10.1155/2018/6849765, eCollection 2018.

206. Ghallab A. **In vitro test systems and their limitations.** Excli J 2013, 12, 1024-1026.

207. Nelson J, Manzella K, Baker OJ. **Current cell models for bioengineering a salivary gland: a mini-review of emerging technologies.** Oral Dis 2013, 19 (3), 236-244.

208. Ponnaiya B, Amundson SA, Ghandhi SA, Smilenov LB, Geard CR, Buonanno M, Brenner DJ. **Single-cell responses to ionizing radiation.** Radiat Environ Biophys 2013, 52 (4), 523-530.

209. Chaurasia M, Bhatt AN, Das A, Dwarakanath BS, Sharma K. **Radiation-induced autophagy: mechanisms and consequences.** Free Radic Res 2016, 50 (3), 273-290.